

INFORMATION TO USERS

This manuscript has been reproduced from the microfilm master. UMI films the text directly from the original or copy submitted. Thus, some thesis and dissertation copies are in typewriter face, while others may be from any type of computer printer.

The quality of this reproduction is dependent upon the quality of the copy submitted. Broken or indistinct print, colored or poor quality illustrations and photographs, print bleedthrough, substandard margins, and improper alignment can adversely affect reproduction.

In the unlikely event that the author did not send UMI a complete manuscript and there are missing pages, these will be noted. Also, if unauthorized copyright material had to be removed, a note will indicate the deletion.

Oversize materials (e.g., maps, drawings, charts) are reproduced by sectioning the original, beginning at the upper left-hand corner and continuing from left to right in equal sections with small overlaps.

Photographs included in the original manuscript have been reproduced xerographically in this copy. Higher quality 6" x 9" black and white photographic prints are available for any photographs or illustrations appearing in this copy for an additional charge. Contact UMI directly to order.

ProQuest Information and Learning
300 North Zeeb Road, Ann Arbor, MI 48106-1346 USA
800-521-0600

UMI[®]

University of Alberta

A novel method to prepare ligand-targeted liposomal drugs for clinical applications.

by

Debbie Lynne Iden



A thesis submitted to the Faculty of Graduate Studies and Research in partial fulfillment
of the requirements for the degree of Master of Science

Department of Pharmacology

Edmonton, Alberta

Spring, 2001



National Library
of Canada

Acquisitions and
Bibliographic Services

395 Wellington Street
Ottawa ON K1A 0N4
Canada

Bibliothèque nationale
du Canada

Acquisitions et
services bibliographiques

395, rue Wellington
Ottawa ON K1A 0N4
Canada

Your file *Votre référence*

Our file *Notre référence*

The author has granted a non-exclusive licence allowing the National Library of Canada to reproduce, loan, distribute or sell copies of this thesis in microform, paper or electronic formats.

The author retains ownership of the copyright in this thesis. Neither the thesis nor substantial extracts from it may be printed or otherwise reproduced without the author's permission.

L'auteur a accordé une licence non exclusive permettant à la Bibliothèque nationale du Canada de reproduire, prêter, distribuer ou vendre des copies de cette thèse sous la forme de microfiche/film, de reproduction sur papier ou sur format électronique.

L'auteur conserve la propriété du droit d'auteur qui protège cette thèse. Ni la thèse ni des extraits substantiels de celle-ci ne doivent être imprimés ou autrement reproduits sans son autorisation.

0-612-60440-3

Canada

University of Alberta

Library Release Form

Name of Author: Debbie Lynne Iden
Title of Thesis: A novel method to prepare ligand-targeted liposomal drugs for clinical applications.
Degree: Master of Science
Year this Degree Granted: 2001

Permission is hereby granted to the University of Alberta Library to reproduce single copies of this thesis and to lend or sell such copies for private, scholarly or scientific research purposes only.

The author reserves all other publication and other rights in association with the copyright in the thesis, and except as herein before provided, neither the thesis nor any substantial portion thereof may be printed or otherwise reproduced in any material form whatever without the author's prior written permission.



1101-10149 Saskatchewan Drive,
Edmonton, Alberta, Canada
T6E 6B6

Jan 5/01

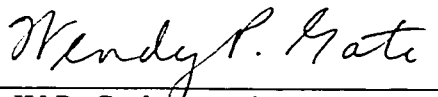
University of Alberta

Faculty of Graduate Studies and Research

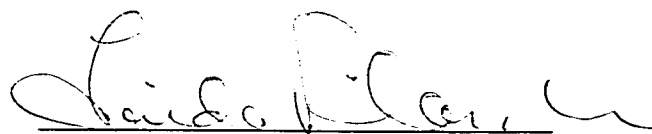
The undersigned certify that they have read, and recommend to the Faculty of Graduate Studies and Research for acceptance, a thesis entitled A novel method to prepare ligand-targeted liposomes for clinical applications submitted by Debbie Lynne Iden, in partial fulfillment of the requirements for the degree of Master of Science.



Dr. T.M. Allen, supervisor



Dr. W.P. Gati, committee member



Dr. L.M. Pilarski, committee member

Jan 4/01

ABSTRACT

Ligand-targeted liposomes have potential in cancer treatment by improving the therapeutic index of chemotherapeutic agents. The application of a novel, combinatorial approach to the preparation of ligand-targeted liposomes that is amenable to clinical application has been evaluated in this thesis. It was shown that IgG- PEG₂₀₀₀-DSPE will transfer from a micelle phase into the bilayer of pre-formed, drug-loaded liposomes in a time- and temperature-dependent manner, resulting in the production of sterically stabilized immunoliposomes. The *in vitro* binding/uptake of post-insertion immunoliposomes targeted to the CD19 receptor (PIL[anti-CD19]) on B-cell lymphoma (Namalwa) cells was similar to immunoliposomes prepared by conventional techniques (SIL[anti-CD19]). In addition, no significant difference was found comparing the *in vitro* cytotoxicity and *in vivo* therapeutic efficacy of DXR-PIL[anti-CD19] with DXR-SIL[anti-CD19]. Importantly, PIL[anti-CD19] showed improved binding/uptake, cytotoxicity, and therapeutic efficacy compared to a non-targeted liposomal formulation. Overall, the results suggest that targeted liposomes prepared using the post-insertion technique may have clinical utility.

ACKNOWLEDGMENTS

First and foremost, I would like to thank my supervisor, Dr. T.M. Allen for her guidance and support throughout my graduate school term. I am especially thankful for the knowledge that I have gained from her in all aspects of my training.

I also wish to thank all of the members of my supervisory committee including Dr. T.M. Allen, Dr. W.P. Gati, and Dr. L.M. Pilarski for their helpful suggestions and constructive criticism. A special thanks is extended to Dr. Gati for her assistance as graduate student coordinator and for nominating me to become the graduate student representative for the HSLAS Animal Policy and Welfare Committee.

I am also extremely grateful to all the members of Dr. Allen's laboratory (from 1998-2000), otherwise known as the 'lipozoids', for their friendship and support: René LeClerc, Darrin Stuart, Marc Kirchmeier, Felicity Wang, Tatsuhiro Ishida, Chris Hansen, Julie Chevrette, Zolt Gabos, Joao Moriera, Jie Mah, Cheryl Santos, Greg Charrois, Puja Sapra, Janny Zhang, Fabio Pastorino, Manuela Colla, Amanda Reichert, Elaine Moase, and Susan Cubitt. My time as a graduate student would not have been the same without them. Special thanks to Tatsuhiro for being my partner and mentor in the early stages of my project and to Elaine and Susan for their technical assistance. Susan is gratefully acknowledged for production of anti-CD19 mAb and Elaine for iodinations and training me in the lab.

Finally, I would like to thank Grant and my friends and family for their support, especially during the writing of this thesis.

Financial support from the Canadian Institutes of Health Research is gratefully acknowledged.

TABLE OF CONTENTS

Chapter 1	Introduction and hypothesis	
1.1	Background and rationale.....	2
1.2	What are liposomes?.....	2
1.3	Liposomes as drug carriers.....	7
1.4	Liposomal anti-cancer drugs.....	7
1.5	Loading drugs into the liposome interior.....	9
1.6	Evolution of long-circulating liposomes.....	10
1.7	Improving the tumor specificity of liposomes: passive targeting.....	14
1.8	Ligand-mediated targeting.....	18
1.9	Coupling techniques.....	20
1.10	Demonstrated potential of ligand-targeted liposomes.....	27
1.11	Choice of target antigen.....	29
1.12	Disadvantages of ligand-mediated targeting.....	33
1.13	Indications for targeted liposomes.....	35
1.14	Barriers and solutions to the clinical approval of ligand-targeted liposomes	36
1.15	The model system.....	40
1.16	Hypothesis and objectives.....	47

Chapter 2 Materials and Methods

2.1	Materials.....	51
2.2	Cell lines.....	52
2.3	Mice.....	52
2.4	Preparation of anti-CD19 mAb.....	53
2.5	Iodination of antibodies.....	54
2.6	Preparation of liposomes.....	54
2.7	Preparation of micelles.....	56
2.8	Antibody coupling to liposomes and micelles.....	57
2.9	Determination of micelle coupling efficiency.....	58
2.10	Micelle transfer.....	59
2.11	Characterization of transfer efficiency.....	59
2.12	<i>In vitro</i> stability of insertion.....	60
2.13	<i>In vitro</i> doxorubicin leakage experiments.....	60
2.14	<i>In vitro</i> binding/uptake.....	61
2.15	<i>In vitro</i> cytotoxicity.....	62
2.16	Pharmacokinetics.....	63
2.17	<i>In vivo</i> therapeutic efficacy.....	64
2.18	Statistical analysis.....	65

Chapter 3	Development and optimization of the post-insertion method to prepare ligand-targeted liposomes	
3.1	Determination of CMC coupling efficiency for micelles.....	67
3.2	Optimization of incubation conditions for transfer.....	69
3.3	Effects of micelle composition on transfer efficiency.....	70
3.4	Effects of liposome composition on transfer efficiency.....	74
Chapter 4	<i>In vitro</i> targeting of post-insertion and conventional immunoliposomes to human B-cell lymphoma cells	
4.1	Binding/uptake.....	83
4.2	Cytotoxicity.....	93
Chapter 5	<i>In vivo</i> targeting of doxorubicin-loaded post-insertion and conventional immunoliposomes to an animal model of human B-cell lymphoma	
5.1	Pharmacokinetics.....	102
5.2	<i>In vivo</i> therapeutics.....	113
	Summarizing discussion and future directions.....	119
	References.....	129

LIST OF TABLES

Table 1.1	Comparison of various coupling methods for the preparation of sterically stabilized immunoliposomes.....	28
Table 4.1	Cytotoxicity (IC ₅₀) of non-targeted and anti-CD19 targeted formulations of DXR against CD19+ Namalwa cells <i>in vitro</i> by the MTT assay.....	95
Table 4.2	Statistical comparison of the 1h and 24 h IC ₅₀ s of non-targeted and CD19 targeted formulations of DXR against Namalwa cells <i>in vitro</i>	96
Table 5.1	Comparison of the clearance rates of ¹²⁵ I-TI Liposomes: variation based on the targeting Ab and coupling method.....	108
Table 5.2	Comparison of the clearance rates of ¹²⁵ I-TI liposomes between BALB/c and SCID mice bearing i.v. CD19+ Namalwa cells.....	110
Table 5.3	Therapeutic efficacy of non-targeted and CD19 targeted formulations of DXR in SCID mice injected i.v. with Namalwa Cells.....	114
Table 5.4	Statistical comparison of MST for SCID mice bearing i.v. Namalwa cells that were treated with untargeted or CD19 targeted formulations of DXR.....	115

LIST OF FIGURES

Figure 1.1	General phospholipid structure.....	3
Figure 1.2	Association patterns of amphiphiles.....	5
Figure 1.3	Liposome classification.....	6
Figure 1.4	Remote loading of doxorubicin by the ammonium sulfate gradient method	11
Figure 1.5	Classical and sterically stabilized (Stealth®) liposomes.....	15
Figure 1.6	Passive targeting of long-circulating liposomes to solid tumors.....	16
Figure 1.7	Coupling strategies	22
Figure 1.8	Techniques for coupling antibodies or other ligands to liposomes.....	23
Figure 1.9	General antibody structure.....	26
Figure 1.10	Routes of intracellular delivery of liposomal drugs.....	31
Figure 1.11	Schematic outlining the post-insertion method to prepare ligand-targeted Liposomes.....	39
Figure 1.12	Schematic showing the combinatorial approach to the preparation of drug-loaded, ligand-targeted liposomes for clinical applications.....	40
Figure 1.13	The stages of lymphocyte differentiation.....	42
Figure 3.1	Separation of free IgG from IgG-PEG-DSPE micelles on a metrizamide gradient.....	68
Figure 3.2	Affect of micelle composition on the transfer of IgG-PEG-DSPE and PEG-DSPE from micelles to preformed liposomes.....	73
Figure 3.3	Effect of liposome PEG ₂₀₀₀ -DSPE content on transfer of IgG-PEG ₂₀₀₀ - DSPE and PEG-DSPE from micelles into preformed liposomes.....	75
Figure 3.4	Comparison of free IgG and IgG-PEG-DSPE micelle transfer to CL....	77
Figure 4.1	<i>In vitro</i> binding/uptake of anti-CD19 targeted liposomes and non-targeted liposomes.....	85

Figure 5.1	Blood clearance of tyraminyl-inulin loaded SIL[anti-CD19], PIL[anti-CD19], SIL[sheep IgG], PIL[sheep IgG], and non-targeted SL in Balb/C or Alt BM mice.....	103
Figure 5.2	Comparison of the clearance rates of ¹²⁵ I-TI liposomes: variation based on the targeting Ab and coupling method.....	106

LIST OF ABBREVIATIONS

Ab	antibody
AUC	area under the time concentration curve
CHOL	cholesterol
CL	classical liposomes (non-pegylated)
DSPE	distearoylphosphatidylethanolamine
DXR	doxorubicin
DXR-PIL[anti-CD19]	doxorubicin-loaded sterically stabilized immunoliposomes coupled by the post-insertion method with anti-CD19 monoclonal antibody
DXR-SIL[anti-CD19]	doxorubicin-loaded sterically stabilized immunoliposomes coupled by the conventional method with anti-CD19 monoclonal antibody
DXR-SL	doxorubicin-loaded sterically stabilized liposomes
FBS	fetal bovine serum
h	hour
[³ H]CHE	[1,2- ³ H(N)]cholesterol hexadecyl ether
HEPES	4-(2-Hydroxyethyl)-1-Piperazineethansulfonic Acid
HSPC	hydrogenated soy phosphatidylcholine
H _z -PEG-DSPE	hydrazide-derivatized poly(ethylene glycol) (molecular weight 2000) covalently linked to distearoylphosphatidylethanolamine
IC ₅₀	drug concentration that results in a 50% reduction in absorbance compared to control
IgG	immunoglobulin G
ILS	increased life span (percent increase over control)

i.v.	intravenous
kg	kilogram
LUV	large unilamellar vesicles
MAb	monoclonal antibody
mg	milligram
μg	microgram
μl	microliter
μmol	micromole
min	minute
ml	milliliter
MLV	multilamellar vesicle
MRT	mean residence time
MST	mean survival time
MTD	maximum tolerated dose
MTT	3-(4,5-dimethylthiazol-2-yl)-2,5-diphenyltetrazolium bromide
MW	molecular weight
nm	nanometers
PEG	poly(ethylene glycol)
PIL	post-insertion liposomes
PL	phospholipid
SCID	severe combined immunodeficient
S.D.	standard deviation
SL	sterically stabilized (Stealth [®]) liposomes

SIL	sterically stabilized (Stealth [®]) immunoliposomes
SUV	small unilamellar vesicles
T _{1/2}	half-life
T _M	membrane phase transition temperature
v/v	volume/volume
w/w	weight/weight

Chapter 1
Introduction and Hypothesis

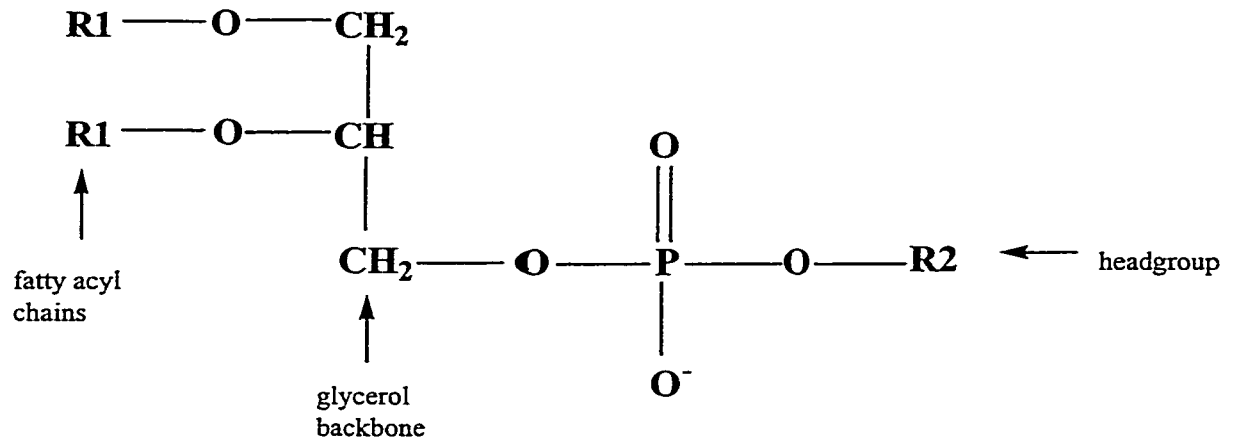
Chapter 1:

1.1 Background and Rationale

The subject of this thesis is the development of a novel method to prepare targeted liposomes for clinical applications. Advancements in liposomal technology have primarily, but not exclusively, centered on the development of liposomal anti-cancer drugs. This is because cancer is a major cause of morbidity and mortality worldwide and current treatments are associated with severe side effects and, sometimes, inadequate responses. Liposomal formulations of anti-cancer drugs, are one of the new treatment strategies to increase the response to chemotherapy and to increase patient quality of life. In this study a novel method for inserting antibodies into liposomes, termed the post-insertion method, was employed to prepare targeted liposomes loaded with the anti-cancer drug doxorubicin. The resulting therapeutic formulation was evaluated in a model of B-cell lymphoma.

1.2 What are Liposomes?

Liposomes were first described by Alec Bangham in 1965 (1). They are composed of amphipathic phospholipids (PL) that spontaneously associate when hydrated to form bilayer spheres or vesicles with an aqueous interior core. The basic structure of a representative phospholipid is illustrated in **Fig. 1.1**. Amphiphilic phospholipids have hydrophobic fatty acyl chains and a hydrophilic headgroup and they tend to associate in an aqueous environment in a pattern that shields the hydrophobic tails. The association patterns are dependent on the size and topology of the hydrophilic and hydrophobic regions. Amphiphilic phospholipids that are tubular in shape tend to produce bilayers, and can form liposomes, while phospholipids that have a large



R1
Saturated Fatty Acids

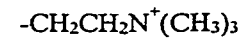
Lauric	$\text{CH}_3(\text{CH}_2)_{10}\text{COOH}$
Myristic	$\text{CH}_3(\text{CH}_2)_{12}\text{COOH}$
Palmitic	$\text{CH}_3(\text{CH}_2)_{14}\text{COOH}$
Stearic	$\text{CH}_3(\text{CH}_2)_{16}\text{COOH}$

Unsaturated Fatty Acids

Palmitoleic	$\text{CH}_3(\text{CH}_2)_5\text{CH}=\text{CH}(\text{CH}_2)_7\text{COOH}$
Oleic	$\text{CH}_3(\text{CH}_2)_7\text{CH}=\text{CH}(\text{CH}_2)_7\text{COOH}$
Linoleic	$\text{CH}_3(\text{CH}_2)_4\text{CH}=\text{CHCH}_2\text{CH}=\text{CH}(\text{CH}_2)_7\text{COOH}$
Linolenic	$\text{CH}_3\text{CH}_2\text{CH}=\text{CHCH}_2\text{CH}=\text{CH}-\text{CH}_2\text{CH}=\text{CH}(\text{CH}_2)_7\text{COOH}$
Arachidonic	$\text{CH}_3(\text{CH}_2)_4(\text{CH}=\text{CHCH}_2)_3\text{CH}=\text{CH}(\text{CH}_2)_3\text{COOH}$

R2
Headgroups

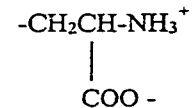
phosphatidylcholine (PC)



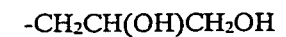
phosphatidylethanolamine (PE)



phosphatidylserine (PS)



phosphatidylglycerol (PG)



phosphatidylinositol (PI)

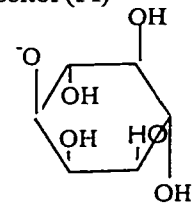


Fig. 1.1 General phospholipid structure.

polar head group compared to the acyl chain size tend to form micelles, as shown in Fig. 1.2. A wide variety of phospholipids from both plant and animal sources can be used to make liposomes. The acyl chains vary in length and can be saturated or unsaturated to various degrees. Some of the commonly used phospholipids are listed in Fig. 1.1. The choice of phospholipid affects several properties of the resulting liposomes, including charge, size, stability, and phase transition temperature (T_M). Above the T_M the bilayer becomes fluid; therefore the stability of liposomes is markedly affected by temperature (2). Cholesterol is often included in the formulation for its 'membrane- stabilizing effects' (*vide infra*).

The hydration of phospholipid results in vesicles that are heterogenous in size, ranging from 300-2000 nm in diameter, composed of multiple bilayers, and are referred to as multilamellar liposomes (MLV). Various techniques have been developed to manipulate the size and lamellarity of the liposomes (3-6). One of the commonly used methods, and the approach employed in this thesis research, is multiple extrusion of the lipid under moderate pressure (≤ 500 psi) through polycarbonate membranes with a uniform pore size. The liposomes are sequentially extruded through membranes of decreasing pore size until the desired vesicle size is reached. This method results in the production of vesicles of a homogenous size distribution. The vesicles are normally classified according to their size and lamellarity into either small or large unilamellar vesicles (SUV or LUV), or large multilamellar vesicles (MLV) (Fig. 1.3). Unilamellar vesicles are normally preferred because the volume of the interior aqueous space is much larger, thereby increasing the amount of drug or other molecules that can be encapsulated.

Association Patterns of Amphiphiles

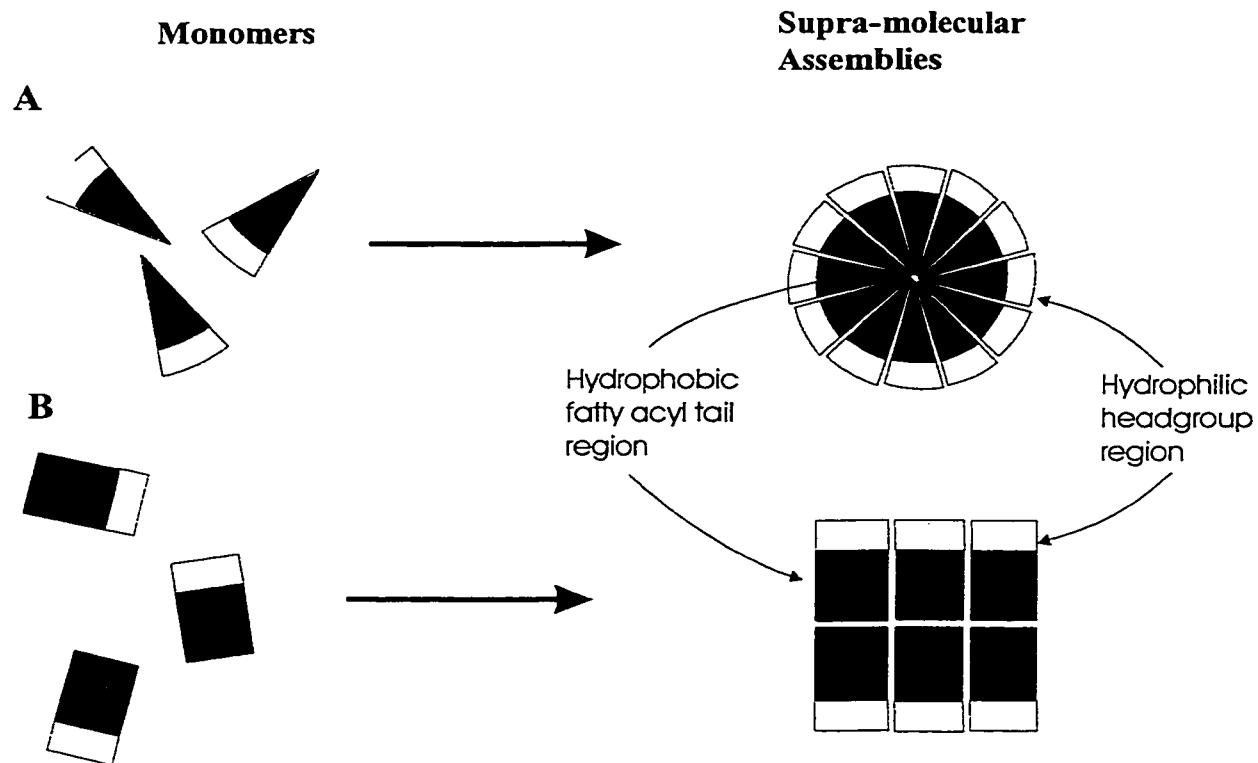


Fig. 1.2 Association patterns of amphiphiles in aqueous environments. Phospholipids associate in aqueous environments in a pattern that shields the hydrophobic regions. The size and topology of the hydrophobic and hydrophilic regions determines the most favorable aggregation pattern. **A.** Phospholipids that have large hydrophilic head groups relative to the size of the hydrophobic tails tend to form micelles. **B.** Phospholipids that are tubular in shape tend to form bilayers.

Liposome Classification

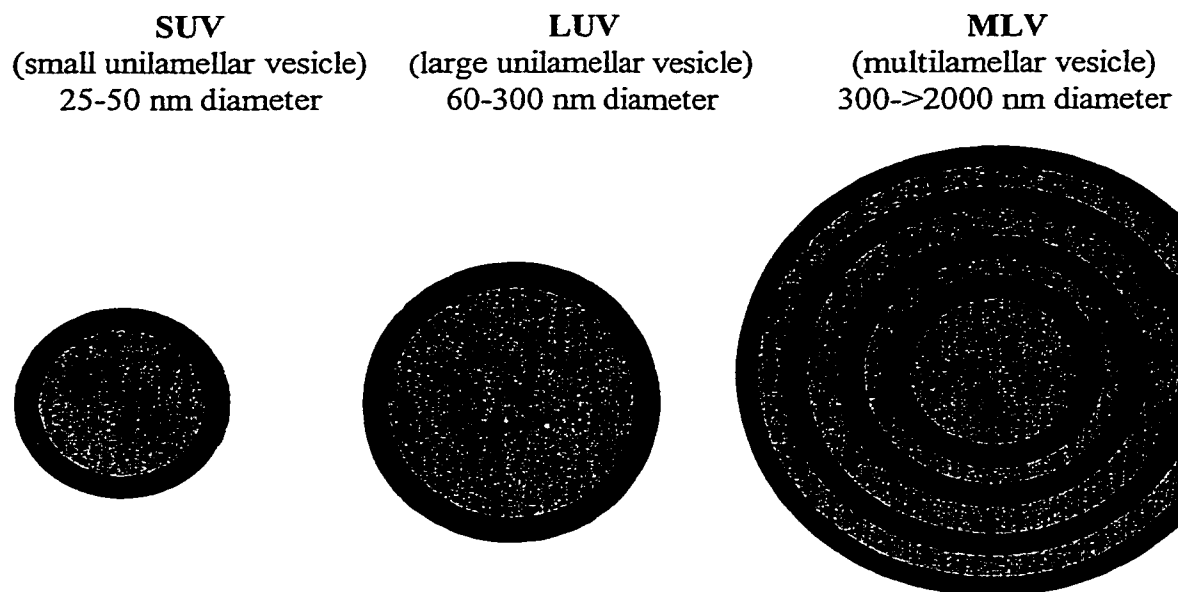


Fig. 1.3 Liposome classification.
Liposomes are classified according to their size and bilayer lamellarity into small unilamellar, large unilamellar, or multilamellar vesicles.

1.3 Liposomes as Drug Carriers

Since their introduction as drug carriers in the 1970's (7, 8), liposomes have been found to have many potential applications as drug carriers. Some advantages of liposomes include low toxicity (due to their similarity to biological membranes) and the ability to manipulate the fate of the liposomes *in vivo* by manipulating their composition. In addition, they can be used to deliver hydrophobic drugs without the need for solvents, and are effective sustained release systems (reviewed in (9, 10)). The latter is an important attribute because increasing the $AUC_{t=0-\infty}$ is known to influence the therapeutic effect of many drugs. Liposomes also alter the pharmacokinetics of the drugs, and provided that the drugs are released slowly, they adopt the pharmacokinetics of the carrier. The possible benefits include an increased half-life for rapidly degraded drugs, and increased therapeutic indices. The latter is particularly advantageous for drugs that are considered too toxic to be administered in the free (i.e. non-encapsulated) form. Anti-cancer drugs are well known for their dose-limiting toxicities; therefore the development of liposomal drugs has primarily, but not exclusively focused on anti-cancer formulations. A reduction in toxicity to non-target tissues has been demonstrated for several liposomal drugs including the anthracyclines, daunorubicin (11-13) and doxorubicin (14-21) and a highly toxic anti-fungal agent, amphotericin B (22). These were among the first liposomal formulations approved for clinical use.

1.4 Liposomal Anti-cancer Drugs

Historically, chemotherapy has been associated with severe side effects because there are very few properties that differentiate malignant cells from normal cells. Due to their mechanism of action, most anti-cancer drugs are marginally selective for malignant

cells because they target rapidly dividing cells. Unfortunately, this means that rapidly dividing non-malignant cells will also be affected, including hematopoietic, gastrointestinal, and germ cells, and hair follicles. For this reason the common side effects of chemotherapy include myelosuppression, mucositis, stomatitis, nausea, alopecia, and reproductive effects. In general, the side effects of anti-cancer drugs are severe, compared to other drugs, and are tolerated in the medical community only because there is no other effective alternative. The modulation of anti-cancer drug pharmacokinetics by encapsulating them in liposomes can be an effective method of increasing the therapeutic index of these drugs. For instance many liposomal anti-cancer drugs have a lower volume of distribution compared to the free drug, which invariably decreases the toxicity to some tissues.

The side effects that are associated with chemotherapy limit the doses that can be administered. This is unfortunate since the therapeutic efficacy of most chemotherapy regimens increases with dose. For this reason, research in the field of anti-cancer therapy has focused on improving the tumor selectivity of chemotherapy in hopes of improving the quality of life for the patients and increasing the likelihood of remission. An effective approach for increasing the therapeutic indices, or the ratio of the effective dose to the toxic dose, of anti-cancer drugs is to alter their pharmacokinetics by delivering them in association with drug carriers, such as liposomes (reviewed in (9)). In fact, research in the field of liposome technology has been traditionally dominated by the development of liposomal anti-cancer drugs, due to their dose limiting toxicities, and several anti-cancer drugs are now available in liposomal formulations.

1.5 Loading Drugs into the Liposome Interior

Drugs can be loaded into liposomes by either active or passive entrapment. The latter occurs at the time of hydration and vesicle formation, and is the simplest method (23). Alternatively, drugs can be taken up actively after vesicle formation by remote loading. In these methods a transmembrane gradient is set up, usually of voltage or pH, which drives the uptake of the drug (23-28). These methods rely on the fact that drugs can permeate membrane bilayers as neutral, but not charged, species. Therefore, the permeability of the drug can be manipulated by the transmembrane gradient, so that the drug can enter but not exit the liposome. The appropriate loading technique depends on the physiochemical properties of the chosen drug. The oil:water and octanol:water partition coefficient (pK) is particularly important and is defined as the log of the ratio of the drug concentration in the two phases. Hydrophobic drugs with high oil:water and octanol:water partition coefficients can be passively loaded within the membrane bilayer. Due to the low volume of this space, the loading can be poor.

Many anti-cancer drugs are amphipathic (low oil:water and variable octanol:water pK) weak bases (cationic). These drugs can be easily remote loaded since their hydrophobic properties make them membrane permeable at neutral pH and their positive charge at low pH keeps them trapped within the liposome aqueous interior, often in association with a counter ion like citrate or sulfate, which lowers their aqueous solubility. Remote loading offers two main advantages. First, the encapsulation efficiencies are generally 98-100%, compared to approximately 30% for passively entrapped drugs. Second, remote-loaded drugs are retained more effectively in the liposomes. This is especially important for drugs with lipophilic character as they can

easily cross membrane bilayers resulting in drug loss. In general the efflux of drug from the liposome interior is slow following remote loading. In one study it was shown that the time to release of 50% ($T_{1/2}$) of encapsulated doxorubicin (DXR) at 37°C could be extended from approximately 1 h to 24 h by changing the loading method from passive entrapment to the pH gradient method (25). It is thought that the transmembrane gradient that is set up at the time of loading makes subsequent efflux of the drug unfavorable due to the acquisition of charge by the drug, or its precipitation in the liposome interior. Doxorubicin is also commonly loaded into liposomes by the ammonium sulfate gradient method (28) and is the method employed in this thesis. A schematic of the loading procedure is shown in **Fig. 1.4**.

1.6 Evolution of Long-circulating Liposomes

Liposomal drug carriers have evolved substantially since their beginning. The first liposomal drug carriers, now known as classical liposomes (CL) (**Fig. 1.5**), have a 'naked' phospholipid bilayer, which attracts the binding of a variety of opsonins/plasma proteins to the liposome surface. This, in turn, results in the rapid clearance of liposomes from circulation by the mononuclear phagocyte system (MPS), sometimes referred to as the reticuloendothelial system (RES). The MPS is comprised mainly of fixed macrophages in the spleen and bone marrow, and Kupffer cells in the liver. These cells have cell surface receptors for opsonins, therefore these proteins promote clearance of liposomes by the MPS. The opsonins promote clearance of liposomes by these cells because they are recognized by receptors on the surface of MPS cells (reviewed in (30) and (31)). The targeted delivery of liposomal drugs to the MPS has led to improved

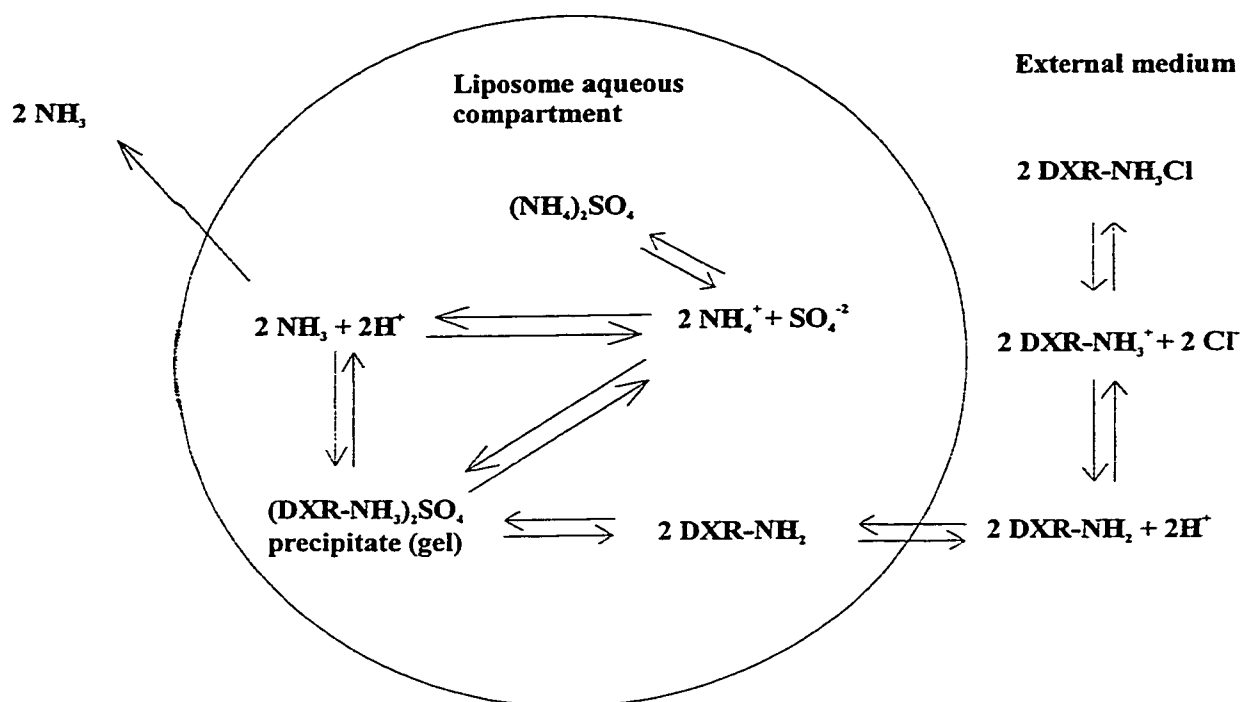


Fig. 1.4 Remote loading of doxorubicin by the ammonium sulfate gradient method. At the liposome exterior an equilibrium exists between the protonated, charged form (NH_3^+) and the neutral form (NH_2) of doxorubicin hydrochloride (DXR-HCl). The neutral form is able to cross into the liposome interior. As this occurs, DXR is protonated and reacts with the sulfate anion to form a precipitate. This drives the further dissociation of ammonium sulfate into its ionic forms by Le Chatelier's principle. NH_4^+ also dissociates into ammonia and hydrogen ions. The efflux of ammonia in exchange for hydrogen ions drives the whole process by creating a transmembrane pH gradient (low internal pH and higher external pH). This facilitates the uptake and trapping of DXR by keeping DXR in its neutral form on the liposome exterior and promoting its precipitation in the liposome interior. Encapsulation efficiencies of 90-100% can be achieved using this method. (Adapted from (29))

therapy of diseases of this system, such as leishmania (32), and delivery of immunomodulators such as muramyl-tripeptide can result in stimulation of macrophages improving immune therapy (33). The latter has been investigated as possible adjuvant therapy for the eradication of metastases. However, most therapeutic applications of liposomes require long circulation times for effective drug exposure at the target cancer cells, which in turn increases the likelihood of a positive clinical outcome (34).

Several strategies have been investigated in attempts to reduce the clearance of liposomes by the MPS, albeit with limited success at first. The stability of the liposomes could be improved by modifying the phospholipid composition to include neutrally charged, high T_M phospholipids, and a high level of cholesterol. The addition of lipids with T_M that exceeded 37°C was intended to decrease the fluidity of the liposome membranes *in vivo*. Cholesterol was included because it promotes the orderly packing of membrane bilayer lipids. Both of these strategies were shown to decrease the ability of opsonins to adsorb to the liposome membrane (35). Since opsonin adsorption has been shown to accelerate liposome clearance (31), these formulations were expected to have longer circulation times. In addition, reducing the vesicle size to between 30 and 60 nm and increasing the phospholipid dose had beneficial effects on clearance rates (36). The reason for the inverse relationship between size and circulation time is likely due to a decrease in the potential for multivalent binding of opsonins to small liposomes exhibiting a high degree of curvature. In the absence of multivalent binding, opsonins interact weakly with liposome bilayers. (37). Increasing the dose, or pre-dosing with empty, or drug-loaded, liposomes is aimed at saturating the uptake processes in the MPS and is referred to as MPS/RES blockade (38, 39). Classical liposomes are often

described as having dose-dependent pharmacokinetics because their MPS uptake is saturable (40). While sufficiently long circulation times were achievable with these formulations, the small vesicle size decreased the stability of the liposomes and limited the amount of drug that could be loaded into the liposomes. For this reason alternatives were sought.

One major difference between liposome membranes and biological membranes is that the former lack surface carbohydrates. Negatively charged sialic acid residues seem to be particularly important in preventing clearance of circulating cells, such as red blood cells, by the MPS. The first successful strategy to reduce liposome uptake by the MPS came out of an attempt to formulate liposomes that resemble biological membranes. The inclusion of optimal concentrations of monosialylganglioside (G_{M1}) in liposomes was shown to substantially decrease their uptake by liver and spleen and increase the amount of liposomes remaining in circulation (41). However, G_{M1} is purified from natural sources and was not considered practical for regular use. This led to the search for alternative molecules that would allow liposomes to evade uptake by the MPS. The inclusion of polyethylene glycol (PEG) in liposomes has since been shown to be even more effective at reducing their uptake by the MPS (34, 42-44) and its use has become common place. These liposomes are termed sterically stabilized liposomes (SL). The addition of PEG is able to extend the half-life of liposomes from less than 10 min (CL) to approximately 12-15h (SL)(40). In addition, the ability of PEG to increase circulation times is independent of liposome PL composition and dose (34, 40, 45). This is an important advantage because flexibility in liposome formulation allows the optimization of their properties for different therapeutic applications. The optimal amount of PEG falls

between 5 and 10 mol% of liposome PL, as this level of incorporation is sufficient to increase circulation times (44) without changing the physical properties of the bilayer (46). This level of PEG also minimizes the extent of drug leakage (43). These liposome formulations that contain PEG, or other molecules/polymers that increase the life time of liposomes in circulation (47, 48) are now referred to as sterically stabilized or 'Stealth[®]' (SL) formulations. Their introduction has been one of the most important advances in liposome technology. The structure of sterically stabilized and classical liposomes is shown in Fig. 1.5.

Several researchers have investigated the mechanism behind the protective effect of PEG. As the name implies, the addition of PEG to sterically stabilized liposomes is thought to sterically hinder the adsorption of plasma proteins/opsonins, which initiate liposome clearance by the MPS (46, 49). An important stabilizing attribute of PEG is its hydrophilicity, which allows PEG to exist in an extended conformation in aqueous environments. This confers mobility to the PEG layer, which is thought to create a barrier to the approach of opsonins or cells towards the liposome bilayer. (37, 50, 51) The effectiveness of the barrier is related to the density and extension length of the polymer and is optimal for PEG densities between 5-10 mol% and molecular weights between 1000-5000 (44, 45, 52). This is due to the amount of coverage the PEG polymer affords.

1.7 Improving the Tumor Specificity of Liposomes: Passive Targeting

An advantage of increased circulation times in plasma is the opportunity for selective localization of liposomal drugs to solid tumors (53-56). This process is known as 'passive targeting' (Fig. 1.6) and it is attainable due to permeability differences in normal

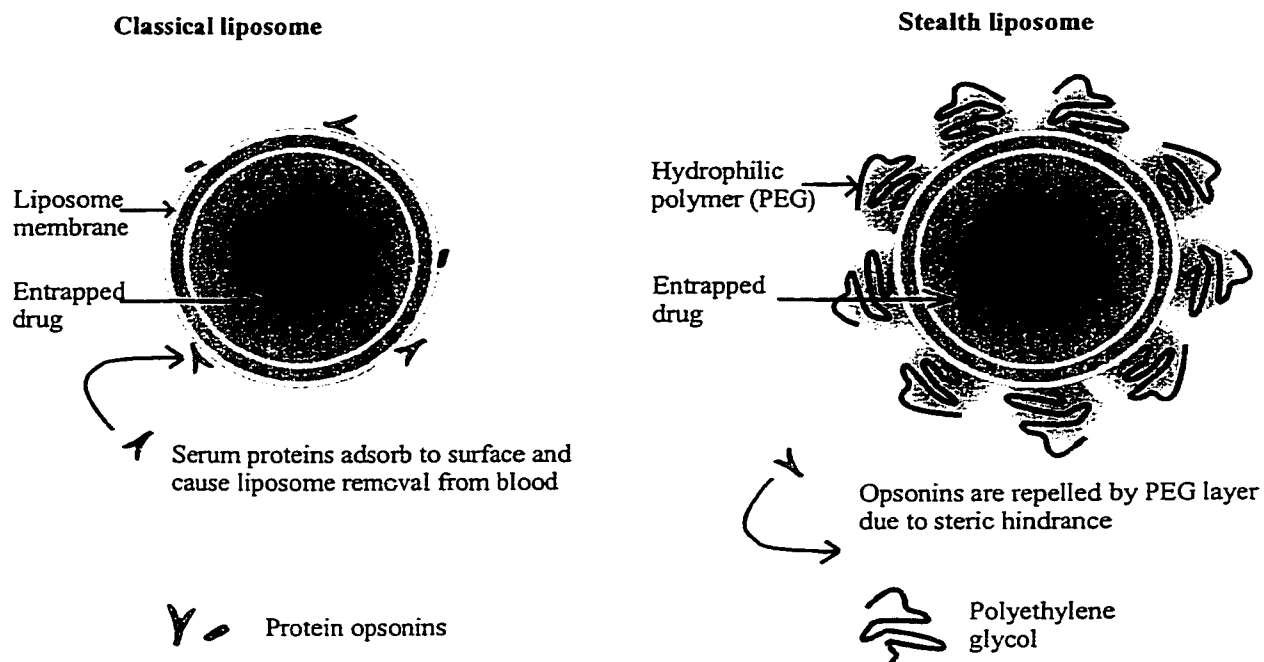


Fig. 1.5 Classical and sterically stabilized (Stealth[®]) liposomes. Classical liposomes have a naked phospholipid bilayer that tends to attract the binding of serum proteins or opsonins to the liposome surface. This accelerates the rate of liposome clearance by the MPS. Sterically stabilized formulations are resistant to opsonization because they are coated with the hydrophilic polymer, PEG that sterically hinders the approach of opsonins to the bilayer. As a result sterically stabilized liposomes are cleared less rapidly from circulation. (From T.M. Allen)

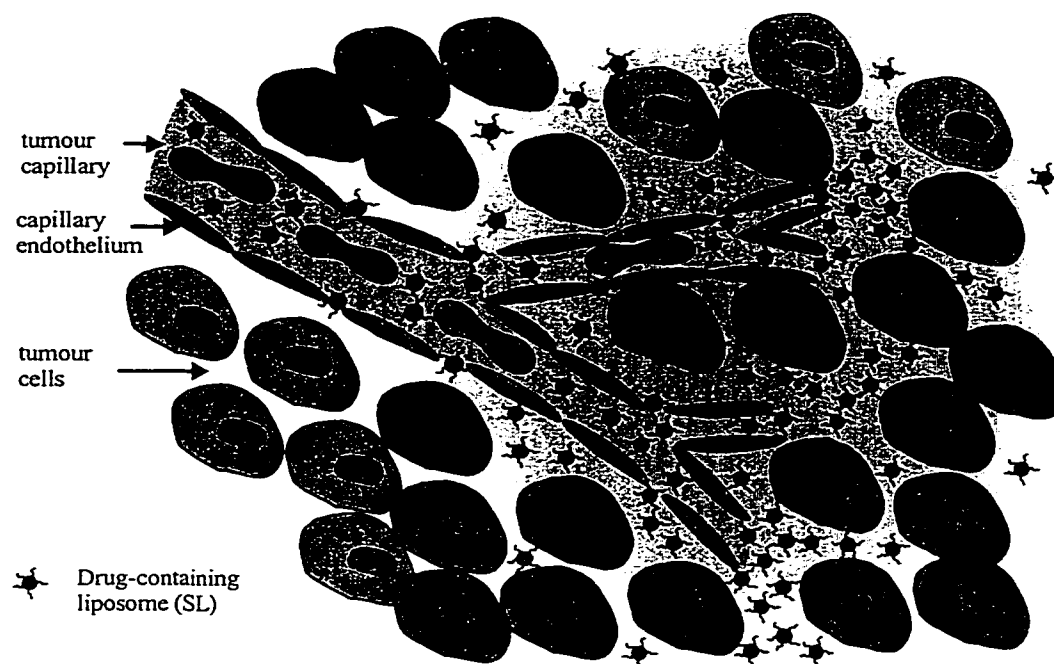


Fig. 1.6 Passive targeting of sterically stabilized liposomes to a solid tumor. Normal vasculature is impermeable to liposomes. However, in areas of angiogenesis, such as occurs in solid tumors, capillaries become permeable to liposomes due to the creation of gaps between endothelial cells that can be up to 800 nm in diameter. The extended circulation times exhibited by sterically stabilized liposomes allows their selective extravasation into tumor tissue by this mechanism (from T.M. Allen).

vs. tumor vascular endothelium. In most tissues the vascular endothelial cells that line capillaries form tight junctions; therefore they are relatively impermeable. Sinusoids in the liver, spleen, and bone marrow contain 100 nm clefts that will allow the passage of some small molecules (57). However, in diseased tissue the permeability of the vascular endothelium increases through the action of inflammatory mediators. In this case, gaps between endothelial cells occur that are sufficiently large in diameter to allow liposomes to extravasate into the tumor interstitium (58). In areas of angiogenesis, such as occurs in solid tumors, the blood vessels are even more 'leaky' as they tend to have discontinuous endothelial layers and basement membranes (59). In these areas the endothelial fenestrations can reach up to 800 nm in diameter (60), which is more than sufficient for 100 nm liposomes to pass through. It may also be possible to pharmacologically manipulate the permeability of the vascular endothelium in order to target the extravasation of liposomes. In this regard it has been shown that substance P is able to selectively increase the endothelial permeability and extent of liposome extravasation in the trachea, esophagus, and urinary bladder (61). On the downside, the blood supply to solid tumors tends to be heterogenous and mainly confined to the periphery. In addition, the interstitial pressure in the center of solid tumors is high; therefore the diffusion potential of particles, such as liposomes, is quite low (61-63). In result, it is unlikely that central or poorly perfused regions will be exposed to cytotoxic levels of drug. Overall, the potential of passive tumor targeting remains suboptimal for the aforementioned reasons.

Some creative approaches to further improve the selectivity of liposomal drugs involve their triggered release from the carrier. First, pH sensitive liposome formulations

have shown some potential in anti-cancer therapy. These formulations include phospholipids that confer instability to the liposomes at certain pH's causing them to fuse with biological membranes or other liposomes (64). Changes in pH in tumor interstitium can then be exploited to promote the intratumoral release of anti-cancer drugs.

Alternatively, liposome formulations exist which can be directed to release their contents in response to localized hyperthermia (65, 66).

1.8 Ligand Mediated Targeting

The search for the 'magic bullet' in anti-cancer therapy, as proposed by Ehrlich in the early 1900's, continues (67). This is a hypothetical agent that has selective toxicity towards a target population of malignant cells, but not 'normal' cells. Unfortunately, there are a limited number of features that distinguish malignant from non-malignant cells and that can be exploited to increase the selectivity of chemotherapy. However, the differential over-expression of cell surface antigens and/or receptors opens up the possibility for antibody-directed therapy. Since the advent, by Kohler and Milstein, of methods to produce large-scale quantities of monoclonal antibodies (mAb's) (68), there has been an increasing trend towards the use of antibodies to target therapeutic agents. Included in the growing list of agents that have been conjugated to mAb are toxins and liposomes. The latter is relevant to this thesis and warrants further discussion.

Antibodies were the first ligands that were coupled to liposomes and the resulting formulations were named immunoliposomes. More recently other ligands, such as peptides that can bind to tumor specific antigens have also been used (69). Collectively, liposomes that have had a ligand coupled to their surface are referred to as 'ligand-targeted liposomes', or abbreviated to 'targeted-liposomes'. The development of these

formulations has focussed on the achievement of certain characteristics that constitute the 'ideal targeted-liposome'.

The first requirement is a rapid and simple method to couple ligands to the liposome surface. In this regard it is important to consider the labile nature of some ligands, particularly antibodies, and potentially some liposome components. This means that they will not endure lengthy, multi-step protocols.

Secondly, the chosen coupling method needs to be efficient to minimize wastage of ligand and coupling lipid. In many cases the ligand is either expensive, or difficult to prepare (in the case of mAb), or both. In addition, because the coupling lipid introduces functional groups (*vide infra*) that may be reactive *in vivo* if left exposed (i.e. not conjugated to antibody), the minimum amount should be incorporated into the liposomes to avoid possible toxicities and potential for opsonization.

Third, the antibody density should be optimized to achieve specific targeting and reasonable circulation times. In this regard, the pharmacokinetics of immunoliposomes have been well studied. Not surprisingly, the attachment of antibodies to liposomes accelerates the rate of liposome clearance from circulation. It is likely that the IgG acts as an opsonin, similar to its normal immunological function. Fortunately, the antibody density can be decreased to a level where reasonable circulation times and effective targeting can be mutually achieved. For whole antibodies (MW=150 000 Da) the optimal density is generally between 30-60 $\mu\text{g}/\mu\text{mol}$ liposome PL. However, the optimal ligand density will be affected by several ligand-dependent factors including its targeting effectiveness, and immunogenicity.

Fourth, the ligand must retain the ability to bind to its target. An important consideration here is the preservation of the ligand structure. Also, the ligand must be accessible for target recognition.

Fifth, the coupling method and the attachment of the chosen ligand should not affect the drug loading and retention characteristics of the resulting liposomes in a negative way.

1.9 Coupling Techniques

There are several techniques available to couple ligands to liposomes (reviewed in (70, 71)). The attachment can be either non-covalent or covalent, although the latter is more common. In general the ligands are coupled to the head group of a long-chain, hydrophobic phospholipid anchor, commonly phosphatidylethanolamine (PE). These properties of the phospholipid are required for its retention in the bilayer with its ligand attached. The attachment of the ligand occurs by the formation of bonds between reactive functional groups on the phospholipid head group and the ligand. A variety of derivatized phospholipids have been synthesized, which have specific functional groups chemically conjugated to the head group. These phospholipids are incorporated into the liposomes, at specified molar ratios, before hydration and extrusion. The functional groups are then made reactive in an activation step. At this time the ligand is also activated for coupling by the introduction of a reactive group, and is incubated with the liposomes to allow for coupling. In the case of antibodies, free amine groups on exposed lysine residues are regularly exploited for activation.

While ligands can be easily coupled directly to the bilayer surface of classical liposomes, the addition of a PEG layer in sterically stabilized liposomes limits the

accessibility of ligands. This can dramatically reduce the coupling efficiency (72-74). In addition, steric interference from the PEG can substantially reduce the access of the ligand to the target and prevent binding (74, 75). The extent of the inhibition is directly related to the extension length of the PEG polymer. Reducing the length of the PEG polymer or PEG content was shown to increase ligand accessibility somewhat, as evidenced by both *in vitro* and *in vivo* binding (74, 76, 77). ELISA using secondary antibody against the ligand has also been employed to study its accessibility, with similar results (70). The extent of improvement in target binding was dependent on the length of the PEG spacer, and remained less than ideal. One study also indicates that the binding potential may be influenced by the ligand itself, by its relative potential to interact with PEG (76).

Alternative coupling strategies were sought. Coupling to the PEG terminus has proven to be an effective strategy to increase ligand accessibility (72, 76, 78). A schematic of the three possible coupling strategies is shown in **Fig. 1.7**. Since classical liposomes have largely been superseded by sterically stabilized liposomes, many of the coupling techniques that were developed for classical liposomes have become obsolete. In fact, the PEG terminal coupling procedures have largely replaced the others; therefore the following discussion will primarily focus on this approach.

Several end-functionalized derivatives of PEG have been synthesized for coupling antibodies to the PEG terminus (reviewed in (79)). Three of the commonly used PEG derivatives include pyridyldithiopropionylamino (PDP)-PEG (80), hydrazide (Hz)-PEG (81), and maleimide (Mal)-PEG (82). A description of each of these coupling reactions is shown in **Fig. 1.8**. The PDP-PEG method was originally developed for CL but has been

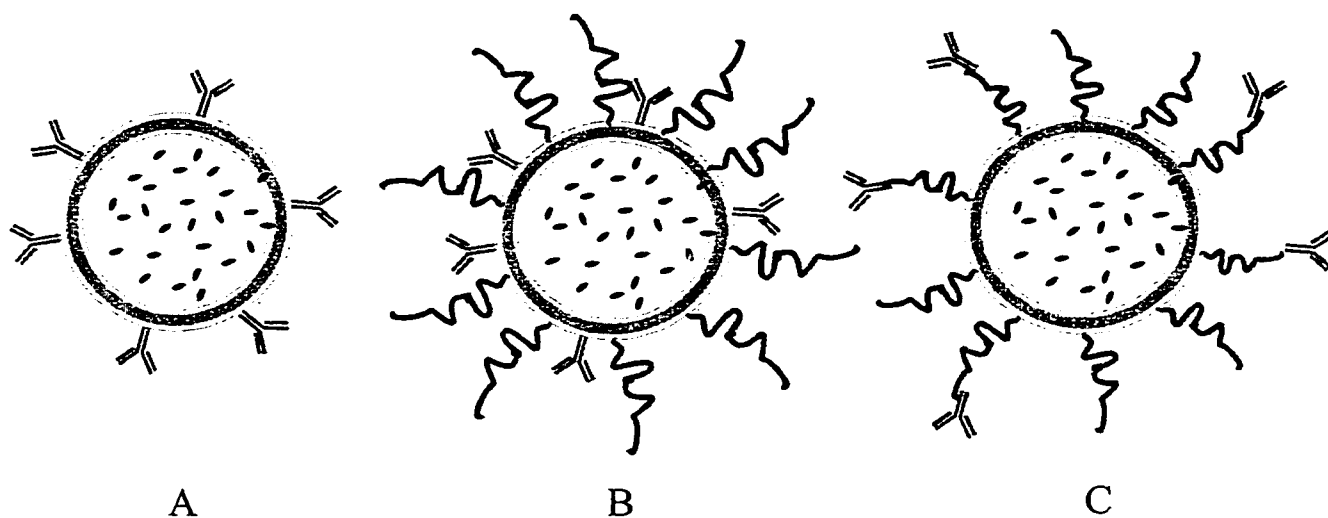


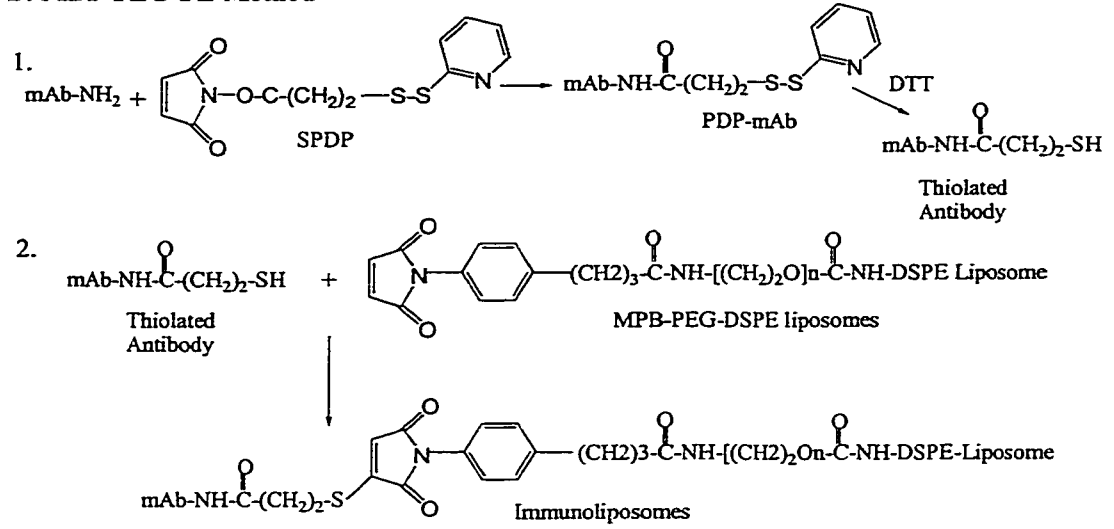
Fig. 1.7 Coupling strategies.

Antibodies or other ligands can be covalently attached to liposomes directly to the liposome surface (A and B) or to the PEG terminus (C). The accessibility of ligands is greater for non-peglyated liposomes (A) or when ligands are coupled to the PEG terminus (C).

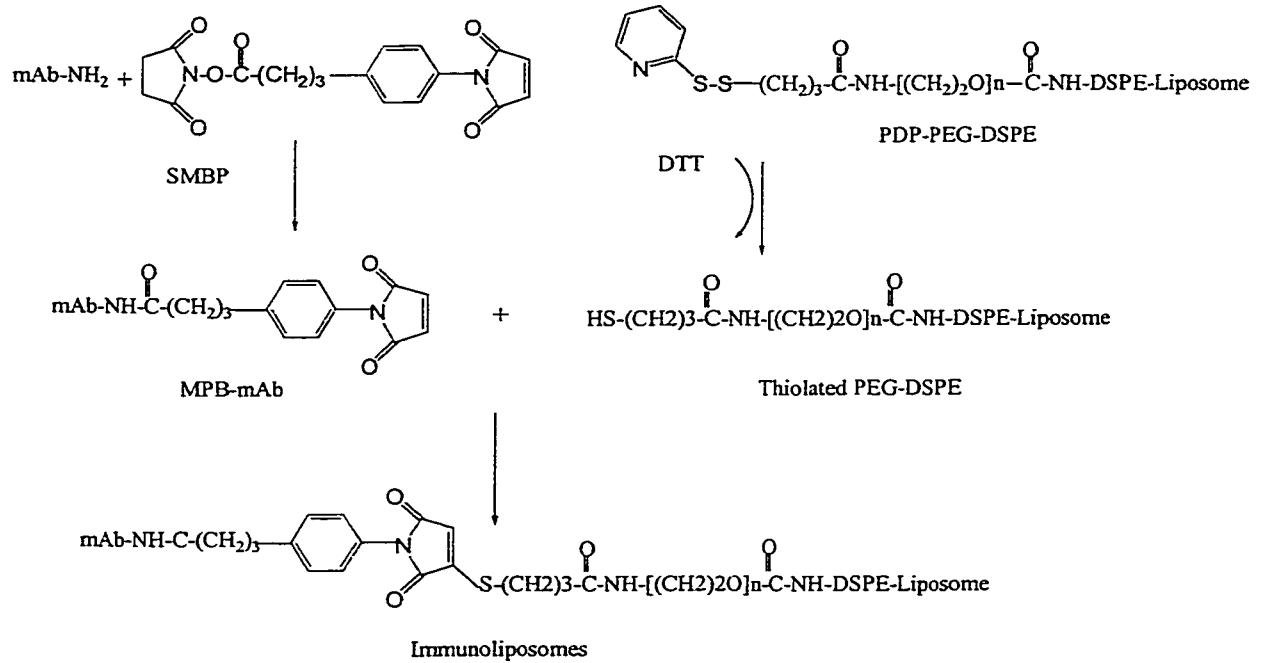
A. Biotin-Avidin Method



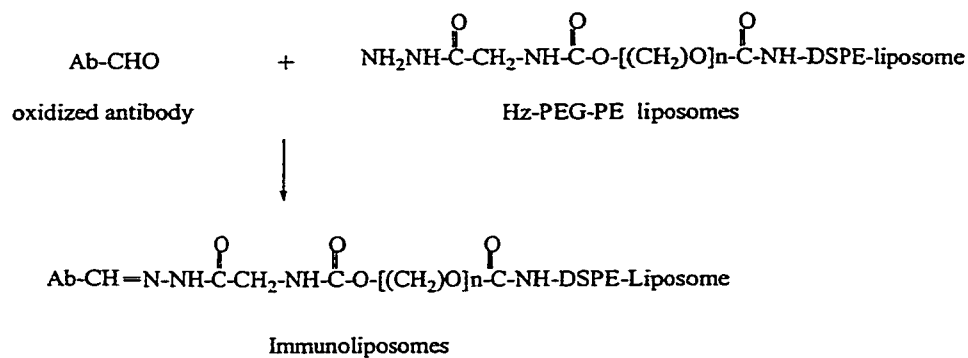
B. MBP-PEG-PE Method



C. PDP-PEG-PE Method



D. HZ-PEG-PE Method



E. Mal-PEG-PE Method

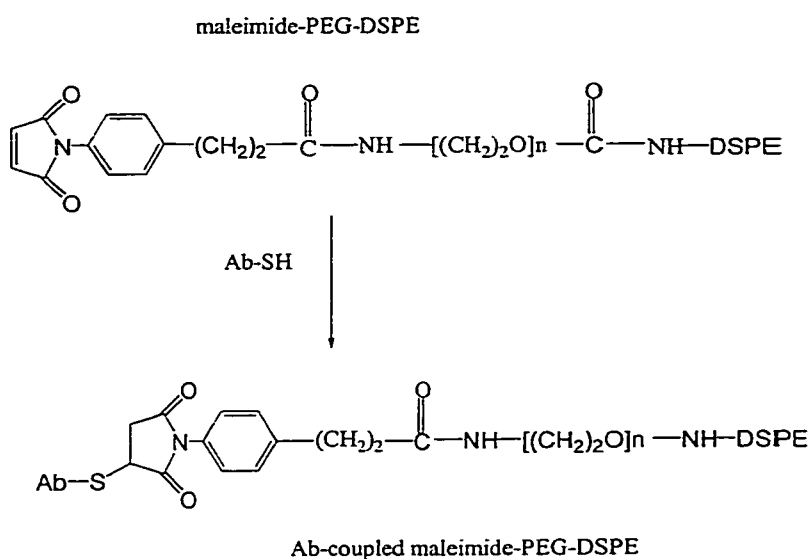


Fig. 1.8 Techniques for coupling antibodies to liposomes.

The abbreviations are as follows: DSPE, distearoyl phosphatidylethanolamine; DTT, dithiothreitol; MBP, *N*-maleimidophenylbutyrate; PDP, *N*-pyridyldithiopropionate; SMBP, succinimidyl-4-(*p*-maleimidophenyl)butyrate; SPDP, *N*-succinimidyl-3-(2-pyridyldithio)propionate. (adapted from (73))

adapted for SL. Both the PDP-PEG and the Mal-PEG coupling techniques both rely on the formation of thioether bonds. This reaction has the advantage of being efficient and the bond is stable. The PDP-PEG method is the most complex of the three, as it involves multiple activation steps. The antibody is activated by the reagent succinimidyl-4-(*p*-maleimidophenyl)butyrate (SMBP) and the PDP-PEG is thiolated with dithiothreitol (DTT). The Mal-PEG method is much simpler, as it only requires thiolation of the antibody with 2-iminothiolane/Traut's reagent. One disadvantage of the Mal-PEG method is the fact that free thiol groups may react with oxygen to produce di-sulfide bonds. Since there are several potential thiolation sites on each antibody (amine groups) it is possible that antibodies will cross-link with each other in the presence of oxygen. However, the use of oxygen-free buffers during liposome preparation minimizes cross-linking.

PDP-PEG and Mal-PEG can also be used to couple antibody fragments to liposomes. The general structure of antibodies is illustrated in **Fig. 1.9**. The cleavage of the interchain disulfide bond of the F(ab')₂ fragment results in the production of two Fab' fragments, each having a single exposed thiol group ready for coupling (84). This eliminates the need for activation of the antibody.

Finally, in the hydrazide method, carbohydrates in the Fc region are oxidized with periodate to form reactive aldehydes, which form a bond with the hydrazide groups on the liposome. This method is less efficient, but has the advantage that coupling is site-directed to the Fc region. This is advantageous because the antibodies are consistently oriented with the antigen binding regions exposed to the target. The coupling of antibody fragments also results in coupling in a predictable orientation that leaves the binding site

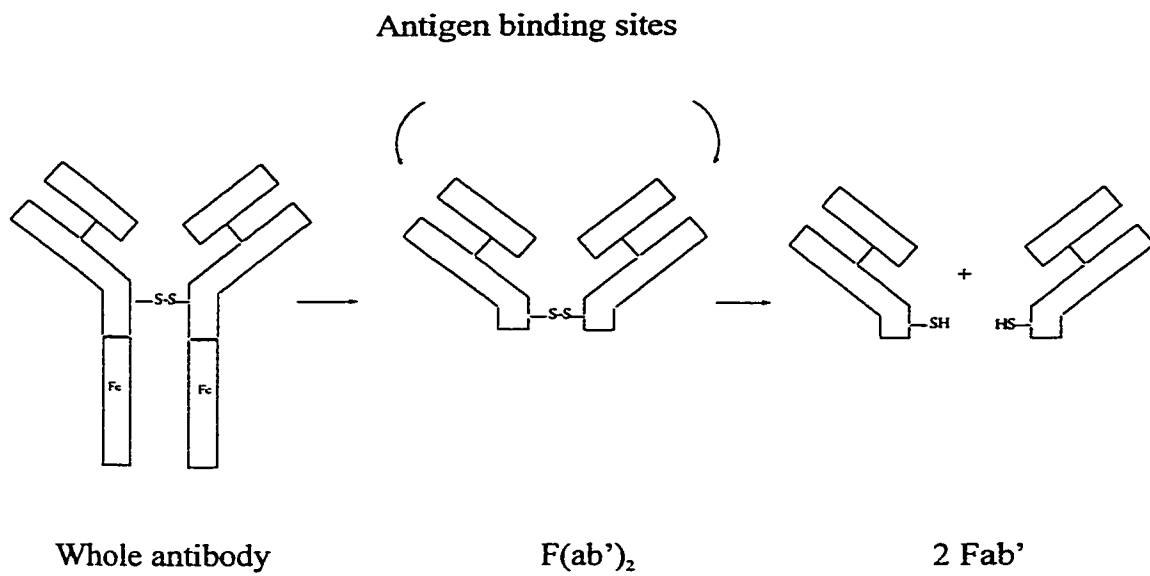


Fig. 1.9 General antibody structure.

The enzymatic cleavage of antibodies removing the Fc portion yields one F(ab')₂ fragment which can be further reduced to two Fab' fragments. The latter can be coupled to liposomes and micelles without the need for chemical activation.
(Adapted from (83))

accessible to its target. This contrasts with the application of the Mal-PEG and PDP-PEG methods for coupling of whole antibody. In both cases multiple coupling sites are created, through the activation of amines, allowing the antibodies to couple in any orientation. In addition, coupling can occur to amines within the antigen-binding region, which may interfere with target binding. The coupling efficiencies, antibody densities, and drug-loading potentials associated with each method are compared in **Table 1.2**. In this thesis the Mal-PEG coupling method has been employed.

1.10 Demonstrated Potential of Ligand-Targeted Liposomes

The utility of therapeutic formulations of ligand-targeted liposomes in animal models of cancer has been widely studied and several models have shown clinical potential. The cell surface antigens that have been targeted are commonly over-expressed on tumor cells. Not surprisingly, these antigens generally facilitate cell growth and proliferation by cell signaling or through the provision of nutrients or co-factors. Some examples include, the folate receptor (74, 85, 86), the transferrin receptor (87), and the receptor tyrosine kinase HER2/Neu/erbB-2 (88-90). In addition, several antigens on hematological cells have been targeted including CD19 (91), the B-cell idiotype (92), and Thy 1.1 (T-cell differentiation antigen) (93). These antigens are generally involved in signaling of lymphocyte differentiation and proliferation. Tumor cells also commonly express aberrant carbohydrates or antigens that have been targeted. For instance MUC₁ (a breast cancer associated mucin involved in cell adhesion (94, 95), the disialoganglioside, GD₂, on melanoma cells (96, 97), and tumor specific antigens on ovarian cancer cells (98) have been targeted. These studies have demonstrated a binding and cytotoxicity advantage for ligand-targeted liposomes to their target cells, compared to

Table 1.2 Comparison of various coupling methods for the preparation of sterically stabilized immunoliposomes.

Coupling Method	mAb Density ($\mu\text{g}/\mu\text{mol PL}$)	Coupling Efficiency (% of initial mAb)	% Drug Loading
Biotin-avidin	8-20	10	95-100
MPB-PE	50-200	50-100	30-50
Hz-PEG-PE	20-40	10-25	95-100
PDP-PEG-PE	50-200	50-85	95-100
PDP-PE	15-30	10	80-95
Mal-PEG-PE	50-200	50-100	95-100

The data presented in this table are for liposomes composed of HSPC:CHOL:mPEG₂₀₀₀-DSPE (2:1:0.1, mol:mol) loaded with doxorubicin by the ammonium sulfate gradient method. (modified from (71))

non-targeted liposomes, *in vitro*, and in some cases *in vivo* as well.

1.11 Choice of Target Antigen

The choice of target antigen is important, not only to minimize cross reactivity with non-malignant cells, but also to maximize the therapeutic effect of the targeted therapy. There are two superior classes of target antigens, the first of which includes receptors that activate cell-signaling pathways. Ligand binding to these receptors has intrinsic antiproliferative effects via the blockade of signaling pathways involved in cell growth and proliferation or the initiation of apoptosis. For this reason, targeting to these receptors results in anti-tumor effects by two separate mechanisms; first by interfering with cell signaling, and second by tumor specific delivery of therapeutic agents. Some examples of the signaling effects are induction of cell cycle arrest (99), blockade of P-glycoprotein (*vide infra*) (100), and inhibition of DNA repair (101, 102). Each of these effects has been shown to involve cytoplasmic second messenger systems that are activated following binding of an antibody to a specific receptor. These mechanisms have the potential to sensitize cancer cells to chemotherapeutic agents and induce synergistic effects on cytotoxicity.

The second important class of antigens includes internalizing receptors. The advantage of these receptors is the intracellular delivery of the entire contents of the liposome. In the case of a non-internalizing receptor the cell will be exposed to much less drug. This is because the drug is released relatively slowly, and in random directions, from the liposome. Only a small proportion of this drug will reach the target cell and cross the membrane into the intracellular site of action, and importantly a proportion of the drug will affect non-target cells. Indeed, the extent of endocytosis of

therapeutic agents has been shown in some cases to correlate with cytotoxicity (87, 103, 104). Some researchers have used an elegant method to evaluate the dependence of cytotoxicity on internalization of liposomal drugs. In these studies analogues of drugs, such as methotrexate- γ -aspartate, that are relatively impermeant to cells and are dependent on liposome uptake have been employed (87, 104).

Evidence that targeted liposomes are internalized has been shown by confocal and electron microscopy of liposomes loaded with the fluorophore 1-hydroxypyrene-3,6,8-trisulfonic acid (HPTS) and colloidal gold, respectively. In both cases targeted liposomes have been shown to initially localize at or near the cell surface, then in the cytoplasm and the nucleus. Conversely, non-targeted liposomes show no intracellular localization. Uptake occurs by the coated pit pathway into endosomes and lysosomes, which is the same pathway by which free ligands are internalized. The route of internalization was determined by the intracellular disposition of gold-laden liposomes as seen using electron microscopy. The localization of the liposomes in the endosomal, low pH, compartment was further corroborated using pH-sensitive fluorophores. The kinetics of receptor uptake and recycling are rapid. For at least some receptors, uptake occurs within min of ligand binding and receptors are released from the ligand and recycled to the membrane several times in 1 hour (105).

Important changes in the intracellular trafficking of anti-cancer drugs occur when they are delivered in targeted liposomes that may have therapeutic implications. The delivery of drugs by receptor-mediated endocytosis provides an alternate route of entry to diffusion across the membrane (**Fig. 1.10**). This may allow targeted liposomes to

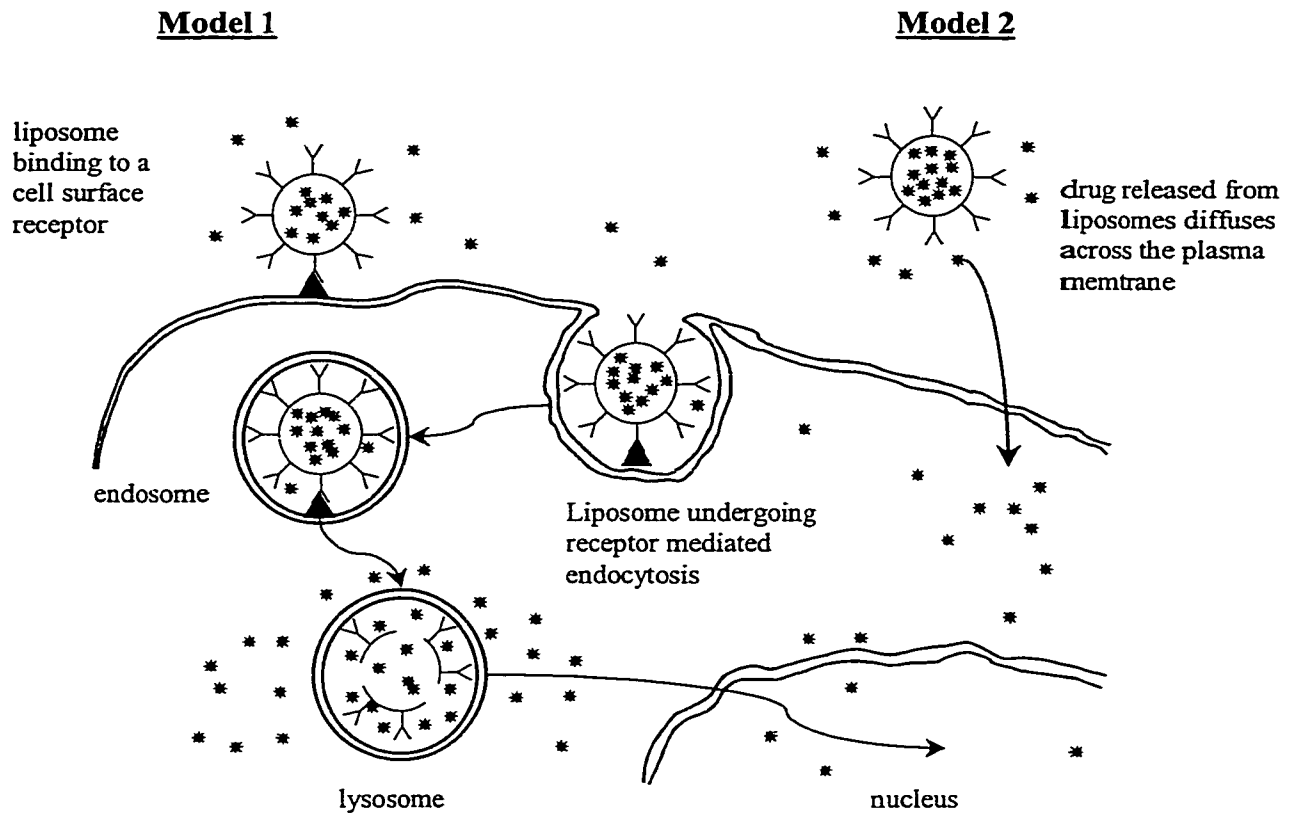


Fig. 1.10 Routes of intracellular delivery of liposomal drugs. Drugs can enter the cell by diffusion, following their release from liposome. Alternatively, entire liposomes can be taken up by receptor-mediated endocytosis. In this case the drug can be released from the liposomes following their destabilization in lysosomes.

overcome multi-drug resistance (MDR), which is the well-defined simultaneous resistance to numerous structurally and functionally unrelated drugs. One of the mediators of MDR is P-glycoprotein (Pgp). It is located in the plasma membrane, nuclear membrane, cytoplasm, (106) and golgi apparatus; where it acts as an ATP-dependent efflux pump that has been shown to expel anti-cancer drugs from cancer cells (107). However, targeted liposomes are capable of transporting large amounts of drug into Pgp drug-resistant cells and this drug is retained much more effectively than free drug. In one study the retention of DXR that had been endocytosed in folate-targeted liposomes was not enhanced by blocking Pgp with verapamil, while 4 times more free doxorubicin was retained in the presence of verapamil (85). This indicates that the drug may have bypassed the membrane pump. In addition, much higher drug levels in the cellular nuclear fraction were achieved with the targeted formulation, compared to free DXR, despite the likely presence of nuclear Pgp. The authors propose that the drug molecules are self-associated and at high concentrations the lag time for their dissolution is lengthy. This stacking of the drug molecules was thought to inhibit the ability of Pgp to pump it out. Interestingly, the cytotoxicity was not enhanced in comparison with free drug and it was suggested that the association of the drug molecules also limits the activity of the drug. Alternatively, it is possible that the drug has not been released from the liposome. The rate of release of drugs from liposomes in the endosomal/lysosomal apparatus is a subject of current research. This is the second main therapeutic implication of receptor-mediated endocytosis of liposomes. While the internalization of liposomes increases the amount of drug delivered to the target cell, it is not necessarily bioavailable. Investigators have recently explored methods of promoting drug release from the

liposomes. Triggered release formulations have been developed that cause liposome destabilization in the endosomal compartment. The phospholipids utilized in these formulations, such as phosphatidylethanolamine (PE), normally exist in a hexagonal phase, but they can exist in a bilayer phase by the stabilizing effects of PEG-PE and cholesterol. Formulations that include pH sensitive lipids will revert to the hexagonal phase following exposure to the low pH in the endosomal compartment (108). Similarly, the inclusion of thiolytically cleavable derivatives of PEG-PE leads to the loss of PEG and liposome destabilization in the endosomal compartment through the action of thiolytic agents, such as glutathione (109). The net effect for both formulations is triggered intracellular release of liposomal drugs.

1.12 Disadvantages of Ligand-Mediated Targeting

Besides the advantages, there are also several disadvantages of ligand-targeted therapies. A problem that is intrinsic to all chemotherapy is the emergence of resistance. In the case of ligand-targeted therapies, receptor or antigen negative cell populations would be selected for by their insensitivity to treatment. In addition, the rapid proliferation and/or mutation rate of cancer cells can facilitate the development of resistant populations. Another important concern is the modulation of antigens in response to the binding of antibody, as is the tendency for tumor cells to down-regulate or shed cell surface receptors. Antibody or ligand directed therapy may accelerate this process as the tumor cells attempt to evade therapy. However, it is likely that certain antigens, such as those required for malignant progression (e.g. HER2), will show stable expression. In addition, the use of cocktails of ligand-targeted liposomes, or changing the targeting ligand in sequential administrations may be able to circumvent this problem.

The administration of immunoglobulins naturally leads to problems with immunogenicity for two main reasons. First, because mAb are generally of murine origin (produced by murine hybridomas) they tend to elicit the production of human anti-mouse antibodies (HAMA). This is especially limiting when multiple treatments are desired. This problem can be circumvented in at least two ways. First, humanized antibodies can be produced using genetically engineered expression vectors in mammalian cells. These antibodies contain murine variable regions, which are responsible for antigen binding, and human constant regions (110). Since the constant region contains the majority of the antigenic structures (111), these humanized antibodies should be less immunogenic. Although, it is important to note that the antigen binding region can also elicit the production of antibodies (112). Second, Ab fragments can be used. In this case, the most immunogenic portion, the Fc region, has been removed, leaving only the antigen-binding region.

The conjugation of antibodies to PEG-liposomes may enhance the immunogenicity of whole antibody. Harding *et al.* (113) followed the production of antibodies against both humanized free C225 antibody (anti-human epidermal growth factor receptor), and immunoliposomes conjugated with the same antibody, after their repeat administration in mice. They found that when the antibody was conjugated to liposomes it elicited the production of much higher titres of anti-C225 antibody, compared to the free antibody. While this phenomenon of enhanced immunogenicity of antibody remains to be replicated, it is an interesting finding. Since cross-linking of antibodies is known to be involved in B- and T-cell activation, it is possible that the close proximity of antibodies on the surface of a liposome could facilitate the immune

response. Interestingly, the antiserum was primarily directed against the Fc portion of the antibody, which indicates that Fab' fragments may show more clinical utility (113).

Future studies are needed to confirm or refute this finding, and to determine whether Fab'-PEG-immunoliposomes will also show enhanced immunogenicity compared to free antibody. These findings will likely influence the future of ligand-targeted liposomes in the clinic. One study has shown that the administration of mAb specific for the Fc receptor can prevent the acceleration of immunoliposome clearance that is associated with an immune response against them (114).

1.13 Indications for Targeted Liposomes

Another important consideration is target accessibility. When the idea for targeted-liposomes was first conceived they were expected to radically improve the localization of anti-cancer agents. This enthusiasm has since waned due to the finding that targeted liposomes have a limited ability to penetrate solid tumors. This has become known as the 'binding site barrier' because the liposomes seem to be blocked from penetrating into the center of solid tumors and instead they remain localized in the periphery. The 'barrier' is proposed to result from a combination of factors. First, the heterogenous blood flow, coupled with a low potential of colloidal particles to diffuse through the tumor interstitium (due to high interstitial pressure in the core of solid tumors), limits access of the liposomes to poorly perfused areas. Second, the antibody may promote specific or non-specific binding to tumor antigens in the periphery, leaving a limited amount of liposomes to travel further into the tumor. In this regard, the affinity of the ligand for its target antigen may be important because low affinity ligands may allow the liposome to 'percolate' further into the tumor (57). Despite the limitations an

excellent example of success in the targeting of solid tumors is targeting to HER2 (89). An instrumental part of this achievement is likely the use of antibody fragments as a targeting agent because earlier studies with whole antibody did not share this success (90). The relatively small size of Fab' fragments undoubtedly improves the penetration of the immunoliposomes into the tumor. In addition, HER2 is an internalizing receptor, giving it a targeting advantage.

The greatest potential for targeting is expected to be against malignancies where the target cells are more dispersed and easily accessible. This includes hematological malignancies, and early stage metastases. In addition, targeted therapy will likely be useful in an adjuvant setting, for the treatment of minimal residual disease following primary therapy. Furthermore, in these settings chemotherapy is often the only reasonable choice due to the diffuse nature of the malignancies. In addition, some of these malignancies respond poorly to currently available therapies; therefore targeted therapy may be particularly beneficial. Some examples include relapsed B-cell lymphoma, and multiple myeloma.

1.14 Barriers and Solutions to Clinical Approval of Targeted Liposomes

Despite the potential of targeted liposomes, there has been little progress towards clinical approval of these formulations. As mentioned earlier, some of the barriers towards clinical approval have been the problem of immunogenicity and target cell accessibility. However, these problems have been addressed in some form. However, one major obstacle remains. In order to attain successful targeting, that results in enhanced therapeutic efficacy, diversity in the choice of both drug and targeting ligand is necessary. This requirement stems from the heterogeneity of malignant cells between

tumor types, patients, and even within the same tumor. The clinical approval of targeted liposomal anticancer drugs has been prevented, in part, by the impracticality of manufacturing such a diverse array of targeted liposomal formulations. In this regard, the development of a combinatorial approach where liposomes with a variety of targeting ligands could be produced from a small number of precursors would be an attractive alternative to classical coupling techniques. This would allow the production of targeted liposomal anticancer drugs that are tailored to each individual patient's needs.

One possible way to introduce flexibility in the choice of targeting ligand in the preparation of targeted liposomes is to develop a method that allows ligand incorporation at a late stage in liposome preparation. Uster *et al.* (115) have shown that PEG-derivatized phospholipids will transfer from the micelle phase into liposome bilayers in a time-and-temperature dependent manner. Similarly, the insertion of ligand coupled, derivatized PEG-phospholipids by this technique would provide a feasible way to incorporate ligands into preformed, drug-loaded liposomes, resulting in the formation of a ligand-targeted liposome. This approach is described in **Fig. 1.11**. Mal-PEG coupling chemistry is employed, with the substitution of PEG-DSPE micelles for liposomes. Following coupling, the ligand would then transfer into the liposomes during an incubation period under optimized conditions of time and temperature. This method would be advantageous since the ligand is incorporated at a relatively late stage in liposome production; therefore considerable flexibility can be achieved in both the choice liposomal drug and targeting ligand. Theoretically, using a combinatorial approach, it would be possible to produce patient-selective liposomes from any liposome formulation. This approach is described in **Fig. 1.12**. Ideally, liposomal drugs that are currently

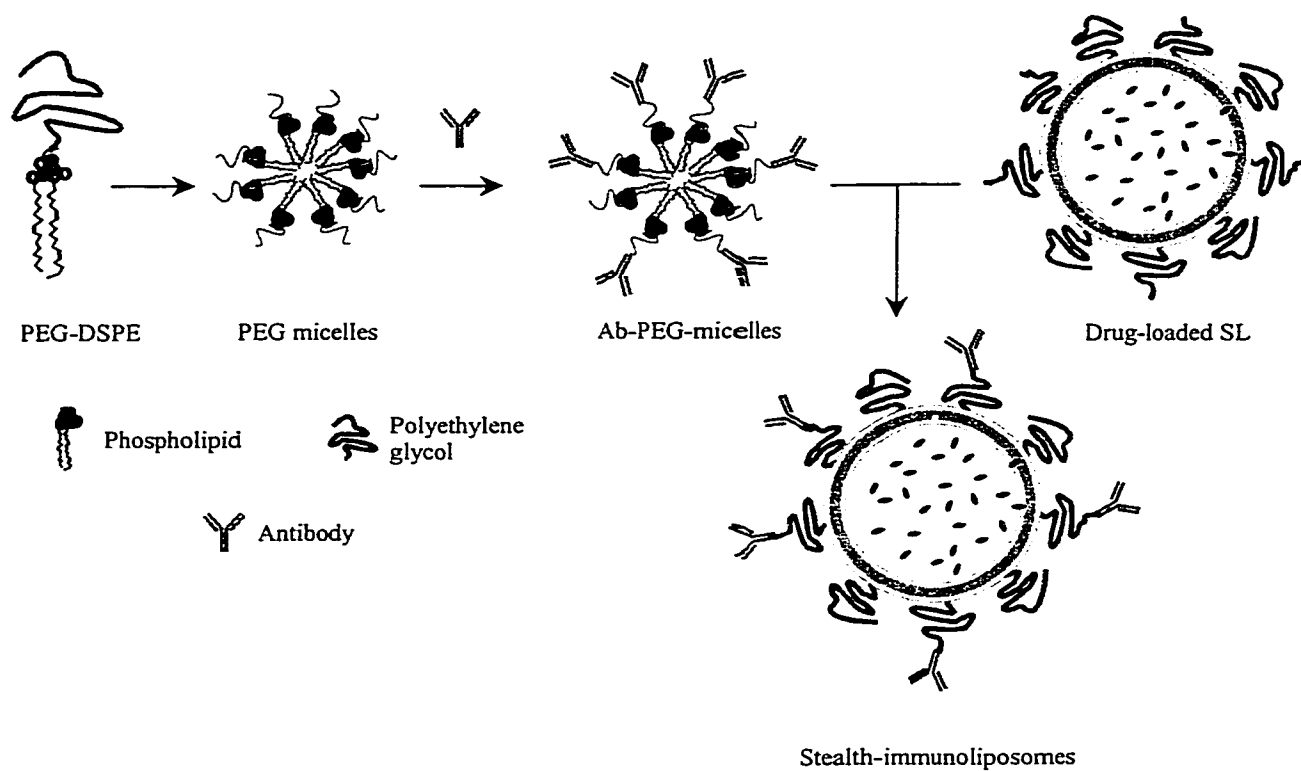


Fig. 1.11 Schematic outlining the post-insertion method to prepare ligand-targeted liposomes.

PEG-DSPE micelles are coupled with antibody by the Mal-PEG method and incubated with preformed, drug-loaded liposomes at specified molar ratios for 1 h at 60°C. Following transfer of the IgG-PEG-DSPE into the liposome bilayer from the micelles, a therapeutic formulation of immunoliposomes results.

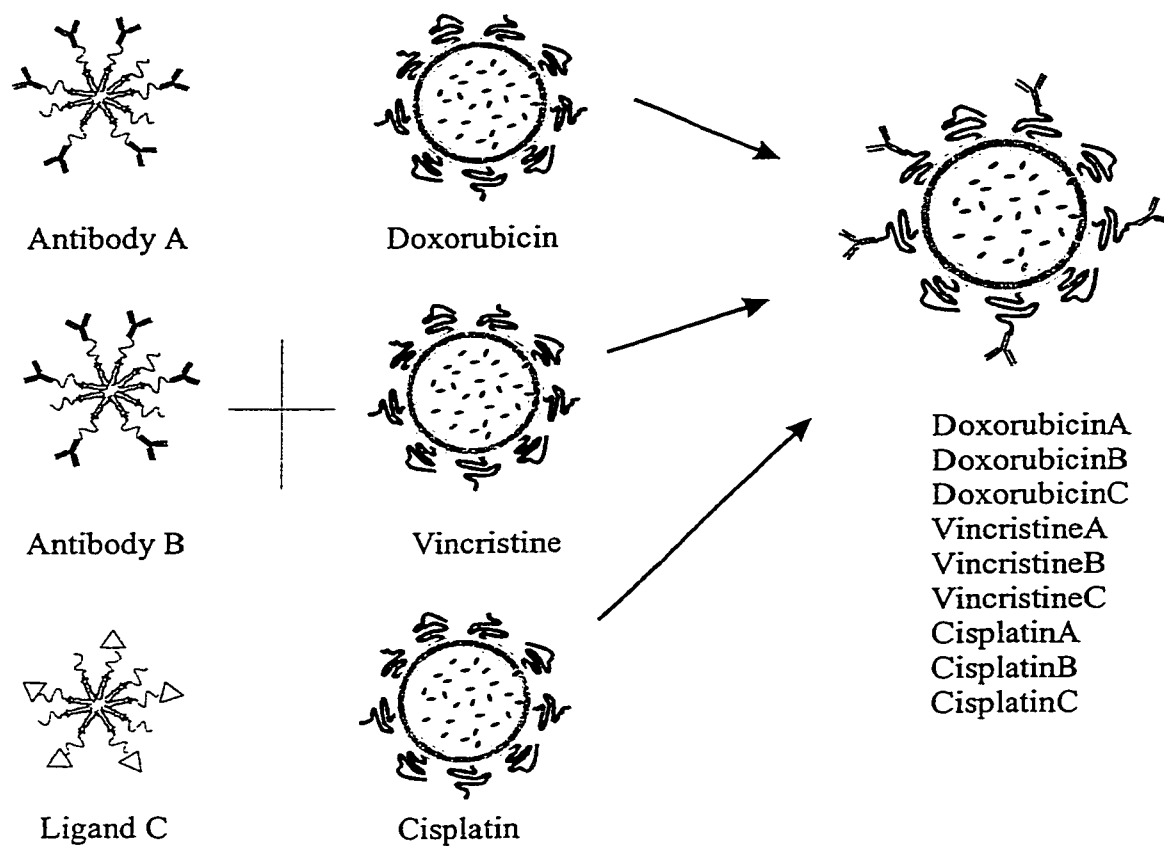


Fig. 1.12 Schematic showing the combinatorial approach to the preparation of drug-loaded, ligand-targeted liposomes for clinical applications.

approved for clinical use, such as liposomal doxorubicin (Caelyx[®]/Doxil[®]) could be used. Given the potential of the combinatorial approach, the aim of this thesis was to develop, what is now called, the 'post insertion technique' into a viable method for producing ligand-targeted liposomes for therapeutic/clinical use.

For the post-insertion method to be useful certain criteria must be met. In general, these criteria model the characteristics of an ideal targeted-liposome that were outlined previously. To reiterate, the method must be simple, rapid, and efficient to avoid wastage of materials, and maintain the structure of the ligand. In the case of the post-insertion technique the incubation conditions used for transfer will also be important, and the transfer efficiency as well as the coupling efficiency must be considered. In addition, the ligand density should be optimized to allow target binding without enhanced clearance from circulation. Finally, the drug loading and retention characteristics should not be compromised by the coupling/transfer procedure.

1.15 The Model System

The clinical applicability of post-insertion liposomes (PIL) was evaluated in this thesis using a model of human B-cell lymphoma. Lymphomas are malignancies that arise in the lymphoid system. They are a heterogenous group of neoplasms and are extensively classified according to their lineage and stage of origin (reviewed in (116)). The incidence of non-Hodgkins lymphoma, which includes the majority of lymphomas, is increasing in prevalence (117) by about 3-4% per year and in the last 15 years has increased by 50% (118). One of the aggressive forms of non-Hodgkin's lymphoma is Burkitt's lymphoma. In this disease the response to currently available therapies is poor and relapses eventually occur. The average six-year survival of patients with advanced

stage Burkitt's lymphoma following intense combination chemotherapy is only 35% (119). In cases of relapse, chemotherapy was shown to result in 5 year survival of 12%, but this increases to 53 % with high dose therapy followed by bone marrow transplant (120). However, it is clear that more effective treatments are needed. The post-insertion approach to the preparation of targeted liposomes may open up new treatment options for the treatment of B-cell lymphoma and other malignancies.

B-cells are the effector cells of humoral (antibody mediated) immunity. The B-cell lineage is derived from pluripotent stem cells in the bone marrow. These cells leave the bone marrow and undergo several stages of differentiation and maturation within lymphoid organs, leading to the production of the end effector cells, which produce and secrete antibodies. These are called plasma cells and they reside in the bone marrow. The stages of lymphocyte differentiation are shown in **Fig. 1.13**. Malignant clones can be derived from any lymphocyte stage, giving rise to the many sub-types of lymphoma. Each lymphocyte lineage and stage expresses a characteristic set of cluster designation (CD) antigens that can be used to identify the origin of a malignant clone. In the case of B-cells, the expression of Ig subtypes is also an important stage specific feature. Burkitt's lymphoma is an undifferentiated stage malignancy and the cells express surface Ig (predominantly IgM), CD10, CD19, CD20, CD22, and CD79a (121). Burkitt's lymphoma cells are also characterized by translocations in the c-myc oncogene. The function of c-myc is to regulate transcription of genes involved in cell proliferation, differentiation, and apoptosis. The deregulation of c-myc expression, as a result of the translocation, is thought to lead to malignant transformation (122).

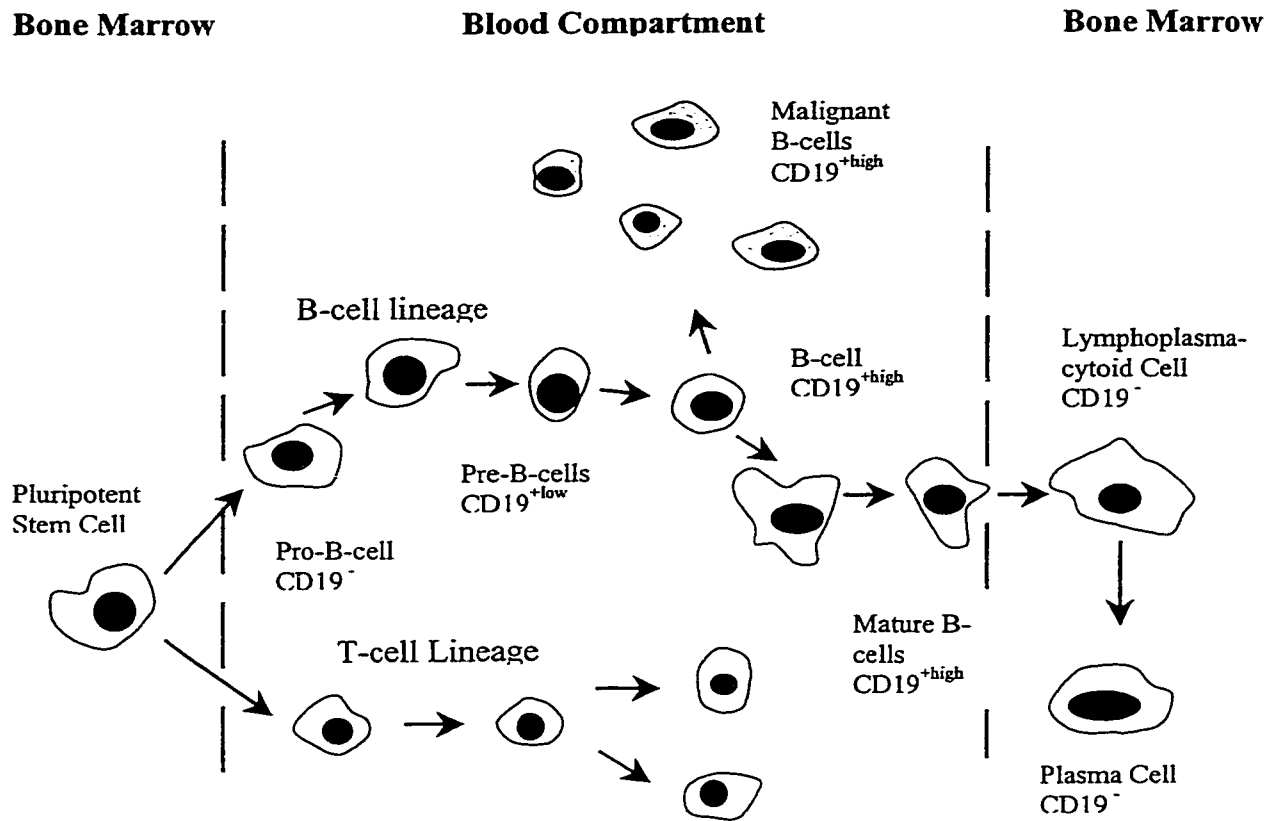


Fig. 1.13 Stages of B-lymphocyte differentiation.

B-lymphocytes are derived from a pluripotent stem cell in the bone marrow and undergo several maturation stages before the end effector cells, plasma cells, that produce antibody are generated. The entire B-cell lineage expresses the CD19 antigen, except the mature lymphoplasmacytoid and plasma cells. Burkitt's lymphoma arises from a malignant clone of the small pre-B-cell stage.

The CD19 antigen is of particular interest to this thesis. It is a member of the IgG superfamily (123) and is expressed on all B-cells from early stages until the final differentiation into plasma cells, when it disappears (124). It is only expressed on B-lineage cells and follicular dendritic cells (125). CD19 consists of extracellular, transmembrane, and cytoplasmic domains and it forms a membrane complex with CD21 (a complement receptor), and several other surface antigens. The function of the complex has not been fully elucidated; however it activates multiple cell signaling cascades. Antibody crosslinking of CD19 has been shown to increase intracellular $[Ca^{2+}]$, activate phospholipase C (PLC) and protein tyrosine kinases (PTKs), and induce homotypic aggregation of B-cells (126). Overall, the evidence to date suggests that the function of CD19 is to regulate B-cell growth and proliferation, as it has been shown to inhibit these processes (127). In addition, the expression of the complex antigens is stage specific; therefore the function of the complex may be developmentally regulated (128). For example, CD21 is only expressed on mature B-cells and both CD19 and CD21 are down-regulated after antigen activation and differentiation into plasma cells. This seems appropriate, given the proposed function of the complex in inhibiting cell proliferation.

Several groups are investigating mAb targeted therapies for the treatment of B-cell lymphoma, many of which employ anti-CD19 antibodies. In fact, B-cell malignancies may be particularly well suited for mAb-based therapy for several reasons. As already mentioned, there is a need for alternative therapies because the response to current therapy can be poor. Other advantages include; the fact that B-cell surface antigens are well characterized, internalizing and cell signaling coupled receptors exist, and a wide variety of mAbs are available. In addition, anti-CD19 antibodies have been

shown to inhibit the function of Pgp (100) and induce cell cycle arrest (99); therefore anti-CD19-based therapies may have synergistic cytotoxicity with other therapeutic agents.

Some responses have been achieved in humans by administering both free anti-CD19 (99) and anti-CD19 that has been conjugated to a plant toxin called ricin (129, 130) (131). In addition, the effect of immunotoxins directed at other CD antigens is enhanced by free anti-CD19 antibody and CD19 immunotoxins (132). In fact, the use of carefully designed cocktails is expected to be much more effective. In one case the use of a triple cocktail of CD19, CD22, and CD38 immunotoxins was shown to be curative of B-cell lymphoma in SCID mice (133). The authors suggest that a small proportion of cells resist treatment with single or dual cocktails because they are negative for one or two of the CD antigens. In their study 0.04% of the cells were negative for two antigens, but none were negative for all three CD antigens. They attribute their success to the ability to overcome resistance to the therapy and maintain that the cocktail approach should be further tested in clinical trials for B-cell malignancy. Finally, mAb-targeted liposomes have also shown success in animal models of B-cell lymphoma. In one study DXR containing sterically stabilized immunoliposomes (DXR-SIL) were targeted using anti-idiotypic antibodies (92), and in another study DXR-SIL were targeted with anti-CD19 (134).

To evaluate the therapeutic potential of immunoliposomes made by the post-insertion technique (PIL) in human B-cell lymphoma we have employed a murine model of Burkitt's lymphoma. Human malignancies are easily studied in the severe combined immunodeficient (SCID) mouse. These mice are immunodeficient because they have a

mutation in the recombinase enzyme needed for immunoglobulin and T-cell receptor gene recombination. In result the mice completely lack mature, functional T- and B-lymphocytes (135). As such, human cells can be xenografted into SCID mice, without rejection. Burkitt's lymphoma cells have been shown to grow in SCID mice without alteration in morphology or antigen expression. In addition, the tumors grow in a disseminated pattern, much like they do in humans. After i.v. injection, the cells localize extensively in the bone marrow in the cranium, vertebrae, and femurs. This results in osteolysis, vertebral fractures, and infiltration of the spinal cord by neoplastic cells. Hind leg paralysis is associated with these changes and its onset accurately predicts death, providing a reliable end point for therapeutic studies (136). In this thesis xenografts of the Burkitt's lymphoma cell line, Namalwa, in SCID mice have been employed to evaluate the therapeutic potential of PIL[anti-CD19]. *In vitro* studies were also performed using the Namalwa cell line.

Doxorubicin (Adriamycin[®]) is commonly included in chemotherapy regimens for the treatment of B-cell lymphoma; therefore it has been employed in this study. This drug belongs to the family of anthracyclines, which are among the most effective and commonly used anti-cancer drugs because they exhibit activity against a wide variety of malignancies. Of the anthracyclines, doxorubicin has the widest spectrum of activity (137, 138). The anthracyclines are antibiotics that were originally isolated from various strains of the mold *Streptomyces spp.* and they are commonly referred to as the 'anti-tumor antibiotics'. The wide spectrum of activity exhibited by doxorubicin, and other anthracyclines, is probably related to the fact that they act through multiple mechanisms. Their most defining feature is that they intercalate into DNA causing strand breaks, and

may be involved in the inhibition of DNA and RNA polymerase that in turn inhibits DNA synthesis. Intercalation in DNA was originally thought to be the only mechanism of action of anthracyclines, however, the importance of several other mechanisms has since been reported. The inhibition of topoisomerases I and II also leads to the production of strand breaks. In addition, the anthracyclines have been reported to directly stimulate well-known apoptosis signaling pathways, independently of DNA damage and cell cycle arrest. More specifically this involves modulation of Fas ligand mRNA levels and ceramide generation (137, 139, 140). However, a full description of this process is beyond the scope of this thesis. The final mechanism of anthracycline cytotoxicity is the induction of oxidative DNA damage resulting from high levels of oxygen free radicals. The reduction of doxorubicin by NADPH-dependent enzymes leads to the generation of oxygen free radicals. In addition, the anthracyclines are able to form complexes with iron that catalyze the production of free radicals by the fenton reaction (141). In addition to causing oxidative DNA damage, these radicals also lead to membrane damage by lipid peroxidation. In summary, anthracyclines act through cytostatic and cytotoxic mechanisms that result in inhibition of RNA and DNA synthesis, DNA damage, and membrane damage. These effects lead to cell cycle arrest (at S-phase or G₂M), depending on dose) and the induction of apoptosis (137).

Side effects that are associated with anthracycline treatment include alopecia, nausea, vomiting, diarrhea, and mucositis. In addition, the dose limiting toxicities of anthracyclines include myelosuppression and cardiotoxicity. Acute cardiotoxicity can occur and this is manifested as electrocardiographic changes, and sometimes pericarditis. However, chronic toxicities are more common and occur with cumulative doses in the

range of 450-550 mg/m² over a lifetime. Cardiomyopathy is the primary effect and this often leads to congestive heart failure and/or death (reviewed in (142)). The heart is particularly sensitive to anthracycline induced oxidative damage as a consequence of low levels of the cytoprotective enzyme, catalase in cardiac cells. In other tissues, the activity of higher levels of free radicals scavengers, such as catalase, are able to limit the build up of damaging free radicals.

1.16 Hypothesis and Objectives

The goal of this thesis was to develop the post-insertion method for the preparation of immunoliposomes into a viable technique for clinical applications, with the potential to extend this technique to other ligands. In addition, we wished to test the hypothesis that targeted liposomes made by the post-insertion technique are equivalent to those made by conventional coupling techniques. Several underlying objectives were considered instrumental to the achievement of this goal.

The first set of objectives aims to evaluate and refine the post-insertion technique so that the product meets the established criteria for ideal immunoliposomes, as described in section 1.8. To this end, we aimed to characterize and optimize the efficiency of both ligand coupling to PEG-DSPE micelles and transfer of IgG-PEG-DSPE to preformed liposomes. An additional objective in these experiments was to determine the optimal micelle composition to achieve specified antibody densities. Second, we aimed to determine the stability of the insertion of IgG-PEG-DSPE. Our third objective was to quantify the amount of drug leakage both during transfer and during incubation in plasma. These studies are important for the following reasons. The therapeutic effectiveness of liposomal drug formulations is related to the amount of drug they can

deliver, and drug leakage rates are formulation dependent. In addition, the potential for drug loss in our model is high because the integrity of the liposome bilayer may be jeopardized during transfer for two reasons. First, the temperature exceeds the liposome T_M during the incubation period, making the bilayer fluid. Second, the insertion of IgG-PEG-DSPE likely creates transient disruptions in the bilayer. The results of these experiments appear in Chapter 3 of this thesis.

The second set of objectives was to determine the *in vitro* targeting effectiveness of PIL. This was evaluated by quantifying the extent of binding and/or uptake by their target cells *in vitro*, and the IC_{50} of doxorubicin-loaded PIL against the same cells. For both the binding and cytotoxicity assays the results were compared to that of immunoliposomes made by conventional coupling techniques (SIL). In this regard, the post-insertion technique was not expected to be a viable alternative for the preparation of targeted liposomes unless they can at least meet the criteria that have been demonstrated for SIL. Overall, the *in vitro* studies were expected to indicate the potential to achieve targeting *in vivo*. These results appear in Chapter 4 of this thesis.

The third set of objectives was to determine the potential therapeutic value of the PIL in the treatment of an animal model of hematological malignancy. An important factor affecting the therapeutic efficacy of any liposome formulation is their rate of clearance from circulation, and disposition *in vivo*. In this case, the evaluation of the pharmacokinetics is particularly important because immunoliposomes may be cleared from circulation at an accelerated rate, and the rate of clearance is affected by small formulation differences. For these reasons we compared the pharmacokinetics of PIL, SIL, and non-targeted liposomes (SL). Subsequently, we compared the therapeutic

efficacy of doxorubicin (DXR)-loaded PIL, DXR-SIL, DXR-SL, and free DXR in a murine model of human B-cell lymphoma. The results of these experiments appear in Chapter 5 of this thesis.

Chapter 2
Materials and Methods

Chapter 2:

2.1 Materials

Hydrogenated soy phosphatidylcholine (HSPC), methoxypoly(ethylene glycol) (molecular weight 2000) covalently linked to distearoylphosphatidylethanolamine (PEG₂₀₀₀-DSPE) (44), hydrazide-derivatized PEG₂₀₀₀-DSPE (HZ-PEG-DSPE) (81), and doxorubicin (DXR) were generous gifts from ALZA Pharmaceuticals, Inc (Mountain View, CA). Maleimide-derivatized PEG₂₀₀₀-DSPE (Mal-PEG-DSPE) was custom synthesized by Shearwater Polymers, Inc. (Huntsville, AL) (82). Cholesterol (CHOL) was purchased from Avanti Polar Lipids (Alabaster, AL). Cholesterol-[1,2-³H-(N)]-hexadecyl ether ([³H]CHE), 1.48-2.22 TBq/mmol, and Na¹²⁵I (185 mBq) were purchased from Mandel Scientific (Mississauga, ON). [Carbamoyl-¹⁴C]mPEG₂₀₀₀-DSPE (17.75 mCi/g) was custom synthesized by Chemsyn Science Laboratories (Lenexa, KS). Nuclepore[®] polycarbonate membranes (pore sizes: 0.2, 0.1, and 0.08 μm) were purchased from Northern Lipids (Vancouver, BC). Sephadex G-25 and G-50, Sepharose CL-4B, aqueous counting scintillant (ASC), and Hi-Trap Protein G columns were purchased from Amersham Pharmacia Biotech (Baie d'Urfé, QC). N-acetylmethionine (NAM), sodium periodate, 3-[4,5-dimethylthiazol-2-yl]-2,5-diphenyltetrazolium bromide (MTT), 2-iminothiolane (Traut's) reagent, and sheep IgG (reagent grade) were purchased from Sigma Chemical Co. (St. Louis, MO). 4-(2-hydroxyethyl)-1-piperazine ethanesulphonic acid (HEPES) was purchased from BDH (Toronto, ON). Florisil[®] lipid filters were purchased from Waters Corporation (Milford, MA) and low protein binding 0.22 μm syringe filters were purchased from Millipore Corporation (Bedford, MA). Iodobeads[®] were purchased from Pierce Chemical Co. (Rockford, IL). Tyraminylinulin (TI)

synthesis and preparation of [125 I]TI have been previously described (143). RPMI 1640 media (without phenol red), penicillin-streptomycin, and fetal bovine serum (FBS) were purchased from Life Technologies (Burlington, ON). All other chemicals were of analytical grade purity.

2.2 Cell lines

The human Burkitt's lymphoma cell line, Namalwa (ATCC CRL 1432), was obtained from American Type Culture Collection (Rockville, MD). The cells were grown in suspension in full RPMI (supplemented with 10% fetal bovine serum (FBS), 50 units/ml penicillin G, and 50 μ g/ml streptomycin sulfate, without phenol red). The cells were maintained in 80 cm² culture flasks at 37°C in 5% CO₂ and 90% humidity at a concentration between 2 x 10⁵ and 1 x 10⁶ cells per ml. *In vitro*, at these concentrations, the cells remained in the exponential growth phase and had a doubling time of 24 h. For experimental purposes, only cells in the exponential phase were used. CD19 expression was previously confirmed by flow cytometry (Becton Dickinson, San Jose, CA).

FMC63 cells for the production of anti-CD19 murine monoclonal antibody (mAb) were grown in RPMI (without phenol red) supplemented with 15% FBS and 5% penicillin-streptomycin. The cells were maintained in 80 cm² culture flasks at 37°C in 5% CO₂ and 90% humidity to a maximum concentration of 8 x 10⁶ cells/ml to ensure that the cells were in logarithmic phase.

2.3 Mice

Female, 6-8 week old Balb/C or Alt BM mice were obtained from Health Sciences Lab Animal Services (University of Alberta, Edmonton, AB) and kept in standard housing. Female, 6-8 week old C.B.-17/ICR-Tac-SCID mice were purchased

from Taconic Farms (German Town, NY). They were housed under virus- and- antigen free conditions, and received autoclaved food and water. In addition, they were given the antibiotic/antimycotic, trimethoprim-sulfamethoxazole (Novotrimel[®]) in their drinking water for 3 days/week. Both strains of mice were used for experiments after a minimum acclimation period of 1 week, when they were 7-12 weeks old. All experiments were approved by the Health Sciences Lab Animal Services Animal Policy and Welfare Committee of the University of Alberta.

2.4 Preparation of anti-CD19 Antibody

Murine, monoclonal anti-CD19 antibody (IgG2a) was produced by the FMC63 murine hybridoma (144). These cells were injected into 6-8 week old BALB/c or Alt BM mice primed i.p. with Pristane or Freud's incomplete adjuvant. Ascites fluid was collected and purified by centrifugation. The monoclonal antibody containing supernatant was then further purified by sequential filtration through a series of syringe driven filters, including long body Florisil[®] lipid filters, 0.8 μm and low protein binding 0.22 μm filters. This solution was then frozen at -20°C for 2 h, centrifuged at 2000 RPM for 7 min and any remaining lipid or cryoprecipitated proteins were removed. The antibody solution was then either further purified or aliquoted and frozen at -80°C for later use. If frozen, the antibody solution was thawed and re-centrifuged at 2000 RPM for 7 min and any cryoprecipitate or particulate matter was removed before the final purification step. Finally, the IgG was further purified by affinity chromatography over a 5 ml protein G column according to manufacturer's instructions. The eluent was passed through a flow cell of the Ultrospec 3000 Spectrophotometer and the antibody was collected according to the absorbance at 280 nm. The pH of the eluent was adjusted to

pH 8.0 by the addition of 1 M, pH 8.0 Tris buffer. The antibody was then concentrated to a 2 ml volume using a 15 ml Ultrafree concentrator, with a MW cutoff of 30 Kda (Millipore Corporation, Bedford, MA), re-diluted to 10-12 ml with HEPES buffer (25 mM HEPES, 140 mM NaCl), pH 8.0, and re-concentrated to 12-20 mg/ml. The Ab concentration was determined using the Biorad Assay (145), and the solution was aliquoted and frozen at -80°C until needed.

2.5 Iodination of antibodies

IgG was dissolved in 25 mM HEPES, 140 mM NaCl, pH 7.4 (1 mg/0.3 ml) and added to a reaction vial with 185 MBq Na¹²⁵I and 5 iodobeads[®]. The reaction was allowed to proceed at 22°C for 1 h, then the ¹²⁵I-IgG was separated from free ¹²⁵I by chromatography on a Sephadex G-25 column that was pre-equilibrated with pH 7.4 HEPES buffer. The specific activity was calculated from the protein concentration, as determined by the Biorad Protein Assay (145) and from the ¹²⁵I specific activity.

2.6 Preparation of liposomes

Liposomes were composed of HSPC:CHOL:mPEG₂₀₀₀-DSPE at either a 2:1:0.1 or 2:1:0.08 molar ratio of phospholipids (PL). In some formulations a portion of the mPEG₂₀₀₀-DSPE (kept constant at 1 mol% of HSPC) was replaced with Mal-PEG₂₀₀₀-DSPE. Lipids were dried from chloroform on a Büchi rotoevaporator for 1 h, to make a thin film covering the inside of a glass tube, and dried further under high vacuum overnight. In some cases a non-metabolizable, non-exchangeable radioactive tracer, [³H]CHE, (30-60 KBq) was added to the lipid mix. Lipids were then hydrated in buffer at 20-30 mM by warming in a 65 °C water bath and vortexing. The buffer chosen for hydration depended on the intended purpose of the liposomes. Liposomes for binding

assays were hydrated in HEPES buffer, pH 7.4. If doxorubicin-loaded liposomes were required (for *in vitro* cytotoxicity and *in vivo* therapeutic studies) the lipid was hydrated in 250 mM ammonium sulfate at pH 5.5. Finally, liposomes for pharmacokinetic studies were hydrated in pH 7.4 HEPES buffer, ^{125}I -TI (14–18 MBq) at pH 7.4. The lipid was then sequentially extruded (Lipex Biomembranes Extruder, Vancouver, BC) through a series of polycarbonate membranes (Northern Lipids, Vancouver, BC) with pore sizes ranging from 0.2 down to 0.08 μm . This procedure results in the production of primarily large unilamellar vesicles (3, 146). The mean liposome diameter was determined by dynamic laser light scattering using a Brookhaven BI 90 submicron particle size analyzer (Brookhaven Instruments Corp., Holtsville, NY) and were in the range of 100 ± 10 nm.

Following extrusion, ^{125}I -TI loaded liposomes were chromatographed on a Sepharose CL4B column that was pre-equilibrated with HEPES buffer, pH 7.4 to remove free ^{125}I -TI. For doxorubicin-loaded liposomes DXR was loaded by the ammonium sulfate gradient method (28). Following extrusion the external buffer (surrounding the liposomes) was exchanged by chromatography over a Sepharose CL-4B column that was pre-equilibrated in 100 mM Na acetate, 70 mM NaCl at pH 5.5, where the sample volume was approximately 10% of the total column volume. At this time DXR, dissolved in 10% sucrose (6 mg/ml) was incubated with liposomes at 65°C at a ratio of 0.26 μmol DXR/ μmol HSPC for 30 min. Free DXR was separated from the liposomal DXR by chromatography over a Sepharose CL-4B column that was equilibrated in HEPES buffer, pH 7.4. The DXR concentration was determined from the absorbance of the loaded liposomes in methanol by spectrophotometry ($\lambda = 450$ nm) and the phospholipid concentration was determined by the Bartlett colorimetric assay (147). The final loading

ratio was approximately 0.26 $\mu\text{mol DXR}/\mu\text{mol PL}$, which translates into approximately 95% efficiency.

If liposomes were intended for coupling with antibody they were chromatographed on a Sepharose CL-4B column that was pre-equilibrated with deoxygenated HEPES buffer, pH 7.4. This column was run following extrusion (for empty or ^{125}I -TI-loaded liposomes), or following doxorubicin loading and was intended to minimize antibody cross-linking. In addition, the liposomes were kept under nitrogen until the antibody was thiolated and ready for coupling. The thiolated antibody was added as quickly as possible, and not more than 4 h following the initial hydration of the phospholipid because the maleimide groups degrade rapidly in buffer, particularly when the pH exceeds pH 6.7.

For liposomes that were intended for *in vivo* administration, the final Sepharose CL-4B column was pre-equilibrated with pH 7.4 HEPES buffer that was prepared with pyrogen free saline. In addition, the liposomes were sterile filtered (0.22 μm , low protein binding filter) and diluted in sterile pH 7.4 HEPES buffer to the dosing concentration.

2.7 Preparation of Micelles

Lipid mixtures were composed of Mal-PEG₂₀₀₀-DSPE or mPEG₂₀₀₀-DSPE: Mal-PEG₂₀₀₀-DSPE at various molar ratios (9:1 or 4:1 mol:mol), and in some cases trace amounts of ^{14}C -mPEG-DSPE was added to follow the insertion of micellar lipid into the liposomes. These lipids were dried from chloroform for 1 h using a rotor-evaporator to make a thin film covering the inside surface of a glass tube and then further dried overnight under high vacuum. The lipids were hydrated immediately before coupling at

10 mM in deoxygenated 25 mM HEPES, pH 7.4, by heating in a 65°C water bath with occasional gentle vortexing.

2.8 Antibody Coupling to Liposomes and Micelles

Antibodies were covalently coupled to PEG termini on liposomes and micelles using the Mal-PEG coupling method (82). The antibody was dissolved in deoxygenated, HEPES buffer, pH 8.0 to give a final concentration (following the addition of the remaining reactants) of 10 mg/ml to couple Ab to liposomes, and 12 mg/ml to couple Ab to micelles. A small amount of ^{125}I -radiolabeled IgG was added for later determination of protein concentration from the specific activity. Finally, Traut's reagent (15 mM in HEPES buffer, pH 8.0) was added to the antibody at a 20:1 molar ratio of Traut's: IgG for liposomes and a 10:1 molar ratio of Traut's: IgG for micelles. The reaction was allowed to proceed at 22°C for one h with occasional mixing. The IgG was then chromatographed over a Sephadex G-50 column equilibrated in deoxygenated HEPES buffer, pH 7.4 (sample volume was equivalent to 10% of the column volume) to remove un-reacted Traut's reagent. The protein concentration of the thiolated antibody was determined by Biorad Assay, and γ -counts were taken, using a Beckman 8000 gamma counter, for determination of the specific activity (cpm ^{125}I /mg IgG). The thiolated antibody was then promptly added to the liposomes or micelles at a specified molar ratio of IgG:PEG₂₀₀₀-DSPE, taking care to avoid exposure to oxygen. In the case of liposomes, approximately 45 μg Ab was added per μmol PL, which corresponds to a molar ratio of 1: 3333 (Ab:liposome PL). Micelles were coupled at a molar ratio of 10:1, Mal-PEG₂₀₀₀-DSPE: IgG. The reaction mixture was left under nitrogen overnight at 22°C on a magnetic mixer to allow for coupling to occur.

Following the incubation, the resulting SIL were chromatographed on a Sepharose CL-4B column pre-equilibrated with HEPES buffer, pH 7.4 to remove non-coupled antibody. The liposome fractions were pooled and the phospholipid concentration was determined from the liposomal cpm ^3H -CHE and the specific activity (cpm/ μmol PL) or by the method of Bartlett (147). In addition, the protein concentration was determined from the cpm ^{125}I -IgG and the specific activity (cpm/ μg IgG). The coupling ratio (μg IgG/ μmol liposome PL) was also calculated. The antibody incorporation was between 25-40 $\mu\text{g}/\mu\text{mol}$ liposome PL.

To prepare PIL the IgG-PEG-DSPE micelles were incubated with liposomes for transfer (see section 2.10).

2.9 Determination of Micelle Coupling Efficiency

Coupling efficiency was determined for IgG-PEG-DSPE micelles composed of 4:1 mPEG₂₀₀₀-DSPE: Mal-PEG₂₀₀₀-DSPE (mol:mol). IgG-micelles were separated from free IgG by ultracentrifugation on a discontinuous metrizamide gradient (40/50/60%, 3/4/3 ml) for 14 h at 37 000 rpm in a SW41 rotor using an L8-70 Ultracentrifuge (Beckman, CA, USA). Ten 1 ml fractions were collected from the bottom of the gradient and an elution profile was drawn based on cpm for ^{125}I and ^{14}C , which are tracers for IgG and mPEG₂₀₀₀-DSPE, respectively. The elution profile for free IgG alone was used as a reference to locate the free IgG peak. An approximate coupling efficiency was determined by integrating the area under the curve for free IgG versus IgG-PEG₂₀₀₀-DSPE.

2.10 Micelle Transfer

Following coupling, the IgG-micelles were filtered through a 0.22 μm , low protein binding filter to remove cross-linked, large diameter micelles. Varying amounts of micelles (ranging from 0.5-5.0 mol% of liposome HSPC) were then incubated with preformed liposomes for 1 h at 60°C. The mPEG₂₀₀₀-DSPE content in the liposomes varied from 0-9.2 mol% of HSPC. For experiments appearing in chapters 4 and 5 the liposomes were exclusively composed of 4 mol% mPEG-DSPE. Following transfer the liposome-micelle mixture was cooled and chromatographed over a Sepharose CL-4B column equilibrated with pH 7.4 HEPES buffer (where the sample volume was equivalent to 4% of the column volume) to separate the liposomes from non-inserted micelles and free antibody. The coupling ratio (μg IgG/ μmol liposome PL) was determined from the cpm of ¹²⁵I and ³H and the specific activities for the antibody (¹²⁵I-cpm/mg protein) and liposome phospholipid (³H]CHE-cpm/ μmol PL). In cases where [³H]-CHE was not used as a tracer the PL concentration was determined by the method of Bartlett (147). For experimental purposes the antibody incorporation ranged from 25-40 $\mu\text{g}/\mu\text{mol}$ liposome PL.

2.11 Characterization of Transfer Efficiency

To determine the time and temperature dependence of IgG-PEG-DSPE insertion, 55 μg IgG-PEG-DSPE micelles were incubated with 1 μmol preformed, doxorubicin-loaded liposomes and incubated at either 37°C for 24 h or 60°C for 1 h. IgG-PEG-DSPE insertion was traced using ¹²⁵I-IgG as described in section 2.10. The effect of micelle and liposome composition on PEG-DSPE and IgG-PEG-DSPE insertion was determined by incubating preformed, doxorubicin-loaded liposomes with increasing concentrations of

micelles (0.5:100 to 3.5:100 ratio of micelle PL: liposome HSPC, mol:mol) composed of either a 4:1 or 9:1 ratio of mPEG₂₀₀₀: Mal-PEG₂₀₀₀-DSPE and incubated for 1 h at 60°C. IgG and PEG-DSPE insertion was quantified as described in section 2.10. For determination of non-specific insertion, increasing amounts of free IgG were incubated with CL (liposomes containing 0 mol% mPEG-DSPE). The insertion was compared to that for micelles composed of 4:1 mPEG-DSPE: Mal-PEG-DSPE and similar amounts of IgG, incubated with CL.

2.12 *In vitro* Stability of Insertion

Post insertion liposomes coupled to Sheep IgG (PL[*sheep IgG*]) were prepared by transfer of IgG-PEG-DSPE into SL containing 4 mol% mPEG-DSPE. They were incubated in 50% human plasma (v/v) at 37°C for 48 h. The liposomes were then chromatographed on a Sepharose CL-4B column, equilibrated in HEPES buffer, pH 7.4. The amount of IgG-PEG-DSPE remaining in the liposomes was determined from β and γ counts by the specific activity of IgG (cpm¹²⁵I / μ gIgG) and PL (cpm ³H/ μ mol PL).

2.13 *In vitro* Doxorubicin Leakage Experiments

Liposomes containing entrapped doxorubicin were chromatographed over a Sepharose CL-4B column, to remove traces of free DXR, and promptly incubated with IgG-PEG-DSPE micelles at a PL molar ratio of 3:100 (micelle:liposomal PL) for 1 h at 60°C. The leakage of doxorubicin from the liposomes leads to dequenching of DXR fluorescence, which was measured using a CytoFluor 2350 fluorimeter (Millipore, Bedford, MA) and the excitation/emission wavelengths of 485/590 nm. Doxorubicin leakage was expressed as a percentage of the total encapsulated doxorubicin, given by the

fluorescence of liposomes in 5% (v/v) Triton- X, which results in 100% dequenching of the doxorubicin fluorescence.

2.14 *In vitro* Binding/Uptake

Liposomes of different formulations, including SL, SIL [anti-CD19] and PIL [anti-CD19] were prepared with 55.5 kBq of ^3H -CHE per μmol PL. The phospholipid concentration was determined by the method of Bartlett (147) and the specific activity (cpm/ μmol PL) was determined from β -counts using a Beckman LS-6800 counter. Namalwa cells were plated in 48 well plates (1×10^6 cells/well in a volume of 0.2 or 0.3 ml) in full RPMI. An equal volume of each liposome formulation, at final concentrations ranging from 0.05 to 1.6 $\mu\text{mol}/\text{ml}$, was added to the plates. In competition experiments excess free anti-CD19 (3-fold at the highest PL concentration and 97-fold at the lowest) was added to the wells 20 min before the addition of SIL [anti-CD19] and PIL [anti-CD19]. Following a 1 h incubation period at 37°C the cells were transferred to 5 ml tubes containing 3 ml cold (4°C) phosphate-buffered saline (PBS), pH 7.4 and centrifuged at 1000 RPM for 10-12 min. The supernatant was aspirated and an additional 2 ml of the same buffer was added. This procedure was repeated once more, for a total of three washes, and the cells were re-suspended in 0.5 ml PBS, pH 7.4. Finally, the cells were transferred to scintillation vials with 5 ml of aqueous counting scintillant (ACS) to quantify the amount of cell-associated liposomal marker, [^3H]-CHE. The cpm per million cells was determined in a Beckman LS-6800 counter and was converted into pmol liposomal PL using the specific activity.

The data was plotted using Slide Write Plus™ software (version 5.0, Advanced Graphics Softwear, Inc., Sunnyvale, CA) and the B_{max} and K_D were determined by non-

linear regression using Graph Pad Prism software (SanDiego, CA). B_{\max} and K_D values were determined for each experiment (n=3) and reported as a mean of four experiments \pm SE.

2.15 *In vitro* cytotoxicity

The *in vitro* cytotoxicities of free DXR, DXR-SL, DXR-SIL[anti-CD19], and DXR-PIL[anti-CD19] against Namalwa cells were compared, using the MTT assay (148). Five $\times 10^4$ Namalwa cells were plated in 96 well, round bottom plates in a volume of 0.1 ml. Free DXR, DXR-SL, DXR-SIL[anti-CD19], and DXR-PIL[anti-CD19] were serially diluted 1:4 with serum free RPMI (without FBS, penicillin-streptomycin) to eight different concentrations in separate 96 well, flat bottom plates. A 0.1 ml aliquot of each concentration was transferred to six wells in the plates containing cells and 0.1 ml of serum-free RPMI was transferred to the 12 remaining wells. The outermost wells were not used, and were filled with sterile distilled water (dH₂O) to maintain humidity. The plates were incubated at 37°C, 5% CO₂, and 90% humidity for 1 h or 24 h, centrifuged, and the cells were washed with PBS three times. Following the final wash the cells were re-suspended in 0.2 ml full RPMI and returned to the incubator. Forty-eight h following drug addition the plates were again centrifuged, the media removed and 50 μ L of 3-(4,5-dimethylthiazol-2-yl)-2,5-diphenyltetrazolium bromide (MTT) (5 mg/ml in distilled water, then diluted 1/10 in serum free RPMI) was added. Following incubation at 37°C, 5% CO₂, and 90% humidity for 4 h, 100 μ L of acid-isopropanol (0.1% HCl, 99.8% isopropanol (v/v)) was added and the plates were shaken until all the formazan crystals had dissolved. The absorbance was read on a Titertek Multiskan Plus (Flow Laboratories Inc., Mississauga, ON) at the dual wavelengths 570 and 650 nm. Metabolically active

cells reduce the tetrazolium dye (MTT) to a colored product, formazan crystals; therefore the color yield is proportional to the number of metabolically active cells, and indirectly approximates the cell viability (148). In result, the cytotoxicity of the drug is related to its effect on the color yield of treated cells following MTT exposure. The IC_{50} was defined as the drug concentration that produced a 50% reduction in control absorbance. To determine the IC_{50} , the % of control absorbance was plotted for each concentration (mean of the 6 wells) against the log [drug] using Slide Write Plus™ software (version 5.0, Advanced Graphics Software, Inc., Sunnyvale, CA). A curve was fitted using the same software by non-linear regression, applying the dose response logistic equation, and the IC_{50} was read from this curve.

2.16 Pharmacokinetics

The biodistribution and pharmacokinetics (PK) of ^{125}I -TI-loaded SL, SIL[IgG], and PIL[IgG] were compared. These studies were carried out in both naïve Balb/C or Alt BM mice and in SCID mice bearing i.v. Namalwa cells. These mice were inoculated with 5×10^6 Namalwa cells by the i.v. route, 24 h prior to the initiation of the PK studies. For the targeted formulations, either sheep IgG or anti-CD19 antibodies were coupled to the liposomes. Liposomes were prepared as described in earlier sections. Mice were injected i.v. with 0.5 μ mol PL ($2-5 \times 10^5$ cpm), via the tail vein. At selected time points (10 min, 30 min, 2 h, 6 h, 12 h, 24 h, and 48 h post injection) groups of three mice per liposome formulation were anesthetized with halothane and sacrificed by cervical dislocation. A blood sample was taken by cardiac puncture and the liver, spleen, lungs, heart, kidneys, and thyroid were excised. The blood and organs were counted for radiolabel in a Beckman 8000 gamma counter. ^{125}I -TI is cleared rapidly from circulation

($t_{1/2} < 10$ min) and is retained by intact liposomes; therefore ^{125}I -TI is used as a marker for intact liposomes. The percent of the remaining dose (cpm) in the blood and organs was calculated and the latter was corrected for blood content (47). The % of the remaining dose in blood was fitted to a pharmacokinetic model and pharmacokinetic parameters were calculated using a polyexponential curve stripping and least squares parameter estimation program PKAnalyst Software (Micromath, Salt Lake City, UT).

The pharmacokinetic model that best fit the data varied between formulations and in each case the selected model was chosen because it gave the highest model selection criteria value. PIL[sheep IgG] data was fit to a one compartment model, assuming bolus i.v. input and first-order output (Model 1). SL, SIL[sheep IgG], SIL[anti-CD19] and PIL[anti-CD19] data was fit to a two-compartment model, assuming bolus i.v. input and first-order output (Model 8).

2.17 *In vivo* therapeutic Efficacy

The therapeutic efficacies of free DXR, DXR-SL, DXR-SIL[anti-CD19], and DXR-PIL[anti-CD19] in SCID mice bearing i.v. Namalwa cells were compared with each other and with a saline control group. Cells for injection were pelleted by centrifugation for 10 min at 900 RPM, the media was aspirated, and the cells were re-suspended in PBS. The cell concentration was determined using a Coulter Counter (Coulter, Miami, FL) and adjusted with PBS to give a final concentration of 25×10^6 cells/ml. A total of 5×10^6 cells in a volume of 0.2 ml were injected i.v. via the tail vein. Following the injections the mice were sorted into weight-matched groups of five and each group was randomly assigned to a treatment regimen. In addition, the % viability of leftover cells was determined by Trypan Blue Exclusion. The liposomes were prepared

as previously described. Each formulation was sterile filtered and diluted in pyrogen-free, pH 7.4 HEPES buffer to give an appropriate doxorubicin concentration for injection. The mice were dosed at 2.5 mg DXR/kg according to the mean weight of each treatment group. The treatment was administered i.v., via the tail vein at 24 h following the inoculation of the mice with Namalwa cells. The mice were monitored daily and were euthanized at the onset of hind leg paralysis (HLP), or upon reaching a moribund state.

2.18 Statistical Analysis

Comparisons of binding/uptake, cytotoxicity, pharmacokinetic and therapeutic efficacy results for different formulations were done using the one-way analysis of variance (ANOVA) with InStat software (GraphPad™ software, version 3.0, SanDiego, CA). The Tukey post-test was used to compare the different treatment means and p-values less than 0.05 were considered significant. An unpaired t-test was used to statistically compare the K_D and B_{max} for SIL[anti-CD19] and PIL[anti-CD19] using Graphpad Prism software (SanDiego, CA).

Chapter 3

Development and optimization of the post-insertion method to prepare ligand-targeted liposomes

Chapter 3: Results and discussion

3.1 Determination of the CMC and Micelle Coupling Efficiency

The experiments reported in this chapter concern the development of the post-insertion method to prepare targeted liposomes. These experiments were performed in collaboration with Tatsuhiro Ishida and the results are published in Ishida *et al.*(149).

The phospholipid concentration at which the phospholipid monomers associate in aqueous media to form micelles is called the critical micellar concentration (CMC). To ensure that phospholipid micelles, as opposed to monomers, were formed and maintained throughout our experiments, it was necessary to determine the CMC for the phospholipids employed. Tatsuhiro Ishida determined the CMC for both Mal-PEG-DSPE and mPEG-DSPE by monitoring the turbidity of a solution containing increasing concentrations of phospholipid using spectrophotometry ($\lambda=240$ nm). The CMCs for Mal-PEG-DSPE and mPEG-DSPE were found to be 6.3 and 2.3 μM , respectively. During micelle hydration, coupling and incubation with liposomes the phospholipid concentration exceeded the CMC for Mal-PEG-DSPE.

The efficiency of IgG coupling to PEG-DSPE micelles (4:1 mPEG-DSPE: Mal-PEG-DSPE, mol:mol) was determined by Tatsuhiro Ishida. Due to the size similarity between IgG (150 000 Da) and IgG-PEG₂₀₀₀-DSPE (152 956 Da) it was not possible to separate non-coupled IgG for determination of the coupling efficiency using size exclusion chromatography. Instead, free IgG and IgG-PEG-DSPE were separated on the basis of differential densities by ultracentrifugation on a discontinuous metrizamide gradient. Fractions were collected and an elution profile was drawn on the basis of [¹²⁵I]-IgG and [¹⁴C]-mPEG-DSPE cpm (**Fig. 3.1**). The elution profiles for free IgG and IgG-

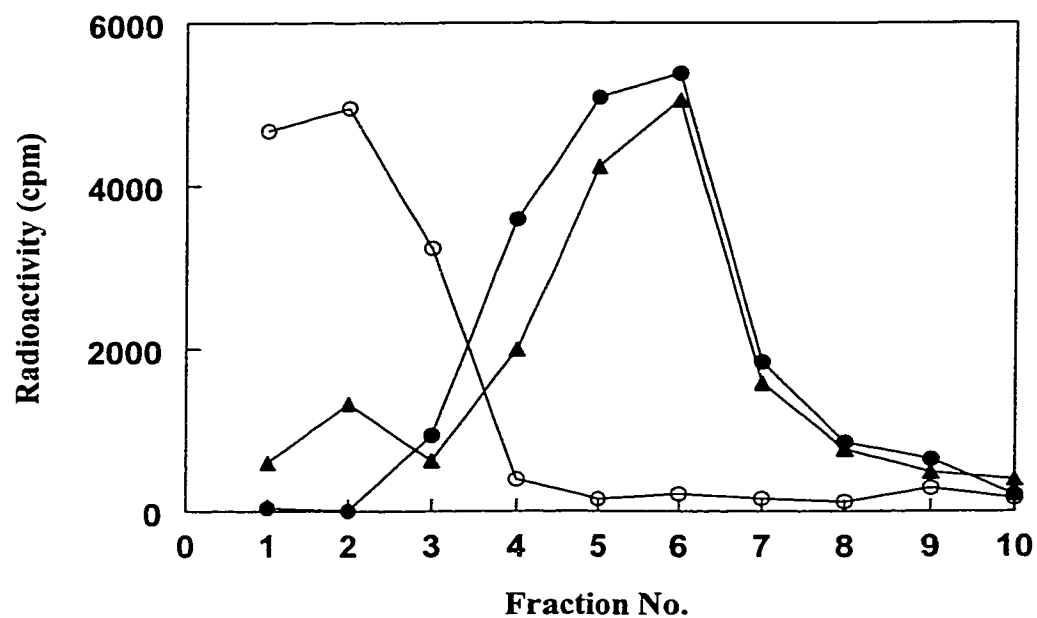


Fig. 3.1. Separation of free IgG from IgG-PEG-DSPE micelles on a metrizamide gradient. IgG-PEG-DSPE micelles were fractionated on a 40/50/60% (3/4/3 ml) discontinuous metrizamide gradient at 37 000 rpm for 14 h in a SW41 rotor using an L8-70 Ultracentrifuge. Ten 1 ml fractions were collected from the bottom of the gradient and counted for radiolabel. Free IgG was also fractionated separately as a control. The elution profiles shown represent cpm ^{125}I -IgG-PEG-DSPE (●), ^{125}I -IgG (○), and ^{14}C -mPEG-DSPE (▲). (From T. Ishida)

PEG-DSPE were previously characterized on identical columns, and used as a reference to identify the peaks. By integrating the area of the peaks corresponding to free IgG and IgG-PEG-DSPE it was concluded that the majority of the antibody was coupled to the micelles.

3.2 Optimization of the Incubation Conditions for Transfer

The next aim was to characterize the efficiency of IgG-PEG-DSPE insertion into preformed liposomes and determine the optimal incubation conditions for this transfer. The amount of mPEG-DSPE inserted into preformed liposomes was previously shown to be time- and- temperature-dependent (115). In addition, the insertion efficiency was found to increase when the incubation temperature exceeded the phase transition temperature (T_M) of the liposomal phospholipid (115). The liposomes employed in this thesis were made with the phospholipid HSPC, which has a T_M of 58°C. For this reason Tatsuhiro Ishida compared the IgG-PEG-DSPE insertion efficiency following incubation at 60°C or 37°C. After 1 h at 37°C only 10.4 % of the IgG transferred, but this amount increased by four times when the incubation time was lengthened to 24 h. However, the transferred amount after 24 h at 37°C was only half the amount observed after incubation for 1 h at 60°C. These results agree with those of Uster *et al.* (115), which showed that transfer of mPEG₂₀₀₀-DSPE is more efficient above the T_M of the liposomal PL. Furthermore, these results extend the finding to include the transfer of IgG-PEG₂₀₀₀-DSPE. It is not surprising that the transfer is more efficient above the T_M . The increased fluidity of the bilayer is likely to facilitate insertion of the IgG-PEG-DSPE monomers. In addition, the higher temperature would provide an obvious thermodynamic advantage. This would provide the requisite activation energy for the uptake of the micelle lipid,

which increases according to the amount of work needed to create a PEG-free area in the bilayer for insertion (150).

As mentioned in the introduction, the preferred methods for preparing targeted liposomes maximize efficiency. In result, wastage of precious materials is minimized and labile components are preserved. For this reason the remaining experiments reported in this thesis have focussed on characterizing post-insertion liposomes (PIL) prepared by transfer of IgG-PEG-DSPE during a 1 h incubation at 60°C because these conditions were found to be most efficient.

3.3 Effects of Micelle Composition on Transfer Efficiency

The next stage of our experiments focused on determining the optimal micelle and liposome composition to efficiently achieve the desired antibody density and PEG-DSPE content in the PIL. In an effort to maximize the efficiency of transfer we began our experiments using micelles composed entirely of the coupling lipid, Mal-PEG-DSPE. However, this resulted in micelle aggregation. The size of non-coupled, PEG-DSPE micelles was measured using a particle sizer and was shown to range between 30-50 nm. In most cases, following the coupling of IgG to the micelles the size increased to approximately 65-80 nm. This is reasonable, given that the maximal linear dimension of IgG is approximately 10.5 nm (151). However, IgG coupled micelles composed of 100% Mal-PEG DSPE could be in excess of 100 nm in diameter. This was proposed to occur by micelle aggregation due to cross-linking between IgG-PEG-DSPE monomers. Given that there are four potential coupling sites per antibody it is likely that multiple lipid molecules were conjugated to the same antibody. The production of aggregated micelles was considered undesirable since they could not be separated from 100 nm liposomes by

size exclusion, gel filtration chromatography. Since chromatography was used to purify PIL (from non-transferred micelles and free IgG) following transfer, the presence of aggregated micelles made the results difficult to interpret. Several approaches were investigated to reduce micelle aggregation. First, the molar ratio of Traut's:Ab was reduced from 20:1 (mol:mol) to 10:1 (mol:mol) to decrease the number of activated coupling sites from 4 to 2 per Ab. This was expected to limit the potential for aggregation by decreasing the likelihood that more than one lipid molecule coupled to the same antibody. Also, protecting the lipids and antibodies from exposure to oxygen during coupling is known to reduce the potential for the formation of disulfide bonds or 'cross-linking', between thiolated antibody molecules. Finally, the composition of the micelles was modified to include mPEG-DSPE, which is a non-coupling lipid. The addition of an inert lipid was expected to reduce the potential for micelle aggregation by reducing the number of lipid molecules that can bind to each antibody. Since the large size of IgG already sterically hinders coupling to adjacent PEG-DSPE molecules, the addition of an inert lipid was not expected to reduce the coupling efficiency to any extent.

Micelles composed of mPEG₂₀₀₀-DSPE and Mal-PEG₂₀₀₀-DSPE at either a 4:1 or 9:1 ratio were prepared and their elution profiles on Sepharose CL-4B were analyzed to evaluate whether the change in micelle composition reduced the micelle size. Molecules greater than 20×10^6 Da are excluded by this column matrix; therefore large micelles elute early, in the void volume of the column, producing a sharp peak early in the elution profile. For both formulations, the absence of a peak at the void volume was taken as evidence for the absence of large micelles (not shown). As an additional control, liposomes and micelles were mixed at room temperature (22°C) and immediately run

down a Sepharose CL-4B column to determine whether separation of the two was possible. By integrating the area under the curves for each peak on the elution profile it was determined that less than 4% of the micelles ran in the liposome fractions (not shown). From this we can conclude that the inclusion of a non-coupling lipid (mPEG-DSPE) at either a 4:1 or 9:1 ratio (mPEG-DSPE: Mal-PEG-DSPE, mol:mol) minimizes micelle aggregation.

While both micelle formulations were relatively resistant to micelle aggregation, the transfer efficiency was substantially lower for micelles composed of mPEG₂₀₀₀-DSPE:Mal-PEG₂₀₀₀-DSPE at a 9:1 ratio. The level of PEG-DSPE and IgG-PEG-DSPE insertion was compared for micelles composed of a 4:1 and 9:1 ratio of mPEG-DSPE:Mal-PEG-DSPE (mol:mol) in **Fig. 3.2 A,B**. Interestingly, the extent of PEG-DSPE transfer (**Fig. 3.2 B**) was much less affected by the micelle composition compared to IgG-PEG-DSPE transfer (**Fig. 3.2 A**). One possible explanation for this observation is that the ligand somehow hindered transfer so that mPEG-DSPE inserted preferentially over IgG-PEG-DSPE. It is also possible that the ligand could promote reverse transfer (desorption) of IgG-PEG-DSPE out of the bilayer, especially during the incubation process when the temperature was elevated and the bilayer was fluid. Finally, the predominance of mPEG-DSPE in the lipid mixture could have increased the probability of its insertion compared to the less prevalent IgG-PEG-DSPE. Given that an equilibrium exists between micelle fusion and desorption it is likely that the more prevalent lipid will be inserted preferentially into the liposome bilayer. However, it is also likely that a combination of factors were important. The micelle composition with the intermediate ratio of

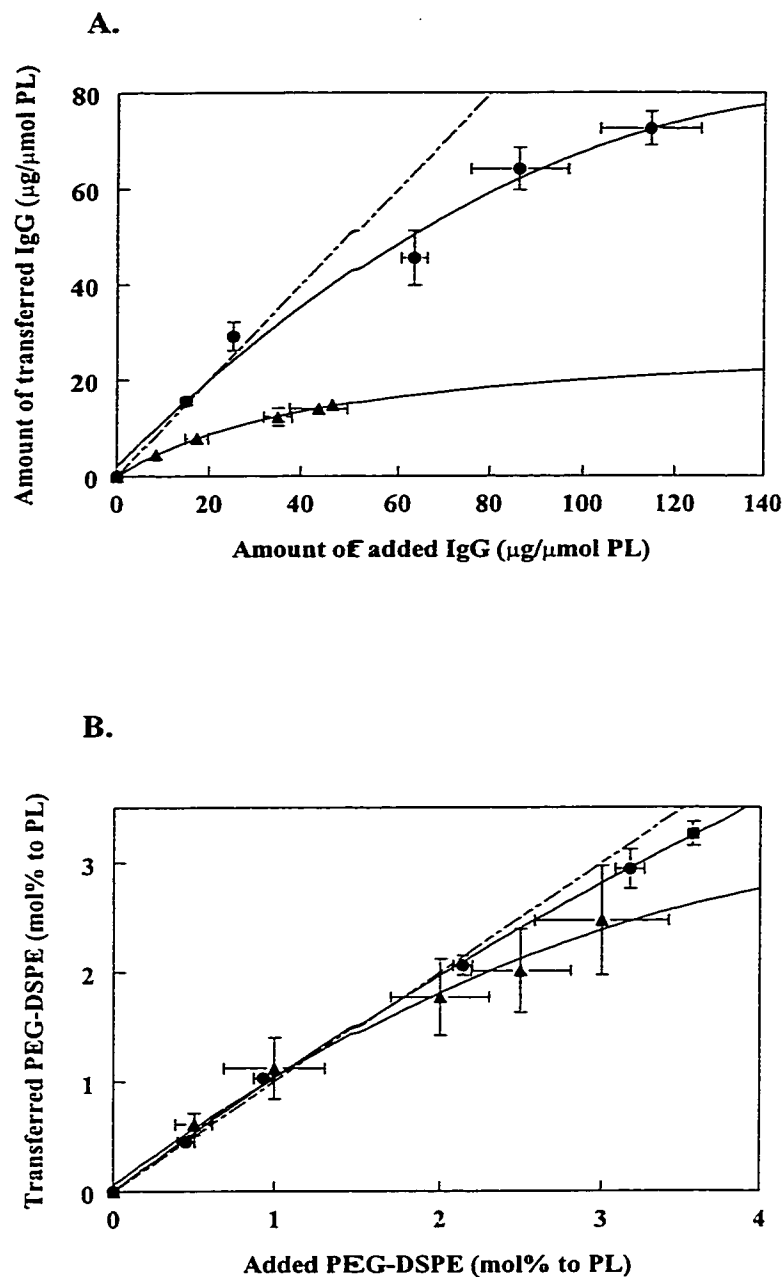


Fig. 3.2 Affect of micelle composition on the transfer of IgG-PEG-DSPE and PEG-DSPE from micelles to preformed liposomes. Liposomes were composed of HSPC:CHOL:mPEG-DSPE at a 2:1:0.08 molar ratio. Micelles were composed of mPEG-DSPE and Mal-PEG-DSPE at a 4:1 (●) or 9:1 (▲) molar ratio (mPEG-DSPE: Mal-PEG-DSPE) and sheep IgG was coupled using the Mal-PEG method at a 10:1 ratio of Mal-PEG-DSPE: IgG (mol:mol). The transfer of IgG-PEG-DSPE is shown in panel A and the transfer of PEG-DSPE is shown in panel B. The dotted line indicates 100% transfer. (From T. Ishida)

mPEG₂₀₀₀-DSPE:Mal-PEG₂₀₀₀-DSPE (4:1, mol:mol) was chosen for future studies in order to maximize the transfer amount as much as possible. However, this was not ideal. The use of higher ratios of coupling lipid would have been preferred because the transfer efficiency would have increased. In the future the use of a different coupling method, other than the Mal-PEG method, may be a viable solution. In particular methods that offer only one potential coupling site per antibody would be useful since cross-linking would be avoided. The Hz-PEG coupling method is site-directed to the Fc region on the antibody, and is one potentially useful method. In addition, Fab' antibody fragments couple via a single exposed thiol group (derived by cleavage of the inter-chain disulfide bond). Preliminary experiments with transfer of IgG-PEG-DSPE micelles that were coupled with either the Hz-PEG method or a modification of the Mal-PEG method for coupling of Fab' fragments suggest that more efficient transfer can be achieved. Further experimentation is needed to characterize the potential of site directed coupling methods for application in the post-insertion approach, but for now the results seem promising.

3.4 Effects of Liposome Composition on Transfer Efficiency

Next, we characterized the efficiency of insertion of both PEG-DSPE and IgG-PEG-DSPE into preformed liposomes with a PEG content ranging from 0-9.2 mol% of liposomal HSPC. These results are shown in **Fig. 3.3**. An inverse relationship existed between the liposomal PEG-DSPE content and the amount of additional PEG-DSPE that transferred into the bilayer from micelles. The most pronounced effect was seen for liposomes composed of 9.2 mol% PEG-DSPE. In this case, less than 50% of the added amount of PEG-DSPE inserted into the bilayer for all micelle concentrations tested and

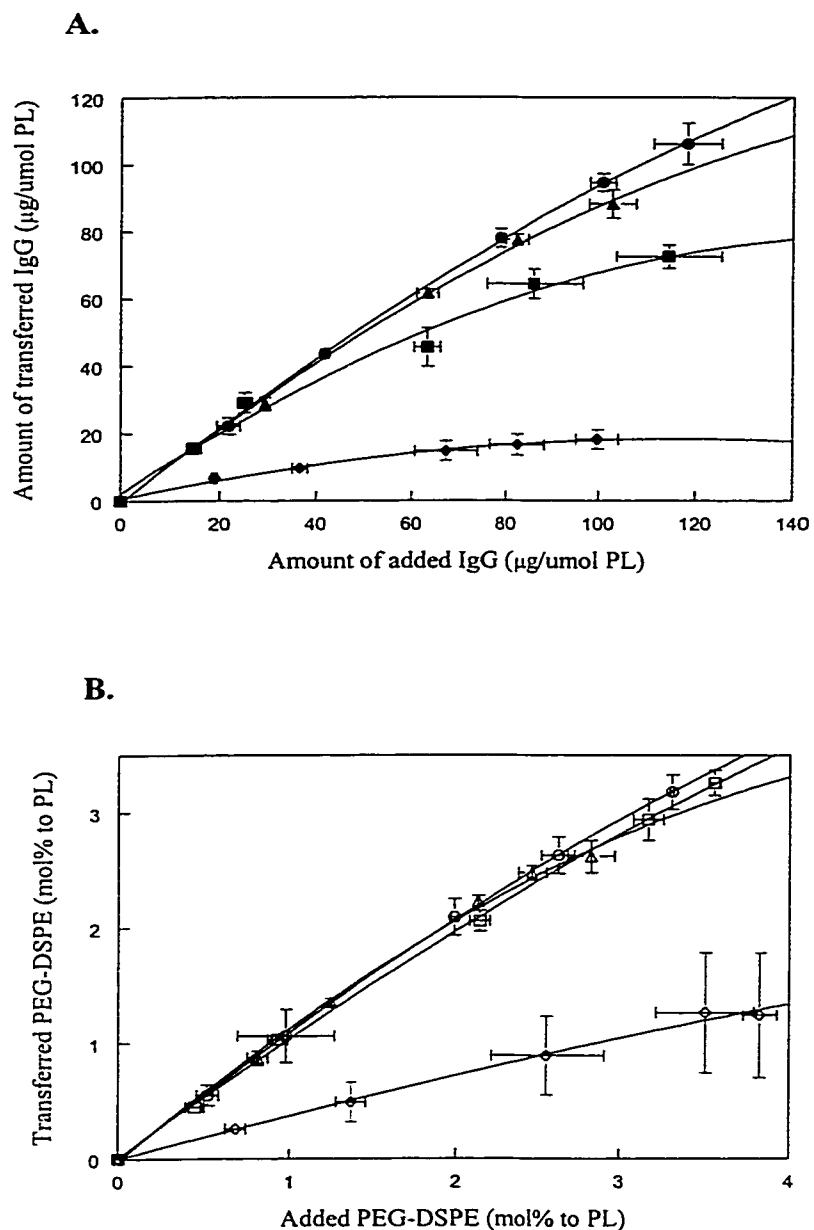


Fig. 3.3 Effect of liposome PEG₂₀₀₀-DSPE content on transfer of IgG-PEG₂₀₀₀-DSPE and PEG-DSPE from micelles into preformed liposomes (HSPC:CHOL, 2:1, mol: mol)(100 ± 10 nm). Aliquots of IgG-PEG₂₀₀₀-DSPE micelles were incubated with liposomes at specified molar ratios for 1 h at 60°C. Transferred IgG is shown in A. and transferred PEG-DSPE is shown in B. The liposome mPEG₂₀₀₀-DSPE content was as follows: CL(0 mol%)(●○), SL(2 mol%)(▲△), SL (4 mol%)(■□), SL(9.2 mol%)(◆◇). (From T. Ishida and D.L. Iden)

the maximal incorporation totaled less than 1.5% of liposomal PL. On the contrary, liposomes composed of 4 mol% PEG-DSPE, or less, showed 100 % transfer of added PEG-DSPE (Fig. 3.2 A). Transfer of IgG-PEG-DSPE, compared to PEG-DSPE alone, was even more inhibited by increasing mPEG-DSPE content in the liposomes. For instance, liposomes composed of 4 mol% PEG or higher showed a substantial decrease in IgG incorporation, compared to liposomes containing less mPEG-DSPE. Again, liposomes composed of 9.2 mol% PEG-DSPE showed poor incorporation, resulting in less than 20 $\mu\text{g Ab}/\mu\text{mol PL}$ at all micelle concentrations tested (20-100 $\mu\text{g Ab}/\mu\text{mol PL}$). A less dramatic decrease in incorporation of IgG-PEG-DSPE was also observed for liposomes composed of 4 mol% PEG. In this case the efficiency began to drop below 100% when more than 35 $\mu\text{g Ab}/\mu\text{mol PL}$ was added, and went as low as 60% when adding 115 $\mu\text{g Ab}/\mu\text{mol PL}$. At this concentration, up to 70 $\mu\text{g Ab}/\mu\text{mol PL}$ was incorporated. Conversely, the transfer of both PEG-DSPE and IgG-PEG-DSPE reached 100 % efficiency for liposomes composed of 0 or 2 mol% PEG-DSPE.

In addition, the extent of IgG insertion into CL (0 mol% PEG-DSPE) was compared for IgG-PEG-DSPE and free IgG. Theoretically, the use of non-pegylated liposomes should maximize the transfer of free IgG due to the absence of steric hindrance. The transfer of free IgG was found to be minimal, compared to the transfer of IgG-PEG-DSPE (Fig. 3.4). This result exemplifies the importance of the lipid anchor in promoting the transfer of IgG into preformed liposomes.

In summary, we have shown that at least 110 $\mu\text{g IgG}/\mu\text{mol PL}$ in the form of IgG-PEG-DSPE can be inserted into the bilayer of preformed, drug-loaded liposomes in a time- and temperature-dependent manner. However, the amount of transfer is inversely

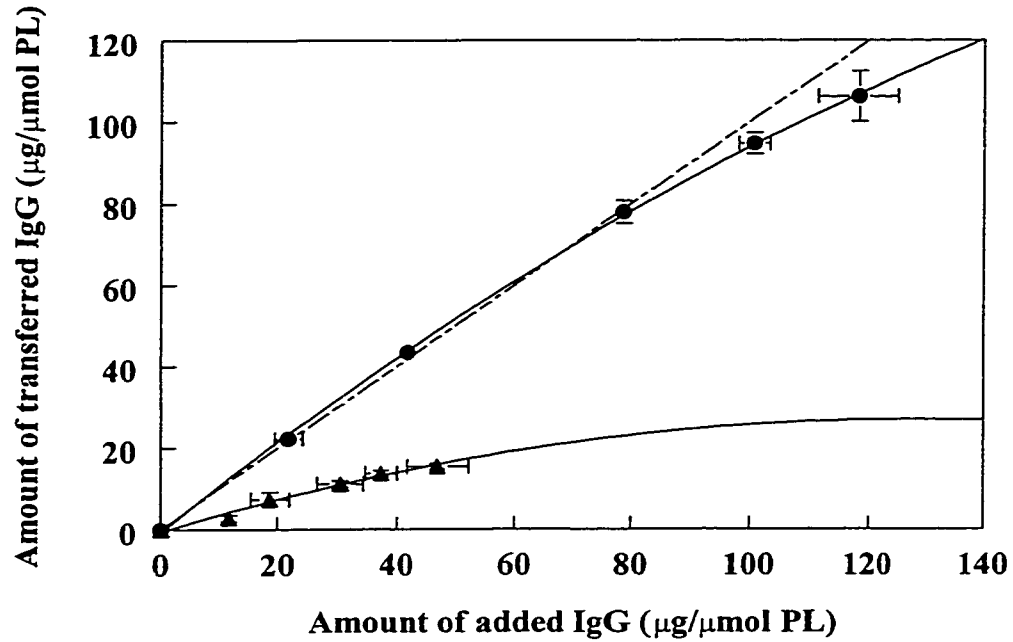


Fig. 3.4. Comparison of free IgG (▲) and IgG-PEG-DSPE micelle (●) transfer to CL. Liposomes were composed of HSPC:CHOL (2:1, mol:mol) and the micelles were composed of mPEG-DSPE and Mal-PEG-DSPE at a 4:1 molar ratio, and were coupled with sheep IgG at a 10:1 ratio of Mal-PEG: IgG (mol:mol) by the Mal-PEG method. Transfer occurred during a 1 h incubation at 60°C and IgG incorporation ($\mu\text{g IgG}/\mu\text{mol}$ liposome PL) was determined from the cpm ^{125}I -IgG and the specific activity. The dotted line indicates 100% transfer. (From T. Ishida and D.L. Iden)

proportional to the content of PEG in the liposomes prior to transfer. These results are consistent with those of Needham *et al.*, who found an inhibition of mono-oleylphosphatidylcholine micelle fusion with pegylated liposomes with increasing concentrations of PEG (150). The authors propose that micelle fusion with liposome bilayers requires contact between the phospholipid head groups and that areas on the membrane free from PEG must be created to allow this interaction to take place. As the concentration of PEG in the bilayer increases, increasing amounts of energy in the form of work is required to clear an area of membrane. In their system, this activation energy requirement was thought to be responsible for prevention of micelle fusion with liposomes containing more than 10 mol% PEG. They maintain that transfer occurs by fusion of monomers and oligomers above this threshold concentration. The present demonstration of reduced transfer to liposomes containing 9.2 mol% PEG is consistent with their finding. The reason that the transfer of IgG-PEG-DSPE is inhibited to a greater degree by the liposome PEG content is unknown. It is possible that the attachment of a ligand to PEG-DSPE alters the transfer behavior of the lipid, akin to the reduction in opsonization by plasma proteins. Perhaps the attachment of IgG to the PEG terminus sterically hinders the interaction of the micelle and bilayer phospholipid headgroups. If this interaction is required to initiate transfer, then IgG may inhibit transfer by this mechanism.

These experiments have shown that it is possible, using the post-insertion approach, to prepare targeted liposomes that have sufficient PEG-DSPE content and high enough antibody densities for therapeutic applications. Specifically, we aimed to achieve 5-10 mol% PEG-DSPE and 25-60 $\mu\text{g Ab}/\mu\text{mol IgG}$ because this is the range of antibody

and PEG contents that are necessary to achieve long circulation *in vivo* (80). However, PEG-DSPE in preformed liposomes is distributed between the outer and inner monolayers, and transferred PEG-DSPE is exclusively situated in the outer monolayer. It is the PEG content in the outer monolayer that is important for steric stabilization. The PEG content in the outer monolayer of preformed liposomes containing 5 mol% total PEG is approximately 2.5-3%. To achieve an equivalent level of PEG in the outer monolayer of liposomes containing 4 mol% PEG (2-2.5 % in the outer monolayer) the transfer of an additional 1-1.5 mol% PEG would be required. We have shown that this level of antibody and PEG-DSPE incorporation could be efficiently attained by transfer to preformed liposomes composed of 0-4 mol% mPEG-DSPE. For the remaining experiments reported in this thesis, liposomes containing 4 mol% mPEG-DSPE were incubated with micelles at either a 4:100 or 5:100 ratio of micelle PL: liposome HSPC (mol:mol).

While we had shown that the appropriate level of IgG-PEG-DSPE insertion was achievable, it was also necessary to show that the ligand was retained in the liposomes following transfer, in order ensure effective targeting. Tatsuhiro Ishida determined the proportion of transferred IgG and PEG-DSPE that remained associated with PIL after 48 h exposure to human plasma. Fortunately, this experiment showed that the stability of insertion is excellent with $102.3 \pm 2.4\%$ of transferred IgG and $99.4 \pm 8.2\%$ of transferred PEG-DSPE remaining associated with the liposomes. Since the mean residence time of immunoliposomes is approximately 24 h, it is reasonable to conclude that the IgG will remain associated with the liposomes for as long as the liposomes circulate. This is provided that the rate of exchange out of the bilayer does not accelerate *in vivo*. While

the presence of additional plasma proteins and lipoproteins *in vivo* may accelerate this process somewhat, the liposomes would be more likely cleared from circulation before a substantial loss of IgG occurred.

Since the drug to phospholipid ratio is an important determinant of the therapeutic efficacy of liposomal drugs and transfer of IgG-PEG-DSPE and PEG-DSPE invariably leads to the production of transient membrane defects, we considered it important to evaluate whether encapsulated drug is lost during transfer. Tatsuhiro Ishida quantified the amount of drug loss during a 6 h incubation at 60°C in the presence and absence of IgG-PEG-DSPE. Approximately 4% of encapsulated doxorubicin was released in the absence of IgG-PEG-DSPE micelles and this increased by only 2-3% in their presence. If a uniform rate of leakage occurred over the 6 h, then the amount of leakage during a 1 h incubation would be negligible. Indeed, the amount of free doxorubicin that can be visualized during chromatography of the PIL indicates that very little drug is released. The disruption of the bilayer might be expected to result in greater drug loss. However, in this case the doxorubicin loading method employed promotes the formation of a doxorubicin sulfate precipitate, which would inhibit drug leakage in the face of transient bilayer disruption. For this reason, future studies will be needed to determine the practicality of the post-insertion method for liposomes loaded by other methods and with other drugs.

In conclusion, these experiments have shown that transfer of IgG-PEG-DSPE from a micelle phase, into the bilayer of preformed liposomes is possible and most efficient above the phase transition temperature of the liposomal phospholipid. The optimal micelle composition consists of a mixture of coupling and non-coupling lipids at

a 4:1 ratio of mPEG-DSPE: Mal-PEG-DSPE. This composition minimizes micelle aggregation and maximizes IgG-PEG-DSPE transfer efficiency. In addition, we have shown that at least 110 $\mu\text{g IgG}/\mu\text{mol PL}$ can be inserted into the bilayer of preformed liposomes, but the amount of transfer is inversely proportional to the content of PEG in the liposomes prior to transfer. Finally, a suitable level of PEG-DSPE and IgG incorporation for *in vivo* administration can be achieved using the post-insertion method. This incorporation is stable and does not result in extensive drug leakage. From the data presented in this chapter it can be concluded that post-insertion liposomes are suitable for further evaluation of potential therapeutic efficacy.

Chapter 4

***In vitro* targeting of post-insertion immunoliposomes and conventional immunoliposomes to human B-cell lymphoma cells**

Chapter 4: Results and Discussion

4.1 Binding/uptake

The aim of the research in this chapter was to evaluate the targeting effectiveness of PIL[anti-CD19] *in vitro* compared to SIL[anti-CD19]. Demonstrating that PIL show an ability to bind to their target cells *in vitro* is an important indicator of potential *in vivo* efficacy. For targeted liposomes to have a therapeutic advantage, they must show specific (antibody-mediated) selectivity and avidity for their target cells. For this reason we evaluated whether PIL[anti-CD19] show enhanced binding/uptake compared to non-targeted liposomes (SL) of similar composition. The term binding/uptake is applied here because the incubation conditions were permissible for endocytosis (37°C) and, with the current protocol, it was not possible to distinguish liposome internalization from cell surface binding. In order to separate these two processes it would have been necessary to block endocytosis by changing the incubation temperature or using metabolic inhibitors.

Since antibodies are proteins that are heat labile it is possible that the optimal time and temperature conditions, shown in Chapter 3, for efficient transfer of IgG-PEG-DSPE into preformed liposomes may have a detrimental effect on the antibody. A disruption of the antibody structure could influence its ability to bind effectively to its target antigen, which in turn could negatively impact the binding/uptake of PIL by their target cells. In addition, targeted liposomes made by the post-insertion method could differ from SIL in other respects that may also affect their interaction with the target cells. For this reason we considered it critical for the future of PIL to evaluate their binding/uptake by the target cells.

It has been previously shown that SIL[anti-CD19] show specific binding/uptake by Namalwa cells. Additionally, DXR-SIL[anti-CD19] were shown to have a therapeutic advantage in an animal model of human B-cell lymphoma (91). We chose to compare the binding/uptake of SIL[anti-CD19] and PIL[anti-CD19] with non-targeted SL. This is a good strategy for multiple reasons. First, the possibility that the preparation of targeted liposomes by conventional techniques provides a superior product, in terms of targeting potential can be confirmed or refuted. Also, comparing the binding/uptake of PIL with a formulation that is known to show effective targeting provides a relevant standard. Theoretically, any negative effects of the post-insertion method on the antibody should impair the binding/uptake of PIL[anti-CD19], compared to SIL[anti-CD19]. In addition, the *in vitro* targeting ability of PIL in a therapeutically relevant model may predict the potential of PIL in the clinic.

The binding/uptake of SL, SIL[anti-CD19], or PIL[anti-CD19] by CD19-expressing Namalwa cells is shown in **Fig. 4.1**. Non-targeted SL were included as a measure of non-specific binding. These liposomes were the same composition as the targeted formulations, except for the absence of antibody and a small percentage of Mal-PEG-DSPE. As expected, the non-specific binding/uptake (SL) increased linearly with increasing concentrations of phospholipid (PL). For the targeted formulations, both the total binding/uptake (**Fig. 4.1 A**) and the specific binding/uptake (**Fig. 4.1 B**) are shown. Specific binding is defined as the total binding/uptake minus the non-specific binding/uptake. The amount of specifically associated PIL and SIL (**Fig. 4.1 B**) increased at PL concentrations below 400 nmol/ml and seemed to saturate above this concentration. At this concentration the total binding/uptake of SIL[anti-CD19] and

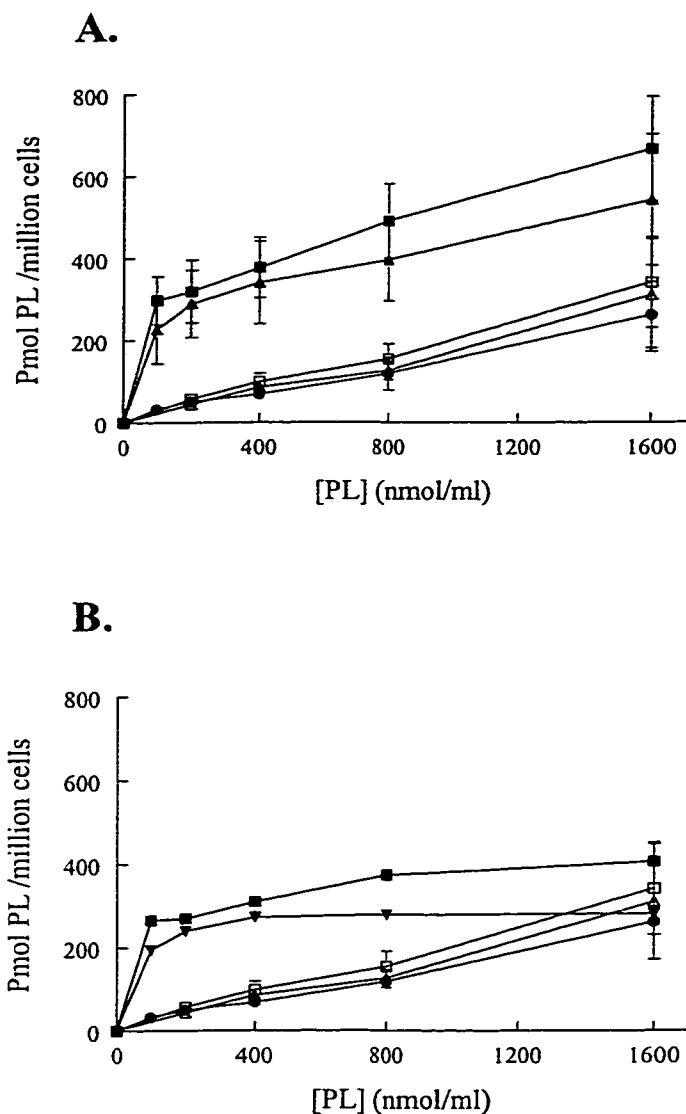


Fig. 4.1 *In vitro* binding/uptake of anti-CD19 targeted liposomes and non-targeted liposomes. Liposomes were 100 ± 10 nm and composed of HSPC:CHOL:mPEG₂₀₀₀-DSPE, 2: 1: 0.1 (mol:mol). Targeted formulations also contained 25-40 μ g anti-CD19/ μ mol PL. Increasing concentrations of ³H-CHE labeled SL (●) (n=10), SIL[anti-CD19] (■) (n=12), and PIL[anti-CD19] (▲) (n=12) were incubated with 1×10^6 Namalwa cells for 1 h at 37°C. In competition experiments 3-97 fold excess free anti-CD19 was incubated at 20 min prior to the addition of SIL[anti-CD19] (□) (n=6) and PIL[anti-CD19] (△) (n=6). Panel A shows the total cell associated PL for all formulations, while in panel B the non-specifically bound PL (SL) was subtracted from the total cell associated PL for SIL[anti-CD19] and PIL[anti-CD19]. Data are expressed as pmol PL \pm S.D. (from the specific activity) per 10^6 cells.

PIL[anti-CD19] was 5.5 and 5.0 fold greater than SL, respectively (Fig. 4.1 A). The fact that both SIL [anti-CD19] and PIL [anti-CD19] displayed increased binding/uptake compared to non-targeted SL, suggests that the antibody mediated specific targeting. Competition experiments with free anti-CD19 were performed to confirm the antibody specificity of the increased binding/uptake. In these studies the CD19 receptors were blocked by pre-incubation of the cells with excess free anti-CD19 antibody, 20 min before the addition of the liposomes. At the highest PL concentration the amount of free antibody added was equivalent to 3 times the amount of antibody present on the surface of the liposomes. Since a constant amount of antibody was added to each well of cells, the amount of excess free antibody increased with decreasing PL concentrations. In these competition experiments the amount of uptake/binding of both SIL[anti-CD19] and PIL[anti-CD19] overlapped that of SL (Fig. 4.1 A,B). There was no significant difference between SL, SIL[anti-CD19]+ free anti-CD19, and PIL[anti-CD19]+free anti-CD19 at all concentrations tested, with one exception. A significant difference was found between SL and SIL in the presence of free Ab for the PL concentration of 400 nmol/ml ($p < 0.01$) for an unknown reason. It should be noted that the standard deviation in the binding/uptake at that concentration was unusually low (± 2.3 pmol). Overall, it can be concluded that the increased binding/uptake of both targeted formulations is an antibody-specific effect. In addition, previous studies using isotype-matched antibodies have demonstrated that this specific binding/uptake is unique to anti-CD19 antibodies (91). Further demonstration of CD19 specificity is beyond the scope of this thesis.

At saturating conditions (400 nmol/ml) SIL showed an overall level of binding that was slightly higher than PIL. However, a significant difference in total binding

occurred at only two concentrations ($p < 0.05$ at 100 and 800 nmol/ml). Since the binding advantage of targeted liposomes is expected to be greatest at low concentrations, where there is a lower potential for non-specific binding, it would be interesting to see whether a significant difference between the binding/uptake for SIL and PIL would occur consistently at lower concentrations.

To further compare the binding/uptake for the two targeted formulations, the number of binding sites (B_{max}) and K_D were also determined. Theoretically, the number of binding sites for anti-CD19 on Namalwa cells should be a function of the number of cell surface CD19 receptors; therefore there should be an equal number of sites for SIL[anti-CD19] and PIL[anti-CD19]. However, this is based on the assumption that the antibody on each liposome has equal affinity for the receptors. In reality the apparent number of binding sites is affected by the affinity of the ligand. In addition, liposomes are capable of multivalent binding; therefore one liposome can potentially bind to more than one CD19 receptor. Since liposome binding/uptake was quantified using radiolabeled liposomes, the number of binding sites was not necessarily related to the number of CD19 receptors. Also, the strength of the binding interaction of all the contributing sites is defined as avidity and it can also affect the number of apparent binding sites. Importantly, any negative change in antibody affinity/avidity that resulted from the transfer conditions was expected to reduce the apparent number of binding sites, or B_{max} , for PIL[anti-CD19] in comparison with SIL. For the remainder of this thesis the strength of the binding interaction will be referred to simply as avidity since the methods employed in this study cannot measure affinity.

The binding/uptake data was expressed in $\mu\text{mol PL per } 10^6 \text{ cells}$; however, with respect to binding sites it is more informative to determine the number of liposomes per $\mu\text{mol PL}$. This was calculated from the literature values for bilayer thickness and the molecular areas for HSPC, CHOL, and PEG-DSPE. With the assumptions that the liposomes were spherical, 100 nm in diameter, and contained unilamellar bilayers with monodisperse PL, the number of liposomes per $\mu\text{mol PL}$ is estimated at 7.7×10^{12} . From this information the number of antibodies for liposomes containing 25-40 $\mu\text{g anti-CD19}/\mu\text{mol PL}$ was calculated to range between 13-21 antibodies per liposome.

The B_{max} was found to be $393 \pm 50 \text{ pmol/million cells}$ for SIL[anti-CD19] and $270 \pm 51 \text{ pmol/million cells}$ for PIL[anti-CD19]. This translates into approximately 3026 and 2067 liposome binding sites per cell for SIL[anti-CD19] and PIL[anti-CD19], respectively. Despite the fact that the binding/uptake of PIL[anti-CD19] saturates at a lower PL concentration, there was no significant difference in the B_{max} for the two targeted formulations. In addition, there was no significant difference in the avidity of SIL[anti-CD19] ($K_D=73 \pm 50 \mu\text{M}$) and PIL[anti-CD19] ($K_D= 78 \pm 37 \mu\text{M}$). It is clear that the avidities are not greatly different and that a proportion of the antibody on the surface of the PIL was able to bind to the target antigen effectively. From this we can conclude that the post-insertion method, and in particular the incubation conditions presently employed, do not adversely affect the avidity of anti-CD19 for its target antigen to any great extent.

The number of binding sites for free anti-CD19 (FMC63) on Namalwa cells has not yet been determined. However, using other anti-CD19 antibodies the number of anti-CD19 binding sites has been determined to be 4×10^4 (103, 152). If this value is also a

reasonable estimate for FMC63 antibodies, then the number of binding sites for liposomes, as determined in this study, is substantially lower than the number of binding sites for free antibody. This may suggest that the liposomal Ab has reduced avidity compared to free antibody, perhaps due to the coupling process, or that the Ab is sterically hindered from binding to its target by the presence of PEG in the liposomes (78). Alternatively, cooperativity in binding may occur. In the case of multivalent binding, more than one receptor will be occupied by each liposome and the apparent number of binding sites may decrease. This is a feasible possibility, since the cross-linking of CD19 antigens by antibodies is involved in signaling from the CD19 receptor.

Interestingly, the amount of binding/uptake for all formulations was much lower than reported in a previous study from our laboratory (91). This resulted in a 10 fold decrease in the estimated number of SIL[anti-CD19] binding sites, compared to the estimate reported by Lopes de Menezes *et al.*, (91). The method used to purify the antibody in the previous study differed from the present one, which may affect the binding/uptake results. However, it is more likely that the use of a different coupling method explains the disparate results. In the previous study the hydrazide method was employed. This method results in the attachment of antibody in a consistent orientation that leaves the antigen-binding region exposed and able to interact with the target. The coupling method employed in this study (Mal-PEG) leads to the incorporation of antibody in several orientations. As a result, it is possible that the apparent number of binding sites was reduced in proportion to the number of antibodies that were oriented in a direction in which the binding region was exposed to the antigen. However, this argument may over-emphasize the importance of antibody orientation considering that

the antibodies are tethered to the liposome at the PEG termini and the PEG layer is mobile. Although it is possible that antibodies in any orientation may be capable of accessing the target, it is also conceivable that there could be some Ab orientations that prevent target access. However, the Mal-PEG coupling method could affect binding in other ways. Antibody activated using Traut's reagent has been shown to bind less effectively to Namalwa cells than un-treated antibody (Elaine Moase, personal communication). This may result from the introduction of sulfhydryl groups to amino acids within the antigen-binding region of the antibody. The coupling of antibodies to micelles via the antigen-binding region would be expected to further interfere with binding. While small changes in the antigen-binding region may not prevent binding of the antibody to CD19, it is possible that receptor activation could be blocked. As a result antibody binding may not lead to endocytosis of the antibody-receptor complex and receptor recycling. A concomitant reduction in liposome binding/uptake would ensue and may explain the disparate results between the present and previous studies.

Further studies comparing binding/uptake of targeted liposomes made by the Mal-PEG and Hz-PEG methods would be useful for interpretation of the present results. It is possible that the application of site-directed coupling methods, such as the Hz-PEG method, may be more appropriate to prepare targeted liposomes. Additionally, the use of antibody fragments as targeting agents may eventually make targeting with whole antibodies obsolete. Antibody fragments are superior for many reasons, including the fact that they are less immunogenic and can be easily coupled to lipids via naturally occurring, inter-chain sulfhydryl groups. They also offer site-directed coupling via a single sulfhydryl group, which may lead to superior binding/uptake by the target. As

discussed in Chapter 3, site-directed coupling might be particularly beneficial for the post-insertion method because the potential for micelle aggregation would diminish. This may in turn result in better transfer efficiency and reduced contamination.

The concept of multivalent binding may be particularly important for targeting to the CD19 receptor and, likewise, the interpretation of the present binding/uptake data for the following reasons. First, antibody-mediated cross-linking or dimerization of CD19 receptors is known to initiate cell-signaling pathways (99, 126) and may be important for the initiation of receptor-mediated endocytosis (153, 154). Endocytosis followed by receptor re-cycling would lead to an increase in the number of available receptors. Then it follows that the triggering of endocytosis by multivalent binding would lead to a difference in the overall level of cell-associated liposomes; therefore a difference in capacity for multivalent binding between the two targeted formulations would be manifested as a change in binding/uptake. It is possible that the small difference in binding/uptake reported here for SIL[anti-CD19] and PIL[anti-CD19] reflects a difference in their capacities for endocytosis. Nevertheless, information regarding this capacity may provide more information about the state of anti-CD19 following transfer.

We have studied the binding/uptake of SL, SIL[anti-CD19] and PIL[anti-CD19] at a temperature that is non-permissive for receptor-mediated endocytosis (4°C) in an attempt to further characterize the binding/uptake of PIL[anti-CD19] vs. SIL[anti-CD19], but the results were inconclusive.

In summary, the binding/uptake data shows that for the majority of PL concentrations tested the amount of total binding/uptake is not significantly different for SIL[anti-CD19] versus PIL[anti-CD19]. It remains possible that the targeting ability is

significantly superior for SIL at lower concentrations than the ones studied here.

However, the important message is that the overall binding/uptake capacity (B_{max}) and affinity (K_D) of PIL does not appear to be significantly different from SIL, at least within a certain PL concentration range. In conclusion, the binding/uptake data reported here shows that the potential exists for effective targeting of Namalwa cells by PIL.

4.2 Cytotoxicity

The increased binding/uptake of PIL[anti-CD19] by Namalwa cells, compared to non-targeted SL, was expected to result in targeted delivery of encapsulated anti-cancer drugs. In theory, this should confer a cytotoxic advantage of DXR-PIL[anti-CD19] against the same cells. Indeed, the extent of internalization has been shown to correlate with cytotoxicity (103). Since the therapeutic potential of drug-loaded PIL depends on their cytotoxicity the following experiments compare the cytotoxicity of DXR-PIL[anti-CD19] with non-targeted DXR-SL, DXR-SIL[anti-CD19] and free DXR. In addition, these experiments were meant to elucidate whether DXR-PIL[anti-CD19] have at least comparable *in vitro* cytotoxicity compared to the available therapeutic alternatives, including doxorubicin-loaded immunoliposomes made by an alternative technique (SIL[anti-CD19]).

The *in vitro* IC_{50} for free DXR, DXR-SL, DXR-SIL[anti-CD19], or DXR-PIL[anti-CD19] were determined for both 1 and 24 h incubations using the MTT assay. This experimental design was meant to highlight any cytotoxic advantage of the targeted formulations for the following reasons. In general, there is a positive correlation between the level of cell exposure to anti-cancer drugs and the cytotoxic effect. For this reason, formulations that have the greatest drug availability will be the most cytotoxic. In this

study, the intracellular delivery of drug was expected to occur by two separate, time-dependent mechanisms; either by diffusion of free DXR across the plasma membrane or by receptor-mediated endocytosis of intact, DXR-loaded liposomes. Free doxorubicin rapidly diffuses across the plasma membrane to enter the nucleus (site of action). On the other hand liposome entrapped doxorubicin must be released before it can diffuse into cells. HSPC:CHOL liposomes release their encapsulated doxorubicin slowly (<10% after 24 h incubation) in buffer and this rate of leakage increases only slightly in the presence of human plasma (16% in 24 h) (155). The interaction of liposomes with cells and serum proteins (FBS) is known to cause bilayer destabilization and accelerated leakage of liposome contents (156, 157). Nevertheless, the amount of drug released from the liposomes in the first hour was likely minimal. In contrast, liposome binding and internalization begins within minutes of incubation (158). Indeed, internalization of the CD19 receptor has been shown to occur rapidly following binding of anti-CD19 (HD37) antibody to a B-cell lymphoma cell line (Daudi) (153, 159). Kinetic studies of other receptors have shown that receptor internalization and recycling occurs many times over the period of 1 h (105). The exact time scale for externalization of anti-CD19 receptors has not been elucidated. However, at least one study indicates that it begins within 1 h (159). Studies in our laboratory that have shown that the amount of cell associated DXR after 1 h incubation is substantially greater for DXR-SIL[anti-CD19], compared to DXR-SL (155). For this reason targeted liposomal doxorubicin was expected to have a cytotoxic advantage at 1 h, but after 24 h the contribution of released doxorubicin was expected to diminish the advantage of targeting.

The *in vitro* IC₅₀ for free DXR, DXR-SL, DXR-SIL[anti-CD19], or DXR-PIL[anti-CD19] are shown in **Table 4.1** and the results of a one-way anova comparing the cytotoxicities is shown in **Table 4.2**. Free doxorubicin was significantly more cytotoxic than DXR-SL ($p < 0.001$), but not DXR-SIL[anti-CD19] and DXR-PIL[anti-CD19] for the 1 h incubation. This was expected since a large amount of free DXR has been found to accumulate in Namalwa cells over the span of 1 h (155). This is likely due to relatively rapid diffusion across the cell membrane because the drug is more available when it is not entrapped within liposomes. In addition, a large proportion of this drug is associated with the nucleus, which one site of drug action (155). As predicted, the targeted formulations also had a cytotoxic advantage after 1h.

After 24 h incubation, free DXR was significantly more cytotoxic than DXR-SL ($p < 0.001$), DXR-SIL[anti-CD19] ($p < 0.05$), and DXR-PIL[anti-CD19] ($p < 0.05$). The fact that the non-targeted formulation was considerably (18.3 fold) less cytotoxic, compared to free DXR implies that a minimal amount of drug was released from the liposome and it was less available. Although a significant difference was found between free DXR and the targeted formulations ($p < 0.05$), the difference was less substantial.

A comparison of the liposomal formulations revealed that targeted ones were considerably more cytotoxic than the non-targeted formulations, with 4.1- and 4.6-fold decrease in the 1 h IC₅₀ for DXR-SIL[anti-CD19] ($p < 0.001$) or DXR-PIL[anti-CD19] ($p < 0.001$), respectively. The fold decrease in the IC₅₀ for the targeted formulations was less substantial after 24 h incubation at 1.9- and 1.8-fold for DXR-SIL[anti-CD19] ($p < 0.001$) and DXR-PIL[anti-CD19] ($p < 0.001$) compared to DXR-SL,

Table 4.1. Cytotoxicity (IC_{50} μ M) of non-targeted and anti-CD19 targeted formulations of DXR against CD19+ Namalwa cells *in vitro* by the MTT assay.

Formulation	1 h IC_{50}	24 h IC_{50}
Free DXR	0.6 \pm 0.3 (n=3)	0.3 \pm 0.1 (n=3)
DXR-SL	142 \pm 27 (n=3)	5.1 \pm 1.3 (n=4)
DXR-SIL[anti-CD19]	35 \pm 25 (n=3)	2.8 \pm 0.7 (n=4)
DXR-PIL[anti-CD19]	31 \pm 8.9 (n=4)	2.8 \pm 0.5 (n=3)

Namalwa cells (5×10^5) were incubated with free DXR, DXR-SL, DXR-SIL[anti-CD19], and DXR-PIL[anti-CD19] for 1 or 24 h at 37°C in an atmosphere of 5% CO₂ and 90% humidity. The liposomes were composed of HSPC:CHOL:mPEG₂₀₀₀-DSPE (2: 1: 0.1, mol:mol) and targeted formulations were coupled with 25-40 μ g anti-CD19/ μ mol PL using the Mal-PEG coupling method. Each plate was incubated for a total of 48 h, after which MTT was added to the plates. The plates were incubated for a further 4 h and then developed with acid-isopropanol and read at the dual wavelengths of 570 and 650 nm. The data is expressed as mean $IC_{50} \pm$ S.D., where each IC_{50} represents the drug concentration which results in a 50% reduction in absorbance (mean of 6 wells) compared to control (mean of 12 wells).

Table 4.2. Statistical comparison of the 1 h and 24 h IC₅₀ of non-targeted and CD19 targeted formulations of DXR against Namalwa cells *in vitro*.

Comparison	p-value
1 h IC₅₀	
SIL[anti-CD19] vs PIL[anti-CD19]	ns
SIL[anti-CD19] vs. SL	<0.001
PIL[anti-CD19] vs. SL	<0.001
Free DXR vs. SL	<0.001
Free DXR vs. SIL [anti-CD19]	ns
Free DXR vs. PIL [anti-CD19]	ns
24 h IC₅₀	
SIL[anti-CD19] vs. PIL[anti-CD19]	ns
SIL[anti-CD19] vs. SL	<0.05
PIL[anti-CD19] vs. SL	<0.05
Free DXR vs. SL	<0.001
Free DXR vs. SIL[anti-CD19]	<0.05
Free DXR vs. PIL[anti-CD19]	<0.05

All liposomes were loaded with doxorubicin. Statistical significance was evaluated using a one-way anova and the IC₅₀ from Table 4.1 were compared using the Tukey post test (Instat version 3.0, Graph Pad Software, San Diego, CA)

respectively. Overall, the results were according to expectation. At the short incubation time, the formulations that were expected to have greater drug availability, including free DXR and the targeted formulations, were most cytotoxic. From this it can be inferred that the targeted formulations allow cytoplasmic delivery of large amounts of DXR, probably by receptor-mediated endocytosis of drug-loaded liposomes. In the case of DXR-SL the drug must be released from the liposome before it can diffuse into the cell. Since very little drug was likely released from the liposomes in the first h of incubation, only a small proportion of the drug was available to enter the cell. The increased cytotoxicity at longer incubation times likely results from the greater opportunity for drug release. This also explains the less dramatic reduction in the IC_{50} for the targeted formulations, compared to DXR-SL. However, the targeted formulations still had approximately 2 fold lower IC_{50} , compared to DXR-SL. This can likely be attributed to receptor-mediated endocytosis of the drug-loaded, targeted liposomes. The delivery of a high percentage of the liposome contents by this mechanism would invariably increase the amount of drug exposure, compared to the amount that is released from the liposomes even after 24 h.

The contribution of released doxorubicin to the cytotoxicity of liposomal doxorubicin can be evaluated by using the cationic exchange resin, Dowex, to scavenge free doxorubicin. Previous studies comparing the 1 and 24 h IC_{50} of DXR-SL, and DXR-SIL[anti-CD19] in the presence and absence of Dowex have demonstrated both the importance of doxorubicin release in the cytotoxicity of DXR-SL and the lack of contribution of released drug towards the cytotoxicity of DXR-SIL[anti-CD19] (155). This data supports the interpretation of the present data.

Anti-CD19 mAb are known to induce cell cycle arrest in B-cell lymphoma cells (99); therefore validation of the proposed targeting effect of anti-CD19 immunoliposomes requires demonstration that the increased cytotoxicity of the targeted formulations of doxorubicin is not mediated by the antibody alone. It has been previously shown that the IC_{50} of free anti-CD19 is considerably higher than the amount of antibody that is incorporated in SIL[anti-CD19]. In addition, the IC_{50} of DXR-SL was not enhanced by the addition of free anti-CD19. This evidence suggests that the specific targeting of DXR-SIL[anti-CD19] is required for the enhanced cytotoxicity. In addition, the requirement for antibody association with the liposomes provides support for the hypothesis that the liposomes are internalized with the antibody-receptor complex. In the present study, preliminary evidence showed that free anti-CD19 is not cytotoxic even at greater concentrations than included with both targeted formulations. Further demonstration of this targeting effect was beyond the scope of this thesis.

A comparison of the 1 and 24 h IC_{50} for DXR-SIL[anti-CD19] and DXR-PIL[anti-CD19] revealed no significant difference. This further demonstrates that targeted liposomes prepared by the post-insertion method have an equivalent *in vitro* targeting capacity, compared to immunoliposomes made by conventional techniques. The data reported here suggests that Namalwa cells were exposed to comparable amounts of drug in the presence of DXR-PIL[anti-CD19] or DXR-SIL[anti-CD19]. Further data is needed to determine whether PIL[anti-CD19] have an equivalent capacity for intracellularly delivery of anti-cancer drugs by endocytosis. It is possible that an increase in the drug release rates could produce a similar cytotoxic effect to an increase in the amount of intracellular delivery of the liposome contents. The leakage of drug from

liposomes is related to the membrane stability, which is in turn related to the PEG-DSPE content through its influence on adsorption of proteins and interactions with cells and other liposomes (43, 46). It is possible that the transfer of IgG-PEG-DSPE resulted in membrane defects that could have, in turn affected drug release. However, the overall PEG-DSPE content is at least equivalent to the amount that was incorporated in the preformed liposomes used for transfer (4 mol% of HSPC content). This amount of PEG-DSPE is likely sufficient to stabilize the membrane, regardless of the transferred amount. However, further studies are needed to characterize the rate of drug release for PIL. Finally, if PIL[anti-CD19] differed from SIL[anti-CD19] in their capacity for endocytosis by Namalwa cells then the binding/uptake should have differed substantially, provided that receptors are re-cycled to the membrane and are available to bind additional liposomes. Since there was no significant difference in the B_{\max} for the two targeted formulations, it is likely that the equivalent cytotoxicity resulted from a similar mechanism of drug delivery to the target cells, probably receptor-mediated endocytosis of intact liposomes.

Interestingly, despite the decrease in binding/uptake in comparison with the study by Lopes de Menezes, *et al.*(91), there was no substantial difference in cytotoxicity. Perhaps there is a threshold amount of liposomal drug internalization required for cytotoxicity. However, there would still likely be some concentration-dependent effects. On the other hand, the discrepancy could be a function of the lower sensitivity of the MTT assay.

Overall it can be concluded that DXR-PIL[anti-CD19] have a cytotoxic advantage compared to non-targeted DXR-SL. This probably results from an improvement in the

cytoplasmic delivery of drug-loaded liposomes by receptor-mediated endocytosis. PIL[anti-CD19] were equivalent in cytotoxicity to immunoliposomes made by the alternative method, and were equally cytotoxic compared to free doxorubicin at longer incubation times. Since none of the therapeutic alternatives appeared to have superior *in vitro* cytotoxicity to DXR-PIL[anti-CD19], and they were more effective than non-targeted DXR-SL, we concluded that PIL may have therapeutic potential.

Chapter 5

***In vivo* targeting of doxorubicin-loaded post-insertion immunoliposomes and conventional immunoliposomes to an animal model of human B-cell lymphoma**

Chapter 5: Results and Discussion

5.1 Pharmacokinetics

The circulation time of liposomal drugs is generally thought to correlate positively with their *in vivo* therapeutic efficacy. For this reason, the next aim of this thesis was to determine whether PIL had suitable pharmacokinetics for *in vivo* administration. As described in the introduction, certain formulations of liposomes are cleared rapidly from circulation by the MPS and are not considered to have clinical potential, except for targeted delivery to the MPS. Conversely, sterically stabilized, non-targeted liposomes have been shown to exhibit long circulation life times. It has also been shown that sterically stabilized immunoliposomes can circulate for therapeutically relevant periods of time provided that optimal antibody densities are employed (80). It follows that if PIL have similar pharmacokinetics to formulations that have been previously established to circulate for sufficient lengths of time, then they should also be appropriate for *in vivo* administration. To this end, the pharmacokinetics of SL, SIL, and PIL were compared.

The liposomes were loaded with tyraminylinulin (TI) as an aqueous space marker (143). It is an appropriate marker to follow intact liposomes because it is retained well within the liposomes, but once it is released it is rapidly eliminated by filtration at the kidneys (within 0.5 h)(41). In this study the mean residence time and half-life of free TI was found to be approximately 1.0 h and 0.7 h, respectively.

The clearance profiles for ^{125}I -TI-loaded SL, SIL[anti-CD19], or PIL[anti-CD19] are shown in **Fig. 5.1**. Both targeted formulations were cleared significantly more rapidly

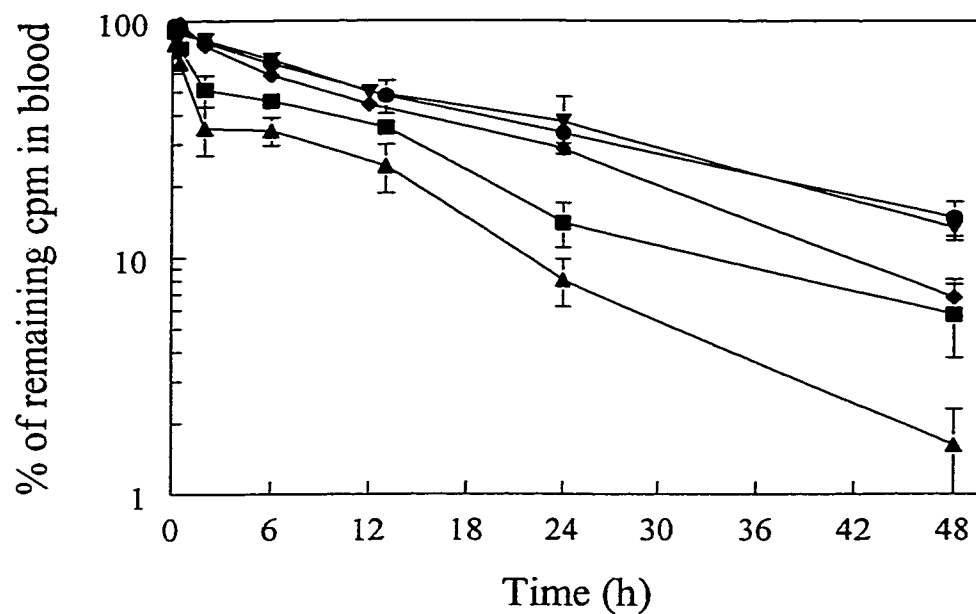


Fig. 5.1 Blood clearance of tyraminylinulin-loaded SIL[anti-CD19] (■), PIL[anti-CD19] (▲), SIL[sheep IgG] (◆), PIL[sheep IgG] (▼), and non-targeted SL (●) in Balb/C or Alt BM mice.

Mice were injected i.v. via the tail vein with a single bolus dose of 0.5 μmol liposome PL. Liposomes were 100 ± 10 nm, composed of HSPC:CHOL:mPEG₂₀₀₀-DSPE (2:1:0.1, mol:mol) and loaded with the aqueous space marker ^{125}I -TI. Targeted formulations were coupled with 25–40 μg Ab/ μmol PL. Data is expressed as the % of the remaining cpm in blood (mean \pm S.D., n=3)

than SL ($p < 0.05$). This was expected, since IgG is known to act as an opsonin that facilitates liposome recognition and clearance by the MPS. The clearance profiles of the targeted formulations were, unlike SL, characterized by an early (first 2 h) rapid phase of clearance that was more apparent for PIL[anti-CD19]. After 2 h the rate of clearance temporarily decreased. The initial rapid phase of clearance seems to be the most pronounced between the two targeted formulations, but it is unknown what is responsible for this phase and why it is exaggerated for PIL. Perhaps this phase represents clearance of a population of liposomes that have higher antibody incorporation. The insertion of IgG-PEG-DSPE into preformed liposomes from a micelle phase, during the preparation of PIL[anti-CD19], is a random event. For this reason it is conceivable that a proportion of the PIL[anti-CD19] with greater IgG-PEG-DSPE incorporation are more susceptible to clearance. Another possibility is that this phase represents clearance of free tyraminylinulin that was released from the liposomes. If liposome membrane defects resulted from the transfer of IgG-PEG-DSPE to PIL that made them more leaky, then the clearance of free TI is a reasonable explanation for the rapid initial phase of clearance. However, HSPC:CHOL liposomes are not generally considered to be leaky, and they were chromatographed to remove free TI before injection. Finally, the rapid clearance phase could be attributed to the deposition of liposomes in tissues such as the bone marrow where CD19 expressing cells are found. This distribution is likely to occur during the first few passages of the blood through these tissues, so it fits with the time course of the clearance. In addition, this explains the lack of a rapid clearance phase for the non-targeted liposomes (SL). However, this mechanism of clearance does not

account for the increased clearance of PIL[anti-CD19]. Probably, a combination of factors was involved.

The later, slower phase of clearance was likely caused by destabilization of liposomes by plasma proteins and lipoproteins and clearance by the MPS. The latter is probably more extensive for the immunoliposomes because the antibody targets the liposomes to phagocytic cells of the MPS via their Fc receptors. This explains the greater slope for the targeted formulations compared to SL.

Previous studies have shown that the clearance profile of immunoliposomes with optimal antibody densities does not differ extensively from SL (80). In addition, SIL[anti-CD19] with an antibody density ranging from 40-60 $\mu\text{g}/\mu\text{mol}$ liposome PL have been previously shown to exhibit circulation times that were comparable to SL(91). This contrasts with the present study in that a pronounced rapid initial phase of elimination and a slightly faster clearance rate was observed. However, in the previous study the Hz-PEG coupling method was employed. It was suspected that the change to the Mal-PEG coupling method, in the present study, might have accelerated the clearance of the resulting immunoliposomes. To confirm this suspicion, the pharmacokinetics of SIL[anti-CD19] prepared by the Hz-PEG method were evaluated for comparison with SIL[anti-CD19] prepared by the Mal-PEG method. Indeed the clearance rate for the Mal-PEG-SIL[anti-CD19] was 13.7% greater than that for SIL[anti-CD19] prepared by the HzPEG method at 2 h and 14.6% greater after 24 h (**Fig. 5.2**). One possible explanation for the difference in clearance rates is the fact that Hz-PEG coupling is site directed to the Fc region of the antibody. Theoretically, the covalent attachment of a PEG chain to the

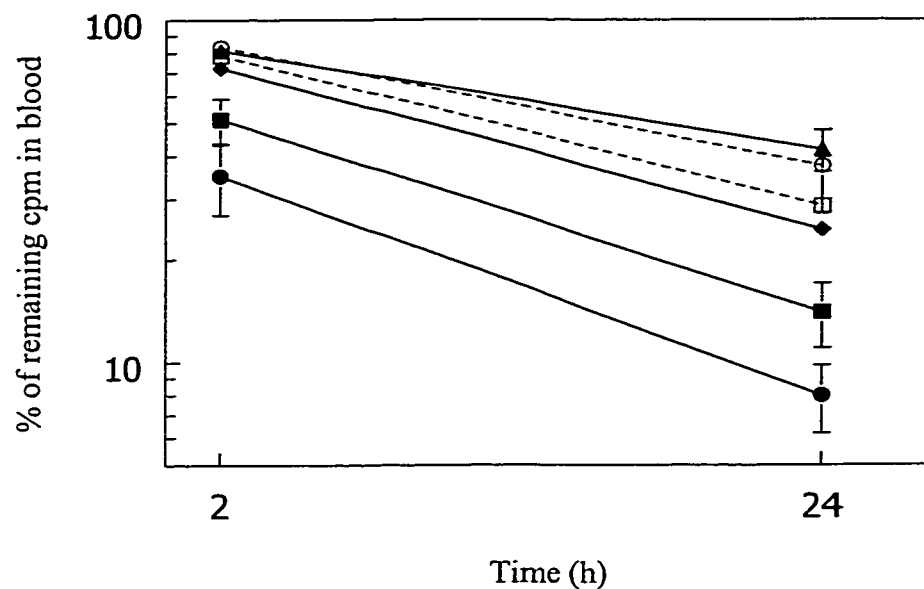


Fig.5.2. Comparison of the clearance rates of ^{125}I -TI liposomes: variation based on the targeting Ab and coupling method.

Mice were injected i.v. via the tail vein with a single bolus dose of $0.5 \mu\text{mol}$ liposome PL. Liposomes were $100 \pm 10 \text{ nm}$, composed of HSPC:CHOL:mPEG₂₀₀₀-DSPE (2:1:0.1, mol:mol) and loaded with the aqueous space marker ^{125}I -TI. The formulations included: SIL[anti-CD19] (■), PIL[anti-CD19] (●), SIL[Sheep IgG] (□, broken line), and PIL[Sheep IgG] (○, broken line) coupled using the Mal-PEG method, SIL[anti-CD19] (◆) coupled using the Hz-PEG method, and non-coupled SL (▲). Targeted formulations were coupled with $25\text{--}40 \mu\text{g Ab} / \mu\text{mol PL}$. Data is expressed as the % of the remaining cpm in blood (mean \pm S.D., $n=3$)

Fc region of the Ab should hinder the binding of liposomes to macrophages and Kupffer cells via their Fc-receptors. In contrast, the Mal-PEG coupling method results in the attachment of antibody via several possible orientations, leaving the Fc region more accessible. For this reason, immunoliposomes prepared by the Hz-PEG coupling method may be less susceptible to clearance by the MPS.

This may have important implications for the choice of coupling methods for preparing targeted liposomes for clinical use. It may be that site-directed coupling methods will be more advantageous, particularly methods that employ antibody fragments because the coupling is more efficient and the liposomes are less immunogenic. While Hz-PEG-coupled liposomes are also potentially less immunogenic than Mal-PEG-coupled liposomes (due to steric hindrance of the Fc region), antibody fragments are likely even less immunogenic because the Fc region has been removed altogether. Indeed, one study has shown that mice produce antisera against the Fc region of Hz-PEG-coupled liposomes (113). In addition, preliminary work by others in our laboratory has shown that SIL[anti-CD19 F'ab] are cleared much less rapidly than SIL[whole anti-CD19] (unpublished data). In these experiments, Mal-PEG was also employed for coupling, which implies that the increased clearance rate observed in the present study may be more related to the site of antibody attachment rather than the Mal-PEG coupling chemistry per se.

Several pharmacokinetic parameters were also calculated and they are shown in **Table 5.1**. The Vd for all formulations closely approximated the mouse blood volume, which ranged from 1.4-1.7 ml. This implies that the liposomes were primarily confined

Table 5.1. Comparison of the pharmacokinetic parameters for non-targeted SL, sheep IgG and anti-CD19 targeted SIL and PIL in Balb/C or Alt BM mice.

Liposome Composition	$t_{1/2\alpha}$ (h)	$t_{1/2\beta}$ (h)	MRT (h)	K_E (h^{-1})	V_D (ml)	Cl (ml/h)	$AUC_{0-\infty}$ (nmol·h/ml)
SL	2.9	21.8	29.5	0.05	1.5	0.1	6798
SIL [anti-CD19]	0.2	15.5	22.1	0.08	1.5	0.1	4264
PIL [anti-CD19]	0.3	17.7	24.6	0.14	1.3	0.2	2742
SIL [sheep IgG]	1.7	16.4	23.0	0.05	1.6	0.1	6275
PIL [sheep IgG]	17.4		25.1	0.04	2.0	0.1	6365

Mice were injected i.v. via the tail vein with a single bolus dose of 0.5 μ mol liposome PL. Liposomes were 100 ± 10 nm, composed of HSPC:CHOL:mPEG₂₀₀₀-DSPE (2:1:0.1, mol:mol) and loaded with the aqueous space marker, ¹²⁵I-TI. Targeted formulations were coupled with 25–40 μ g Ab / μ mol PL. Pharmacokinetic parameters were calculated from the data in Figure 5.1 using a one-compartment or two compartment model, assuming bolus administration and first-order output, and the least squares parameter estimation program PK analyst (Micromath Scientific Software, Salt Lake City, UT). For the formulations that were fitted to a two-compartment model the K_E value was calculated from the β half-life. (n=3)

to the blood compartment. The α and β half-lives ($t_{1/2 \alpha, \beta}$), the mean residence time (MRT), and area under the time concentration curve ($AUC_{0-\infty}$) were greater for SL than the CD19-targeted formulations. Similarly, the elimination rate constant (K_E) and clearance rate (CL) were both lower for SL compared to the CD19-targeted formulations. Interestingly, the pharmacokinetics for sheep IgG targeted liposomes were similar to SL. Also, the α and β half-lives ($t_{1/2 \alpha, \beta}$), the mean residence time (MRT), and area under the time concentration curve ($AUC_{0-\infty}$) were greater, and the K_E and CL were lower, for the sheep IgG liposomes than the anti-CD19 liposomes. Importantly, these studies were carried out in mice that had fully functioning immune systems and likely had a population of CD19-expressing B-cells. For this reason the more rapid clearance of anti-CD19 immunoliposomes, compared to non-targeted and sheep IgG-immunoliposomes can likely be attributed to their binding to B-cells in the blood and tissues, such as the bone marrow. Binding of the liposomes to CD19 expressing cells would trigger their clearance from circulation either by their internalization or destabilization and destruction.

The clearance of SL and anti-CD19 targeted SIL and PIL was also studied in SCID mice that were injected i.v. with Namalwa cells. This model was used to evaluate the therapeutic efficacy of PIL[anti-CD19]; therefore it was necessary to determine whether the liposomes remained in circulation for a therapeutically relevant amount of time. The % of remaining cpm in blood was substantially less in tumor bearing SCID mice than conventional Balb/c mice for both targeted formulations, but not SL (Table 5.2). This is not surprising given that the SCID mice were injected with a large number

Table 5.2 Comparison of the clearance rates of ^{125}I -TI liposomes between naïve BALB/c or SCID mice bearing i.v. CD19+Namalwa cells.

Formulation	% of remaining cpm in blood			
	2 h		24 h	
	SCID	Balb C	SCID	Balb C
SL	91 ± 4.6	81 ± 0.9	38 ± 1.7	42 ± 5.7
SIL[anti-CD19]	23 ± 2.4	51 ± 7.6	1.4 ± 0.8	14 ± 3.0
PIL[anti-CD19]	35 ± 4.2	35 ± 8.1	2.3 ± 0.8	8.0 ± 1.8

SCID mice were injected i.v. with 5×10^6 Namalwa cells via the tail vein, 24 h before the injection of liposomes. Both strains of mice were injected i.v. with $0.5 \mu\text{mol}$ PL of [^{125}I]-TI-loaded liposomes (HSPC:CHOL:mPEG₂₀₀₀-DSPE, 2:1:0.1, mol:mol; 90-100 nm; and for the targeted formulations $25 \mu\text{g}$ anti-CD19/ μmol liposome PL). Groups of 3 mice were sacrificed for each formulation at various time points for blood sampling. Data are expressed as % of remaining cpm in blood (mean ± S.D., n=3).

of Namalwa cells that the liposomes could be taken up by. The fact that clearance of SL was slower in tumor bearing SCID mice compared to BALB/c mice, but clearance of the CD19 liposomes was accelerated suggests that the primary mechanism of clearance may involve binding to CD19 positive cells, rather than clearance by the MPS. The contribution of the MPS to clearance of immunoliposomes may also be reduced in SCID mice due to the small size of their spleens. Although binding to B-cells probably also occurs in BALB/c mice the population of CD19 expressing cells was likely much greater in the SCID mice. This is because a large number of cells were injected (5×10^6) and then were allowed to multiply for 24 h, which is the equivalent of one *in vitro* doubling time.

Interestingly, the decrease in % of remaining cpm in blood for SCID mice bearing Namalwa cells, compared to Balb/c mice was not as dramatic for PIL[anti-CD19] as for SIL[anti-CD19] (Table 5.2). This disparity is most apparent at the 24 h time point, with a 10.3- and 3.5-fold decrease in the % of remaining cpm in blood in tumor bearing SCID mice, compared to BALB/c for SIL[anti-CD19] and PIL[anti-CD19], respectively. One possible explanation for this result is that the PIL[anti-CD19] bind less effectively to Namalwa cells *in vivo*, causing them to be cleared less readily. However, this is unlikely given the *in vitro* binding data and therapeutic data shown in the next section.

Both targeted formulations are cleared rapidly in SCID mice leaving a similar proportion (approximately 25-35%) of the dose in blood after 2 h. While this is not ideal, this amount should be sufficient for targeting given the fact that binding/uptake by Namalwa cells probably occurs rapidly. For instance, binding/uptake occurs within min *in vitro*; therefore even if binding/uptake occurs less rapidly *in vivo*, the remaining dose

at 2h should be sufficient for targeting purposes. Fortunately, the targeted formulations do not depend on drug release from the liposomes for activity, which is more dependent on lengthy circulation times than binding and internalization. Importantly, there was no significant difference in the % of remaining cpm in blood for the two targeted formulations at either time point, which means that the therapeutic efficacy could also be equivalent assuming all other variables were the same.

The % of remaining cpm in tumor bearing SCID between targeted liposomes made by the Hz-PEG and Mal-PEG methods was not directly compared in this study, but would provide useful information. It is not possible to compare the pharmacokinetics in tumor bearing mice with those of Lopes de Menezes *et al.* (91) because in their case the Namalwa cells were injected by the i.p. route. However, it seems reasonable that SIL[anti-CD19] made by the Hz-PEG coupling method are cleared less rapidly in SCID mice, similar to the relationship in BALB/c mice. If this is the case then a change in coupling methods could increase the amount of circulating immunoliposomes to a level that promotes better targeting. This may be important for the clinical approval of PIL.

In summary, the pharmacokinetics data has shown that targeted liposomes made by the Mal-PEG coupling method, either by the conventional or post-insertion technique, are cleared somewhat more rapidly than those made using conventional Hz-PEG coupling method. This indicates that the choice of coupling method may be particularly important and that site-directed methods might be preferred. In addition, the finding that sheep IgG-targeted liposomes were cleared less rapidly than anti-CD19 targeted liposomes suggests that the behavior of immunoliposomes *in vivo* may be partially determined by the antibody specificity. For this reason the results reported in this study

can not necessarily be extended to other antibodies. Finally, a comparison of the two targeted formulations showed that PIL[anti-CD19] are cleared more rapidly than SIL[anti-CD19] in conventional mice. This effect seems to result from a rapid initial phase of clearance, but over time the difference in clearance rates becomes negligible. The converse occurs to a lesser extent in SCID mice bearing a large population of CD19-expressing cells. Overall, the pharmacokinetics of PIL[anti-CD19], although not ideal, seem suitable for in vivo administration. Improvements in the pharmacokinetics may be attained in the future with site-directed coupling and/or the use of antibody fragments.

5.2 *In Vivo* Therapeutics

Finally, the therapeutic efficacy of DXR-PIL[anti-CD19] was compared with some alternative regimens, including CD19 targeted immunoliposomes made by conventional techniques. The aim of this experiment was to determine whether PIL[anti-CD19] have clinical potential; therefore the therapeutic efficacy was evaluated in a murine model of human B-cell lymphoma.

Table 5.3 shows the mean survival times (MST) and % increased life spans (ILS) for mice treated with saline (control mice) or with free DXR, DXR-SL, DXR-SIL[anti-CD19], and PIL[anti-CD19]. The mean survival times for the same formulations are also compared statistically in **Table 5.4**. There was no significant difference in the MST for saline, free DXR, and DXR-SL. However, both anti-CD19 targeted formulations significantly increased the MST compared to saline, and DXR-SL. The ILS for DXR-SIL[anti-CD19] and DXR-PIL[anti-CD19] compared to saline were 36 and 30 %, respectively. The SIL[anti-CD19] group also had a significantly longer MST compared

Table 5.3. Therapeutic efficacy of non-targeted and anti-CD19-targeted formulations of DXR in SCID mice injected i.v. with Namalwa cells.

Formulation	MST in days (\pmS.D.)	ILS (%)
Saline Control (n=6)	28 \pm 2.1	N/A
Free DXR (n=5)	31 \pm 3.7	9.9
DXR-SL (n=5)	30 \pm 2.6	5.7
DXR-SIL[anti-CD19] (n=7)	38 \pm 4.2	36
DXR-PIL[anti-CD19] (n=5)	36 \pm 3.2	30

Namalwa cells ($5 \times 10^6/0.2$ ml) were injected i.v. 24 h before a single treatment with 2.5 mg/kg DXR. The drug was injected i.v. in a volume of 0.2 ml. Liposomes were composed of HSPC:CHOL:mPEG-DSPE (2:1:0.1, mol:mol) with or without 25 μ g anti-CD19/ μ mol liposome PL, coupled by the Mal-PEG method. Doxorubicin was loaded into liposomes by the ammonium sulfate gradient method at 0.2 mg DXR/mg PL. MST denotes mean survival time and ILS denotes increased life span.

Table 5.4. Statistical comparison of MST for SCID mice bearing i.v. Namalwa cells, that were treated with untargeted or CD19 targeted formulations of DXR.

Comparison	p-value
Saline vs. SIL[anti-CD19]	< 0.001
Saline vs. PIL[anti-CD19]	< 0.01
Saline vs. Free DXR	Ns
Saline vs. SL	Ns
SIL[anti-CD19] vs. PIL[anti-CD19]	Ns
SL vs. Free DXR	Ns
SL vs. SIL[anti-CD19]	< 0.05
SL vs. PIL[anti-CD19]	< 0.05
Free DXR vs. SIL[anti-CD19]	< 0.05
Free DXR vs. PIL[anti-CD19]	Ns

All liposomes were loaded with doxorubicin. Statistical significance was evaluated using a one-way anova and the MST from Table 5.4 were compared using the Tukey post test (InStat version 3.0, Graph Pad Software, San Diego, CA)

to the free DXR group. In the case of DXR-PIL[anti-CD19] there was an 18.1% increased life span compared to the free DXR group, but this was not significant.

The therapeutic advantage of the targeted formulations is likely an anti-CD19-specific effect. Confirmation of this specificity has been previously shown by Lopes de Menezes *et al.* (134). In this study, doxorubicin-loaded liposomes targeted with isotype control antibodies were ineffective at prolonging the survival of SCID mice bearing i.v. Namalwa cells. Since anti-CD19 mAb is known to have cytotoxic effects by itself, experimental evidence is needed to show that the cytotoxicity of the DXR-SIL[anti-CD19] is not due to effects of the antibody alone on immunoliposomes, in the absence of drug. Lopes de Menezes *et al.* showed that drug-free SIL[anti-CD19] did not have any therapeutic effect (134). Although, treatment with a combination of free anti-CD19 and non-targeted DXR-SL was more effective than DXR-SL alone, it was not as effective as DXR-SIL[anti-CD19](134). This suggests that DXR-SIL[anti-CD19] have therapeutic efficacy beyond that due to the cytotoxic effects of the anti-CD19 and DXR alone. Furthermore, this supports the argument that anti-CD19 coupled to liposomes is able to mediate the delivery of DXR to Namalwa cells.

A comparison of the two targeted formulations showed no significant difference in MST. This is in agreement with the *in vitro* binding/uptake and cytotoxicity results, which showed that the two formulations had equivalent targetability to Namalwa cells. Similarly, the therapeutic results were as predicted from the pharmacokinetics data, which showed no substantial difference in the final amount of circulating PIL[anti-CD19] compared to SIL[anti-CD19] in tumor-bearing SCID mice. Assuming that a similar proportion of SIL[anti-CD19] and PIL[anti-CD19] were cleared by deposition in tumor

infiltrated regions, then the therapeutic effect should not be expected to differ between the two formulations.

Given that the pharmacokinetics for SIL[anti-CD19] and PIL[anti-CD19] prepared by the Mal-PEG coupling method were less favorable than the pharmacokinetics previously reported for SIL[anti-CD19] prepared by the Hz-PEG method (91); it could be expected that the therapeutic efficacy would also decrease. Using an identical model, Lopez de Menezes *et al.* reported an ILS of 60% for mice treated with 3 mg/kg DXR-SIL[anti-CD19](91). A slightly higher dose was administered (3 mg/kg compared to 2.5 mg/kg) but the same number of Namalwa cells ($5 \times 10^6/0.2\text{ml}$) were injected by the same route (i.v.) and the treatment was given by the same route (i.v.), 24 h after the cells. In the present study the ILS was only 36.2%. It is unknown whether the small decrease in dose could be responsible for the poorer response. It is more likely explained by a combination of the increased rate of clearance and a possible reduction in binding/uptake by the target cells, as predicted by the 10-fold lower binding/uptake shown *in vitro*. In addition, it cannot be ruled out that the cells have drifted and the tumor model differs slightly.

In this study no long-term survivors were achieved (MST < 150 days). This is in agreement with the results of a previous study that employed an equivalent tumor burden and treatment schedule (91). However, in the previous study when the tumor burden was reduced long term survivors were achieved in the group that was treated with SIL[anti-CD19], but not other groups (91). Since disease remission does occur in clinical practice, it is possible that the tumor burden in our model of B-cell lymphoma more closely

approximates refractory disease. For this reason it is possible that our model underestimates the therapeutic potential of targeted-liposomal therapy.

Tseng *et al.* have also reported promising results using anti-idiotypic antibodies for targeting of liposomes in a model of B-cell lymphoma (92). This further validates the potential of immunoliposomes in B-cell lymphoma and demonstrates that a clinically viable approach to the preparation of targeted liposomes is warranted.

In conclusion, it was shown that DXR-PIL[anti-CD19] are capable of improving the survival time of mice that were injected i.v. with Namalwa cells. This is encouraging, since the mice had a fairly large tumor burden. It is conceivable that with multiple doses remission could be achieved. In addition, DXR-PIL[anti-CD19] were at least as effective as DXR-SIL[anti-CD19] and free DXR and more effective than the non-targeted liposomal formulation. Given that there was an a significant increase in the life span of mice treated with DXR-PIL[anti-CD19], the potential exists that they would be more effective than free DXR with multiple dosing. While there was no therapeutic advantage found for DXR-PIL[anti-CD19] over DXR-SIL[anti-CD19], this was according to expectation. However, PIL[anti-CD19] may have an advantage in that the post-insertion approach to preparing targeted liposomes lends itself to a combinatorial approach, which is more versatile given the pleomorphic nature of clinical disease.

Summarizing discussion and future directions

The potential benefits of ligand-targeted liposomes in improving the therapeutic index of anti-cancer drugs are well documented for animal models of cancer. This study demonstrates that the post-insertion method may be a viable approach to promote the clinical approval of ligand-targeted liposomes because it offers flexibility in the choice of targeting ligand and liposomal drug. There are several advantages to this approach and there are also some areas that need improvement.

One of the goals in developing the post-insertion method was to ensure that the resulting immunoliposomes met the criteria that were outlined in the introduction for ideal immunoliposomes. The post-insertion method fulfills the first requirement in that it is rapid and simple, in fact more so than conventional coupling methods. For the Mal-PEG coupling method, the antibody activation step is the same for the conventional and post-insertion techniques. However, the preparation of micelles for coupling using the post-insertion technique is simpler than the preparation of liposomes for conventional coupling techniques. The former simply involves a short (5 min) hydration step, while the latter requires a lengthy liposome preparation phase involving extrusion, drug-loading, and chromatography. One complicating factor is that the thiolation of the antibody and the preparation of the liposomes or micelles must be coordinated in time. This is because the antibody must be incubated with liposomes or micelles immediately after thiolation and must be protected from oxygen. Also, the liposomes must not be prepared too far in advance because the maleimide groups degrade in buffer. In contrast, using the post-insertion method the liposomes may be prepared at any time. Overall, the post-insertion method is substantially less cumbersome.

However, one of the main reasons that a rapid and simple coupling method is desired is to reduce the probability that the antibody or ligand becomes compromised during the procedure. Since the post-insertion methodology that was employed in this thesis required exposing the antibody to elevated temperatures (60°C) for 1 h, this requirement is partially violated. Fortunately, the experiments reported in this thesis have provided evidence that the antibody is not overtly affected in a negative manner by this method because the PIL retained their targeting capacity.

The second feature that is required of an ideal immunoliposome is the efficient use of antibody. This is important because mAbs are expensive and laborious to produce. Although the efficiency of coupling antibody to micelles was shown to be quite good, the efficiency of IgG transfer to SL containing 4 mol% PEG or greater was poor. Therefore one limitation of the post-insertion approach for the preparation of whole antibody-targeted liposomes using the Mal-PEG coupling method is an inefficiency in the use of antibody. While the efficiency in the transfer of IgG to non-pegylated liposomes (CL) approached 100%, it would be more practical from a clinical standpoint to utilize liposomes containing 5-8 mol% PEG for transfer. This is because the benefits of the combinatorial approach can only be realized if a broad range of liposomal formulations, preferably ones that are already in clinical use, can be employed.

In this thesis it was shown that an appropriate level of PEG-DSPE (5-10 mol%) and IgG (25-60 µg Ab/µmol liposome PL) insertion for *in vivo* targeting purposes, as per the literature ((44, 47, 52, 80)) as well as the observed therapeutic results, could be achieved. However, the results were not as promising for a liposomal formulation of doxorubicin, called Caelyx[®], which was in clinical use. The maximal level of IgG

transfer to Caelyx[®], which contains 9.2 mol% PEG, from IgG-PEG-DSPE micelles was below 20 $\mu\text{g Ab}/\mu\text{mol liposome PL}$. In general, it is believed that at least 25-30 $\mu\text{g Ab}/\mu\text{mol liposome PL}$ is required for effective targeting, depending on the antibody. Caelyx[®] was one of the formulations that were originally intended for application to the post-insertion method. Unfortunately, using the current protocol it appears that the resulting immunoliposomes would be unlikely to exhibit effective targeting. In addition, the inefficiency in transfer of IgG would preclude the use of Caelyx[®] for production of targeted liposomes using the post-insertion method from a manufacturing standpoint.

In the present case, the efficiency of transfer was limited by the necessity of including non-coupling lipids to minimize micelle aggregation. In this regard, it may be more appropriate to choose site directed coupling methods for application to the post-insertion method. Indeed, preliminary results have validated further research into the use of the Hz-PEG method, or the selection of antibody fragments as a ligand. The latter approach has been studied by Kirpotin *et al.* (unpublished results) and found to be remarkably efficient with respect to ligand transfer, even to liposomes containing relatively large amounts of PEG (Caelyx[®]). In this case, the micelles were composed of 100% coupling lipid, which is not possible for coupling whole antibodies by the Mal-PEG method. It is not surprising that eliminating non-coupling lipid in the micelle formulation lead to improvements in transfer to Caelyx[®]. The insertion of PEG-lipid is limited to a maximal total PEG-lipid content of approximately 10 mol% (3-6 mol% in the outer monolayer), depending on the anchor lipid (115, 150). Since Caelyx[®] already contains 9.2 mol% PEG-DSPE (4.5-5 mol% in the outer monolayer), it is only possible, theoretically, to insert approximately 1 mol% additional PEG-DSPE. Therefore,

achievement of reasonable levels of IgG incorporation requires that the majority of the transferred lipid be accompanied by IgG. Theoretically, this should be possible when higher ratios of coupling lipid are employed. Therefore, the use of 100% coupling lipid, by Kirpotin *et al.* (unpublished results) likely was instrumental in their success.

Finally, it was shown that the post-insertion method meets the remaining criteria for ideal immunoliposomes in that the ligand insertion was shown to be stable and the method did not compromise the drug -loading characteristics of the liposomes. Therefore, aside from the sub-optimal efficiency of transfer, the post-insertion liposomes seem to meet the requirements for ideal immunoliposomes.

The hypothesis that PIL[anti-CD19] have equivalent *in vitro* and *in vivo* targeting capacity was confirmed by the results of *in vitro* binding and cytotoxicity assays, and *in vivo* pharmacokinetics and therapeutic studies. So despite exposure of the antibody to elevated temperatures using the post-insertion technique the liposomes were able to retain their targeting capacity.

The demonstration that DXR-PIL[anti-CD19] and DXR-SIL[anti-CD19] did not differ in therapeutic efficacy in a murine model of B-cell lymphoma shows that targeted liposomes prepared by the post-insertion technique are no less effective than targeted formulations made by alternate methods. However, the post-insertion technique is amenable to a combinatorial approach, and therefore is more advantageous for the treatment of pleomorphic diseases like cancer because the targeted formulation can be tailored to each patient's needs.

The %ILS was not as substantial as previously reported for anti-CD19 immunoliposomes (134) and anti-idiotypic immunoliposomes (92) in murine models of B-

cell lymphoma. In the latter case, the choice of antigen could be important. That aside, it is not surprising that a difference in response occurred, given that small variations in experimental protocol can influence the results greatly. In the case of the study by Lopes de Menezes *et al.*, (134) the experimental protocol was similar. The difference in therapeutic response compared to this study could be related to the choice of coupling method by its affect on the rate of liposome clearance. An increased rate of clearance could limit the opportunity for liposome targeting and this is likely manifested as changes in therapeutic efficacy.

The fact that antibody, mouse strain and coupling method specific changes in the clearance rate were demonstrated could have important implications towards the future development of ligand-targeted liposomes. The possibility that the choice of antibody could affect the clearance rate, as evidenced by the difference in clearance rates of sheep IgG and anti-CD19 targeted liposomes, means that the results of any therapeutic study that employs ligand-targeted agents cannot necessarily be extended to other situations. The same argument can be applied to changes in coupling method, as shown in this thesis by the disparate rates of clearance for Hz-PEG coupled SIL and Mal-PEG coupled SIL. Similarly, the data showing a difference in clearance rates for anti-CD19 immunoliposomes in Balb/c mice and SCID mice bearing Namalwa cells could be important. Perhaps the response to therapy using these liposomes could be subject to individual patient differences in tumor type and burden by their possible affects on the rate of clearance of the liposomes.

The targeted formulations both showed improved efficacy over a non-targeted liposomal formulation of DXR, indicating that the use of targeted formulations may be a

superior strategy to the treatment of some malignancies, at least B-cell lymphoma. While the efficacy of DXR-PIL[anti-CD19] was not improved over free doxorubicin it remains possible that the targeted formulation could be superior in the face of multiple injection protocols and/or dose escalation.

Importantly, the toxicity to non-malignant tissues is likely reduced with the targeted liposome formulation. While liposomal anti-cancer drugs are also subject to their own dose-limiting toxicities, such as palmar plantar syndrome (160) the opportunity for dose escalation is still greater than with free doxorubicin. This is because the maximum tolerated dose is greater for liposomal doxorubicin (161) and the toxicities associated with liposomal drugs are generally not as severe or life threatening. In the present experiment free doxorubicin was administered at its maximum tolerated dose and this resulted in some signs of toxicity in the mice. Conversely, the liposomal formulations were not given at the maximum tolerated dose; therefore dose escalation would have been possible. In the future it would be interesting to compare the therapeutic efficacies for the different formulations of doxorubicin at their respective maximum tolerated doses. It is logical to predict that with increasing doses the efficacy of DXR-PIL[anti-CD19] may be significantly better than for free DXR. Nevertheless, DXR-PIL[anti-CD19] may offer benefits with respect to patient quality of life, without impairing the therapeutic effect due to an increase in the therapeutic index. In addition, the dose limiting toxicities differ for liposomal and free forms of doxorubicin, as well as from other drugs. This allows the opportunity for combination chemotherapy. The benefits of combination chemotherapy using free drugs (119) and the use of multiple targeting ligands (162) in the treatment of cancer have already been separately

recognized. In addition, promising results were obtained in a clinical trial that evaluated the use of standard cocktail of non-liposomal chemotherapeutic agents with anti-CD20 mAb in low grade B-cell lymphoma (163). The use of multiple drugs with varying mechanisms of action should, theoretically, improve the cytotoxicity against a heterogenous population of cells. For these reasons the cocktail approach, using a combination of various liposomal and free drugs as well as the use several targeting ligands will likely lead to an improvement in the responses to chemotherapy. Overall, it can be concluded that PIL[anti-CD19] may offer a suitable clinical alternative for the treatment of B-cell lymphoma. In addition, the potential exists for the achievement of improved response rates in B-cell lymphoma patients using treatment regimens that include PIL.

This study shows that the post-insertion approach is amenable to the preparation of CD19 targeted immunoliposomes, loaded with doxorubicin by the ammonium sulfate method. However, for the combinatorial approach to the manufacture and administration of targeted liposomes to be effective it is necessary to demonstrate that the post-insertion approach is widely applicable to the preparation of targeted liposomes using other antibodies or ligands and other drugs. In the future it would be useful to repeat these studies using other ligands and liposomes containing other drugs. In this regard, it is necessary to determine the transfer efficiency for other ligands, especially considering the proposition that the attachment of IgG to PEG-DSPE might interfere with its insertion into liposome bilayers. In addition, the insertion stability may differ between ligand-lipid conjugates. Finally, the extent of drug leakage during transfer may be affected by the choice of drug and loading procedure. Since the bilayer integrity is compromised by

heating above the T_M and by transient membrane packing defects during lipid transfer it is likely that drug leakage could occur. The physicochemical characteristics of the drug and the potential for drug precipitation after encapsulation could markedly affect the extent of drug leakage. In particular the precipitation of drug could reduce the potential for leakage, therefore it is important to evaluate the effect of changes in loading procedure.

Another possible future direction of the post-insertion approach would be to evaluate the potential use of liposomes composed of other phospholipids. This could extend the available liposome formulations for application to the post-insertion approach. Perhaps the use of lipids with a lower phase transition temperature would allow the insertion of micelle conjugated ligands at room temperature. This could have potential benefits in maintaining ligand structure, and also facilitate the preparation of PIL. The latter could improve the clinical feasibility of the use of ligand-targeted liposomes by allowing their preparation at bed-side.

One major drawback of immunoliposomes is their immunogenicity, which accelerates their rate of clearance. This is an important concern because the therapeutic efficacy of immunoliposomes is related to their circulation time in that the liposomes must circulate long enough to bind to their target. The use of peptides or natural occurring ligands, such as folate, rather than antibodies, as well as humanized antibodies or antibody fragments are all effective strategies to decrease the immunogenicity of ligand-targeted liposomes. For this reason, it is likely that the use of antibody fragments or peptides that will be more clinically applicable than the use of whole antibodies as targeting ligands.

Another concern with ligand-targeted liposomes is the possibility of target antigen or receptor down-regulation. The failure of therapy due to a lack of stable expression of the target antigen can be circumvented in two ways. First, the use of cocktails of therapeutic agents that target several receptors or antigens would decrease the likelihood of targeting failure. Second, targeting to antigens that are required for malignant progression would reduce the probability of target antigen or receptor down-regulation.

Overall, the results presented in this thesis support the hypothesis that PIL have equivalent *in vitro* and *in vivo* efficacy compared to SIL. In addition, it can be concluded that the post-insertion technique is a viable approach to the preparation of ligand-targeted liposomes for clinical applications. While more research is necessary to gain a thorough understanding of the potential of the post-insertion approach, the data presented here have importance in validating the applicability of the approach. Unfortunately, the post-insertion method as it was applied in this thesis would be unlikely to gain clinical approval due to problems with efficiency. In addition, the clinical approval of any ligand-targeted formulation will likely be subject to the resolution of problems with immunogenicity. However, it is not unreasonable to predict that with modifications the post-insertion method will find clinical utility. In this regard, the use of antibody fragments will likely be instrumental. In any case, the potential of the combinatorial approach and the positive *in vitro* and *in vivo* results presented in this thesis warrant further investigation in this area.

References

1. Bangham, A. D., Standish, M. M., and Watkins, J. C. Diffusion of univalent ions across the lamellae of swollen phospholipids, *J. Mol. Biol.* *13*: 328-252, 1965.
2. Lasic, D. D. *Liposomes: from physics to applications*, p. 1-575. Amsterdam: Elsevier Science Publishers B.V., 1993.
3. Olson, F., Hunt, C. A., Szoka, F. C., Vail, W. J., and Papahadjopoulos, D. Preparation of liposomes of defined size distribution by extrusion through polycarbonate membranes, *Biochim. Biophys. Acta.* *557*: 9-23, 1979.
4. Szoka, F. and Papahadjopoulos, D. Procedure for preparation of liposomes with large internal aqueous space and high capture by reverse-phase evaporation, *Proc. Natl. Acad. Sci. USA.* *75*: 4194-4198, 1978.
5. Gregoriadis, G. *Liposome technology: liposome preparation and related techniques.* , Vol. 1. Boca Raton, FL.: CRC Press, 1993.
6. Mayer, L. D., Hope, M. J., Cullis, P. R., and Janoff, A. S. Solute distributions and trapping efficiencies observed in freeze-thawed multilamellar vesicles, *Biochim. Biophys. Acta.* *817*: 193-196, 1985.
7. Gregoriadis, G. The carrier potential of liposomes in biology and medicine. Part 1, *New Engl. J. Med.* *295*: 704-710, 1976.
8. Gregoriadis, G. The carrier potential of liposomes in biology and medicine. Part 2, *New Engl. J. Med.* *295*: 765-770, 1976.
9. Allen, T. M. *Oncologic agents in sterically stabilized liposomes: basic considerations*, p. 19-29. Georgetown, TX: Landes Bioscience, 1998.

10. Allen, T. M. Liposomal drug formulations: rationale for development and what we can expect for the future, *Drugs*. 56: 747-756, 1998.
11. Eckardt, J. R., Campbell, E., Burries, H. A., Weiss, G. R., Rodriguez, G. I., Fields, S. M., Thurman, A. M., Peacock, N. W., Cobb, P., Rothenberg, M. L., Ross, M. E., and Von Hoff, D. D. A Phase II trial of DaunoXome, liposome encapsulated daunorubicin, in patients with metastatic adenocarcinoma of the colon, *Am. J. Clin. Oncol. Cancer Clin. Trials*. 17: 498-501, 1994.
12. Schurmann, D., Dormann, A., Grunewald, T., and Ruf, B. Successful treatment of AIDS-related Kaposi's sarcoma with liposomal daunorubicin, *Eur. Respir. J.* 7: 824-825, 1994.
13. Gill, P. S., Espina, B. M., Muggia, F., Cabriaes, S., Tulpule, A., Esplin, J. A., Liebman, H. A., Forssen, E., Ross, M. E., and Levine, A. M. Phase I/II clinical and pharmacokinetic evaluation of liposomal daunorubicin, *J. Clin. Oncol.* 13: 996-1003, 1995.
14. Cowens, J. W., Creaven, P. J., Greco, W. R., Brenner, D. E., Tung, Y., Osto, M., Pilkiewicz, F., Ginsberg, R., and Petrelli, N. Initial clinical (phase I) trial of TLC D-99 (doxorubicin encapsulated in liposomes), *Cancer Res.* 53: 2796-2802, 1993.
15. Northfelt, D. W., Martin, F. J., Kaplan, L. D., Russell, J., Andersen, M., Lang, J., and Volberding, P. A. Pharmacokinetics, tumour localization and safety of Doxil (liposomal doxorubicin) in AIDS patients with Kaposi's sarcoma (Meeting abstract)., *Proc. Am. Soc. Clin. Oncol.* 12: A8, 1993.

16. Schwartz, G. K. and Gasper, E. S. A phase II trial of doxorubicin HCL liposome injection in patients with advanced pancreatic adenocarcinoma, *Invest. New Drugs*. *13*: 77-82, 1995.
17. Muggia, F., Hainsworth, J., Jeffers, S., Groshen, S., Tan, M., and Greco, F. A. Liposomal doxorubicin (Doxil) is active against refractory ovarian cancer, *Proc. Am. Soc. Clin. Oncol.* *15*: 287, 1996.
18. Ranson, M., O'Bryne, K., Carmichael, J., Smith, D., Stewart, S., and Howell, A. Phase II dose-finding trial of DOX-SL (Stealth® liposomal doxorubicin HCl) in the treatment of advanced breast cancer, *Proc. Am. Soc. Clin. Oncol.* *15*: 124, 1996.
19. Conley, B. A., Egorin, M. J., Whitacre, D., Carter, C., and Zuhowski, E. G. Phase I and Pharmacokinetic trial of liposome-encapsulated doxorubicin., *Cancer Chemother. Pharmacol.* *33*: 107-112, 1993.
20. Casper, E. S., Schwartz, G. K., Sugarman, A., Leung, D., and Brennan, M. F. Phase I trial of dose-intense liposome-encapsulated doxorubicin in patients with advanced sarcoma, *J. Clin. Oncol.* *15*: 2111-2117, 1997.
21. Northfelt, D. W., Dezube, B. J., Thommes, J. A., Levine, R., Von Roenn, J. H., Dosik, G. M., Rios, A., Krown, S. E., DuMond, C., and Mamelok, R. D. Efficacy of pegylated-liposomal doxorubicin in the treatment of AIDS-related Kaposi's sarcoma after failure of standard chemotherapy, *J. Clin. Oncol.* *15*: 653-659, 1997.
22. Lopez-Berestein, G., Fainstein, V., Hopfer, R., Mehta, K., Sullivan, M. P., Keating, M., Rosenblum, M. G., Mehta, R., Luna, M., Hersh, E. M., Reuben, J.,

- Juliano, R. L., and Bodey, G. P. Liposomal amphotericin B for the treatment of systemic fungal infections in patients with cancer : A preliminary study, *J. Infect. Dis.* *151*: 704-710, 1985.
23. Mayer, L. D., Bally, M. B., Hope, M. J., and Cullis, P. R. Techniques for encapsulating bioactive agents into liposomes, *Chem. Phys. Lipids.* *40*: 333-345, 1986.
24. Mayer, L. D., Bally, M. B., Hope, M. J., and Cullis, P. R. Uptake of antineoplastic agents into large unilamellar vesicles in response to a membrane potential, *Biochim. Biophys. Acta.* *816*: 294-302, 1985.
25. Mayer, L. D., Bally, M. B., and Cullis, P. R. Uptake of adriamycin into large unilamellar vesicles in response to a pH gradient, *Biochim. Biophys. Acta.* *857*: 123-126, 1986.
26. Mayer, L. D., Madden, T. D., Bally, M. B., and Cullis, P. R. pH gradient-mediated drug entrapment in liposomes, Vol. II, p. 27-44. Florida, USA: CRC Press, Inc., 1993.
27. Harrigan, P. R., Wong, K. F., Redelmeier, T. E., Wheeler, J. J., and Cullis, P. R. Accumulation of doxorubicin and other lipophilic amines into large unilamellar vesicles in response to transmembrane pH gradients, *Biochim. Biophys. Acta.* *1149*: 329-338, 1993.
28. Haran, G., Cohen, R., Bar, L. K., and Barenholz, Y. Transmembrane ammonium sulfate gradients in liposomes produce efficient and stable entrapment of amphipathic weak bases, *Biochim. Biophys. Acta.* *1151*: 201-215, 1993.

29. Bolotin, E. M., Cohen, R., Bar, L. K., Emanuel, S. N., Lasic, D. D., and Barenholz, Y. Ammonium sulphate gradients for efficient and stable remote loading of amphipathic weak bases into liposomes and ligandosomes, *J. Liposome Res.* 4: 455-479, 1994.
30. Devine, D. V. and Marjan, J. M. The role of immunoproteins in the survival of liposomes in the circulation, *Crit. Rev. Ther. Drug. Carrier Syst.* 14: 105-131, 1997.
31. Chonn, A., Semple, S. C., and Cullis, P. R. Association of blood proteins with large unilamellar liposomes in vivo. Relation to circulation lifetimes, *J. Biol. Chem.* 267: 18759-18765, 1992.
32. Alving, C. R., Steck, E. A., Chapman, W. L., Jr., Waits, V. B., Hendricks, L. D., Swartz, G. M., Jr., and Hanson, W. L. Therapy of leishmaniasis: superior efficacies of liposome-encapsulated drugs, *Proc. Natl. Acad. Sci. U S A.* 75: 2959-2963, 1978.
33. Killion, J. J. and Isaiah, J. F. Therapy of cancer metastasis by tumoricidal activation of tissue macrophages using liposome-encapsulated immunomodulators., *Pharmacol. Ther.* 78: 141-154, 1998.
34. Papahadjopoulos, D., Allen, T. M., Gabizon, A., Mayhew, E., Matthey, K., Huang, S. K., Lee, K. D., Woodle, M. C., Lasic, D. D., Redemann, C., and Martin, F. J. Sterically stabilized liposomes: improvements in pharmacokinetics and antitumor therapeutic efficacy, *Proc. Natl. Acad. Sci. USA.* 88: 11460-11464, 1991.

35. Semple, S. C., Chonn, A., and Cullis, P. R. Influence of cholesterol on the association of plasma proteins with liposomes, *Biochemistry*. 35: 2521-2525, 1996.
36. Abra, R. M. and Hunt, C. A. Liposome disposition in vivo. III. Dose and vesicle-size effects, *Biochim. Biophys. Acta*. 666: 493-503, 1981.
37. Lasic, D. D., Woodle, M. C., and Papahadjopoulos, D. On the molecular mechanism of steric stabilization of liposomes in biological fluids, *J. Liposome Res.* 2: 335-353, 1992.
38. Daemen, T., Hofstede, G., Ten Kate, M. T., Bakker-Woudenberg, I. A., and Scherphof, G. L. Liposomal doxorubicin-induced toxicity: depletion and impairment of phagocytic activity of liver macrophages, *Int. J. Cancer*. 61:, 1995.
39. Abra, R. M., Bosworth, M. E., and Hunt, C. A. Liposome disposition in vivo: effects of pre-dosing with liposomes, *Res. Commun. Chem. Pathol. Pharmacol.* 29: 349-360, 1980.
40. Allen, T. M. and Hansen, C. B. Pharmacokinetics of Stealth versus conventional liposomes: effect of dose, *Biochim. Biophys. Acta*. 1068: 133-141, 1991.
41. Allen, T. M. and Chonn, A. Large unilamellar liposomes with low uptake into the reticuloendothelial system, *FEBS Lett.* 223: 42-46, 1987.
42. Blume, G. and Cevc, G. Liposomes for the sustained drug release in vivo, *Biochim. Biophys. Acta*. 1029: 91-97, 1990.
43. Blume, G. and Cevc, G. Molecular mechanism of the lipid vesicle longevity in vivo, *Biochim. Biophys. Acta*. 1146: 157-168, 1993.

44. Allen, T. M., Hansen, C. B., Martin, F., Redemann, C., and Yau-Young, A. Liposomes containing synthetic lipid derivatives of poly(ethylene glycol) show prolonged circulation half-lives in vivo, *Biochim. Biophys. Acta. 1066*: 29-36, 1991.
45. Woodle, M. C., Matthay, K. K., Newman, M. S., Hidayat, J. E., Collins, L. R., Redemann, C., Martin, F. J., and Papahadjopoulos, D. Versatility in lipid compositions showing prolonged circulation with sterically stabilized liposomes, *Biochim. Biophys. Acta. 1105*: 193-200, 1992.
46. Needham, D., McIntosh, T. J., and Lasic, D. D. Repulsive interactions and mechanical stability of polymer-grafted lipid membranes, *Biochim. Biophys. Acta. 1108*: 40-48, 1992.
47. Allen, T. M., Hansen, C. B., and Lopes de Menezes, D. E. Pharmacokinetics of long circulating liposomes, *Adv. Drug Del. Rev. 16*: 267-284, 1995.
48. Torchilin, V. P. and Trubetskoy, V. S. New synthetic amphiphilic polymers for steric protection of liposomes in vivo, *J Pharm Sci. 85*: 85-133, 1995.
49. Needham, D., Kristova, K., McIntosh, T. J., Dewhirst, M., Wu, N., and Lasic, D. D. Polymer-grafted liposomes, Physical basis for the "Stealth" property, *J. Liposome Res. 2*: 411-430, 1992.
50. Torchilin, V. P. and Papisov, M. I. Why do polyethylene glycol-coated liposomes circulate so long? molecular mechanism of liposome steric protection

with polyethylene glycol: role of polymer chain flexibility, *J. liposome Res.* 4: 725-739, 1994.

51. Torchilin, V. P., Omelyanenko, V. G., Papisov, M. I., Bogdanov, A. A., Trubetskoy, V. S., Herron, J. N., and Gentry, C. A. Poly(ethylene glycol) on the liposome surface: on the mechanism of polymer coated liposome longevity, *Biochim. Biophys. Acta.* 1195: 11-20, 1994.

52. Kenworthy, A. K., Simon, S. A., and McIntosh, T. J. Structure and phase behaviour of lipid suspensions containing phospholipids with covalently attached poly(ethylene glycol), *Biophys. J.* 68: 1903-1920, 1995.

53. Gabizon, A. and Papahadjopoulos, D. Liposome formulations with prolonged circulation time in blood and enhanced uptake by tumors, *Proc. Natl. Acad. Sci. USA.* 85: 6949, 1988.

54. Gabizon, A., Catane, R., Uziely, B., Kaufman, B., Safra, T., Cohen, R., Martin, F., Huang, A., and Barenholz, Y. Prolonged circulation time and enhanced accumulation in malignant exudates of doxorubicin encapsulated in polyethylene-glycol coated liposomes, *Cancer Res.* 54: 987-992, 1994.

55. Wu, N. Z., Da, D., Rudoll, T. L., Needham, D., Whorton, A. R., and Dewhirst, M. W. Increased microvascular permeability contributes to preferential accumulation of Stealth liposomes in tumour tissue, *Cancer Res.* 53: 3765-3770, 1993.

56. Allen, T. M., Newman, M. S., Woodle, M. C., Mayhew, E., and Uster, P. S. Pharmacokinetics and anti-tumor activity of vincristine encapsulated in sterically stabilized liposomes, *Int. J. Cancer.* 62: 199-204, 1995.

57. Weinstein, J. N. and Van Osdol, W. The macroscopic and microscopic pharmacology of monoclonal antibodies., *Int. J. Immunopharmac.* 14: 457-463, 1992.
58. Lum, H. and Malik, A. B. Regulation of vascular endothelial barrier function., *Am. J. Physiol.* 267: L223-L241, 1994.
59. Brown, M. J. and Giaccia, A. J. The unique physiology of solid tumors: opportunities (and problems) for cancer therapy., *Cancer Res.* 58: 1408-1416, 1998.
60. Yuan, F., Dellian, M., Fukumura, D., Leunig, M., Berk, D. A., Torchilin, V. P., and Jain, R. K. Vascular permeability in a human tumor xenograft: molecular size dependence and cutoff size., *Cancer Res.* 55: 3752-3756, 1995.
61. Jain, R. K. and Baxter, L. T. Mechanisms of heterogenous distribution of monoclonal antibodies and other macromolecules in tumors: significance of elevated interstitial pressure., *Cancer Res.* 48: 7022-7032, 1988.
62. Jain, R. K. Transport of molecules in the tumor interstitium: a review., *Cancer Res.* 47: 3039-3051, 1987.
63. Jain, R. K. Physiological barriers to delivery of monoclonal antibodies and other macromolecules in tumors., *Cancer Res.* 50: 814s-819s, 1990.
64. Allen, T. M., Hong, K., and Papahadjopoulos, D. Membrane contact, fusion, and hexagonal (HII) transitions in phosphatidylethanolamine liposomes, *Biochemistry.* 29: 2976-2985, 1990.
65. Huang, S. K., Stauffer, P. R., Hong, K., Guo, J. W., Phillips, T. L., Huang, A., and Papahadjopoulos, D. Liposomes and hyperthermia in mice: increased

tumor uptake and therapeutic efficacy of doxorubicin in sterically stabilized liposomes, *Cancer Res.* 54: 2186-2191, 1994.

66. Weinstein, J. N., Magin, R. L., Yatvin, M. B., and Zaharko, D. S.

Liposomes and local hyperthermia: selective delivery of methotrexate to heated tumors, *Science.* 204: 188-191, 1979.

67. Ehrlich, P. The relations existing between chemical constitution,

distribution and pharmacological action, p. 404-443. New York: John Wiley and Sons, Ltd, 1906.

68. Kohler, G. and Milstein, C. Continuous cultures of fused cells secreting

antobody of predetermined specificity, *Nature (London).* 256: 495-497, 1975.

69. Dokka, S., Toledo-Velasquez, D., Shi, X., Wang, L., and Rojanasakul, Y.

Cellular delivery of oligonucleotides by synthetic import peptide carrier., *Pharm. Res.* 14: 1759-1764, 1997.

70. Allen, T. M., Agrawal, A. K., Ahmad, I., Hansen, C. B., and Zalipsky, S.

Antibody-mediated targeting of long-circulating (Stealth®) liposomes, *J.*

Liposome Res. 4: 1-25, 1994.

71. Allen, T. M., Hansen, C. B., and Zalipsky, S. Antibody-targeted Stealth®

liposomes. *In:* D. D. Lasic and F. Martin (eds.), *Stealth Liposomes*, pp. 223-244.

Boca Raton, FL: CRC Press, Inc., 1995.

72. Blume, G., Cevc, G., Crommelin, M. D., Bakker-Woudenberg, L. A.,

Kluft, C., and Storm, G. Specific targeting with poly(ethylene glycol)-modified

liposomes: coupling of homing devices to the ends of the polymeric chains

combines effective target binding with long circulation times, *Biochim. Biophys. Acta. 1149*: 180-184, 1993.

73. Hansen, C. B., Kao, G. Y., Moase, E. H., Zalipsky, S., and Allen, T. M. Attachment of antibodies to sterically stabilized liposomes: evaluation, comparison and optimization of coupling procedures, *Biochim. Biophys. Acta. 1239*: 133-144, 1995.

74. Maruyama, K., Takizawa, T., Takahashi, N., Tagawa, T., Nagaike, K., and Iwatsuru, M. Targeting efficiency of PEG-immunoliposome-conjugated antibodies at PEG terminals, *Adv. Drug Del. Rev. 24*: 235-242, 1997.

75. Klibanov, A. L., Maruyama, K., Beckerleg, A. M., Torchilin, V. P., and Huang, L. Activity of amphipathic poly(ethyleneglycol) 5000 to prolong the circulation time of liposomes depends on the liposome size and is unfavorable for immunoliposome binding to target, *Biochim. Biophys. Acta. 1062*: 142-148, 1991.

76. Gabizon, A., Horowitz, A. T., Goren, D., Tzemach, D., Mandelbaum-Shavit, F., Qazen, M. M., and Zalipsky, S. Targeting folate receptor with folate linked to extremities of poly(ethylene glycol)-grafted liposomes: in vitro studies., *Bioconjugate Chem. 10*: 289-298, 1999.

77. Vertutdoi, A., Ishiwata, H., and Miyajima, K. Binding and uptake of liposomes containing a poly(Ethylene Glycol) derivative of cholesterol (stealth liposomes) by the macrophage cell line J774: influence of peg content and its molecular weight, *Biochim. Biophys. Acta. 127*: 19-28, 1996.

78. Maruyama, K., Takizawa, T., Yuda, T., Kennel, S. J., Huang, L., and Iwatsuru, M. Targetability of novel immunoliposomes modified with amphipathic poly(ethylene glycol)s conjugated at their distal terminals to monoclonal antibodies, *Biochim. Biophys. Acta.* 1234: 74-80, 1995.
79. Zalipsky, S. Functionalized poly(ethylene glycol) for preparation of biologically relevant conjugates, *Bioconjug Chem.* 6: 150-165, 1995.
80. Allen, T. M., Brandeis, E., Hansen, C. B., Kao, G. Y., and Zalipsky, S. A new strategy for attachment of antibodies to sterically stabilized liposomes resulting in efficient targeting to cancer cells, *Biochim. Biophys. Acta.* 1237: 99-108, 1995.
81. Zalipsky, S. Synthesis of end-group functionalized polyethylene glycol-lipid conjugates for preparation of polymer-grafted liposomes, *Bioconjugate Chem.* 4: 296-299, 1993.
82. Kirpotin, D., Park, J. W., Hong, K., Zalipsky, S., Li, W.-L., Carter, P., Benz, C. C., and Papahadjopoulos, D. Sterically stabilized anti-HER2 immunoliposomes: design and targeting to human breast cancer cells *in vitro*, *Biochemistry.* 36: 66-75, 1997.
83. Martin, F. J. and Papahadjopoulos, D. Irreversible coupling of immunoglobulin fragments to preformed vesicles. An improved method for liposome targeting, *J. Biol. Chem.* 257: 286-288, 1982.
84. Martin, F. J., Hubbell, W. I., and Papahadjopoulos, D. Immunospecific targeting of liposomes to cells: a novel and efficient method for covalent

attachment of Fab' fragments via disulfide bonds, *Biochemistry*. *20*: 4229-4238, 1981.

85. Goren, D., Horowitz, A. T., Tzemach, D., Tarshish, M., Zalipsky, S., and Gabizon, A. Nuclear delivery of doxorubicin via folate-targeted liposomes with bypass of multidrug-resistance efflux pump., *Clinical Cancer Research*. *6*: 1949-1957, 2000.

86. Reddy, J. A. and Low, P. S. Enhanced folate receptor mediated gene therapy using a novel pH sensitive formulation., *Journal of Controlled Release*. *64*: 27-37, 2000.

87. Matthey, K. K., Abai, A. M., Cobb, S., Hong, K., Papahadjopoulos, D., and Straubinger, R. M. Role of ligand in antibody-directed endocytosis of liposomes by human T-leukemia cells, *Cancer Res*. *49*: 4879-4886, 1989.

88. Papahadjopoulos, D., Kirpotin, D. B., Park, J. W., Keelung, H., Shao, Y., Shalaby, R., Colbern, G., and Benz, C. C. Targeting of drugs to solid tumors using anti-HER2 immunoliposomes., *Journal of Liposome Research*. *8*: 425-442, 1998.

89. Park, J. W., Hong, K., Kirpotin, D. B., Meyer, O., Papahadjopoulos, D., and Benz, C. C. Anti-HER2 immunoliposomes for targeted therapy of human tumors, *Cancer Lett*. *118*: 153-160, 1997.

90. Goren, D., Horowitz, A. T., Zalipsky, S., Woodle, M. C., Yarden, Y., and Gabizon, A. Targeting of stealth liposomes to erB-2 (Her/2) receptor: in vitro and in vivo studies, *Br. J. Cancer*. *74*: 1749-1756, 1996.

91. Lopes de Menezes, D., Pilarski, L. M., and Allen, T. M. In vitro and in vivo targeting of immunoliposomal doxorubicin to human B-cell lymphoma, *Cancer Res.* 58: 3320-3330, 1998.
92. Tseng, Y., Hong, R., Tao, M., and Chang, F. Sterically stabilized anti-idiotype immunoliposomes improve the therapeutic efficacy of doxorubicin in a murine B-cell lymphoma model., *Int. J. Cancer.* 80: 723-730, 1999.
93. Debs, R. J., Heath, T. D., and Papahadjopoulos, D. Targeting of anti-Thy 1.1 monoclonal antibody conjugated liposomes in Thy 1.1 mice after intravenous administration, *Biochim. Biophys. Acta.* 901: 183-190, 1987.
94. Regimbald, L. H., Pilarski, L. M., Longnecker, B. M., Reddish, M. A., Zimmerman, G., and Hugh, J. C. The breast mucin MUC1 as a novel adhesion ligand for endothelial intracellular adhesion molecule 1 in breast cancer., *Cancer Res.* 56: 4244-4249, 1996.
95. Moase, E. H., Qi, W., Ishida, T., Gabos, Z., Longnecker, B. M., Zimmerman, G. L., Ding, L., Krantz, M., and Allen, T. M. Anti-MUC-1 immunoliposomal doxorubicin in the treatment of murine models of breast cancer., *Biochem. Biophys. Acta. in press.*, 2000.
96. Pagnan, G., Montaldo, P. G., Pastorino, F., Chiesa, L., Raffaghello, L., Kirchmeier, M., Allen, T. M., and Ponzoni, M. GD₂ -mediated melanoma cell targeting and cytotoxicity of liposome-entrapped fenretinide., *Int. J. Cancer.* 81: 268-274, 1999.
97. Pagnan, G., Stuart, D. D., Pastorino, F., Raffaghello, L., Montaldo, P., Allen, T. M., Calabretta, B., and Ponzoni, M. Delivery of c-myb antisense

oligodeoxynucleotides to human neuroblastoma cells via disialoganglioside GD2-targeted immunoliposomes: antitumor effects., *J. Nat. Cancer Inst.* 92: 253-261, 2000.

98. Straubinger, R. M., Lopez, N. G., Debs, R. J., Hong, K., and Papahadjopoulos, D. Liposome-based therapy of human ovarian cancer: parameters determining potency of negatively charged and antibody-targeted liposomes, *Cancer Res.* 48: 5237-5245, 1988.

99. Ghetie, M. A., Picker, L. J., Richardson, J. A., Tucker, K., Uhr, J. W., and Vitetta, E. S. Anti-CD19 inhibits the growth of human B-cell tumor lines in vitro and of Daudi cells in SCID mice by inducing cell cycle arrest, *Blood.* 83: 1329-1336, 1994.

100. Ghetie, M.-A., Ghetie, V., and Vitetta, E. S. Anti-CD19 antibodies inhibit the function of the P-gp pump in multidrug-resistant B lymphoma cells., *Clinical Cancer Research.* 5: 3920-3927, 1999.

101. Pietras, R. J., Fendly, B. M., Chazin, V. R., Pergram, M. D., Howell, S. B., and Slamon, D. J. Antibody to HER-2/*neu* receptor blocks DNA repair after cisplatin in human breast and ovarian cancer cells., *Oncogene.* 9: 1829-1838, 1994.

102. Baselga, J., Norton, L., Shalaby, R., and Mendelsohn, J. Anti-HER2 humanized monoclonal antibody (MAb) alone and in combination with chemotherapy against breast carcinoma xenografts., *Proc. Am. Soc. Clin. Oncol.* 13: 63, 1994.

103. Goldmacher, V. S., Scott, C. F., Lambert, J. M., McIntyre, G. D., Blattler, W. A., Collinson, A. R., Cook, S. A., Slayter, H. S., Beaumont, E., and Watkins, S. Cytotoxicity of gelonin and its conjugates with antibodies is determined by the extent of their endocytosis., *J. Cell. Phys.* *141*: 222-234, 1989.
104. Berinstein, N., Matthay, K. K., Papahadjopoulos, D., Levy, R., and Sikic, B. I. Antibody-directed targeting of liposomes to human cell lines: role of binding and internalization on growth inhibition, *Cancer Res.* *47*: 5954-5959, 1987.
105. Schwartz, A. L., Fridovich, S. E., and Lodish, H. F. Kinetics of internalization and re-cycling of the asialoglycoprotein receptor in a hepatoma cell line., *J. Biol. Chem.* *257*: 4230-4237, 1982.
106. Baldini, N., Scotlandi, K., Serra, M., Shikita, T., Zini, N., Ognibene, A., Santi, S., Ferracini, R., and Maraldi, N. M. Nuclear immunolocalization of P-glycoprotein in multidrug-resistant cell lines showing similar mechanisms of doxorubicin distribution., *European Journal of Cell Biology.* *68*: 226-239, 1995.
107. Germann, U. A. P-glycoprotein--- A mediator of multidrug resistance in tumor cells., *European Journal of Cancer.* *32A*: 927-944, 1996.
108. Connor, J. and Huang, L. pH-sensitive immunoliposomes as an efficient and target-specific carrier for antitumor drugs, *Cancer Res.* *46*: 3431-3435, 1986.
109. Kirpotin, D., Hong, K., Mullah, N., Papahadjopoulos, D., and Zalipsky, S. Liposomes with detachable polymer coating: destabilization and fusion of dioleoylphosphatidylethanolamine vesicles triggered by cleavage of surface-grafted poly(ethylene glycol), *FEBS Lett.* *388*: 115-118, 1996.

110. Winter, G. and Harris, W. J. Humanized antibodies, *Trends Pharmacol. Sci.* *14*: 139-143, 1993.
111. Jaffers, G. J., Fuller, T. C., Cosimi, A. B., Russel, P. S., Winn, H. J., and Colvin, R. B. Monoclonal antibody therapy. Anti-idiotypic and non-anti-idiotypic antibodies to OKT3 arising despite intense immunosuppression., *Transplantation.* *41*: 572-578, 1986.
112. Novotny, J., Handschumacher, M., and Haber, E. Location of antigenic epitopes on antibody molecules., *J. Mol. Biol.* *189*: 715-721, 1986.
113. Harding, J. A., Engbers, C. M., Newman, M. S., Goldstein, N. I., and Zalipsky, S. Immunogenicity and pharmacokinetic attributes of poly(ethyleneglycol)-grafted immunoliposomes, *Biochim. Biophys. Acta.* *1327*: 181-192, 1997.
114. Aragnol, D. and Leserman, L. Immune clearance of liposomes inhibited by an anti-Fc receptor antibody in vivo, *Proc. Natl. Acad. Sci. U S A.* *83*: 2699-2703, 1986.
115. Uster, P. S., Allen, T. M., Daniel, B. E., Mendez, C. J., Newman, M. S., and Zhu, G. Z. Insertion of poly(ethylene glycol) derivatized phospholipid into preformed liposomes results in prolonged in vivo circulation time, *FEBS Lett.* *386*: 243-246, 1996.
116. Skarin, A. T. and Dorfman, D. M. Non-Hodgkin's Lymphomas: Current classification and managment., *CA Cancer J. Clin.* *47*: 351-372, 1997.
117. Ries, L. A. G., Wingo, P. A., Miller, D. S., Howe, H. L., Weir, H. K., Rosenberg, H. M., Vernon, S. W., Cronin, K., and Edwards, B. K. The annual

report to the nation on the status of cancer, 1973-1997, with a special section on colorectal cancer., *Cancer*. 89: 2398-2424, 2000.

118. Devesa, S. S. and Fears, T. Non-Hodgkin's lymphoma time trends: United States and international data., *Cancer Res*. 52 (*Suppl*): 5432S--5440S, 1992.

119. Fisher, R. I., Gaynor, E. R., Dahlberg, S., and al, e. Comparison of a standard regimen (CHOP) with three intensive chemotherapy regimens for advanced non-Hodgkin's lymphoma., *N. Eng. J. Med*. 328: 1002-1006, 1993.

120. Philip, T., Guglielmi, C., Hagenneck, A., and al, e. Autologous none marrow transplantation as xompared with salvage chemotherapy in relapses of chemotherapy sensitive non-Hodgkin's lymphoma., *N. Eng. J. Med*. 333: 1540--1545, 1995.

121. Shipp, M. A., Mauch, P. M., and Harris, N. L. Non-hodgkin's lymphomas. *In*: V. T. DeVita, S. Hellman, and S. A. Rosenberg (eds.), *Cancer: principles and practice of oncology*, Vol. 2, pp. 2165-2220. Philadelphia: Lippincott-Raven, 1997.

122. Gaidano, G. and Dalla-Favera, R. Lymphomas. *In*: V. T. DeVita, S. Hellman, and S. A. Rosenberg (eds.), *Cancer: principles and practice of oncology*, Vol. 2, pp. 2131-2145. Philadelphia: Lippincott-Raven, 1997.

123. Tedder, T. F. and Isaacs, C. M. Isolation of cDNA encoding the CD19 antigen of human and mouse B lymphocytes. A new member of the immunoglobulin superfamily, *J. Immunol*. 143: 712-717, 1989.

124. Anderson, K. C., Bates, M. C., Slaughenhaupt, B. L., Pinkus, G. S., Schlossman, S. F., and Nadler, L. M. Expression of human B-cell-associated

antigens on leukemias and lymphomas: a model of human B-cell differentiation.,
Blood. 63: 1424-1433, 1984.

125. Nadler, L. M., Anderson, K. C., Marti, G., Bates, M., Park, E., Daley, J. F., and Schlossman, S. F. B4, a human B lymphocyte-associated antigen expressed on normal, itogen-activated, and malignant B lymphocytes, *J. Immunol.* 131: 244-250, 1983.

126. Tedder, T. F., Zhou, L.-J., and Engel, P. The CD19/CD21 signal transduction complex of B lymphocytes, *Immunol. Today*. 15: 437-442, 1994.

127. Pezzutto, A., Dorken, B., Rabinovitch, P. S., Ledbetter, J. A., Moldenhauer, G., and Clark, E. A. CD19 monoclonal antibody HD37 inhibits anti-immunoglobulin-induced B-cell activation and proliferation., *J. Immunol.* 138: 1389-, 1988.

128. Bradbury, L. E., Kansas, G. S., Levy, S., Evans, R. L., and Tedder, T. F. The CD19/CD21 signal transducing complex of human B-lymphocytes includes the target of antiproliferative antibody-1 and leu-13 molecules, *J. Immunol.* 149: 2841-2850, 1992.

129. Grossbard, M. L., Freedman, A. S., Ritz, J., Coral, F., Goldmacher, V. S., Eliseo, L., Spector, N., Dear, K., Lambert, J. M., Blattler, W. A., Taylor, J. A., and Nadler, L. M. Serotherapy of B-cell neoplasms with anti-B4-blocked ricin: A phase I trial of daily bolus infusion, *Blood*. 79: 576-585, 1992.

130. Grossbard, M. L., Lambert, J. M., Goldmacher, V. S., Spector, N. L., Kinsella, J., Eliseo, L., Coral, F., Taylor, J. A., Blattler, W. A., Epstein, C. L., and

Nadler, L. M. Anti-b4-blocked ricin-- A phase-I trial of 7-day continuous infusion in patients with B-cell neoplasms., *J. Clin. Oncol.* *11*: 726-, 1993.

131. Stone, M. J., Sausville, E. A., Fay, J. W., Headlee, D., Collins, R. H., Figg, W. D., Stetler Stevenson, M., Jain, V., Jaffe, E. S., Solomon, D., Lush, R. M., Senderowicz, A., Ghetie, V., Schindler, J., Uhr, J. W., and Vitetta, E. S. A phase I study of bolus versus continuous infusion of the anti-CD19 immunotoxin, IgG-HD-37-dgA, in patients with B-cell lymphoma, *Blood.* *88*: 1188-1197, 1996.

132. Ghetie, M.-A., Richardson, J., Uhr, J. W., and Vitetta, E. S. The anti-tumor activity of an anti-CD22-immunotoxin in SCID mice with disseminated Daudi lymphoma is enhanced by either an anti-CD29 antibody or and anti-CD19 immunotoxin., *Blood.* *80*: 2315-, 1992.

133. Flavell, D. J., Noss, A., Pulford, K., Ling, N., and Flavell, S. U. Systemic therapy with 3BIT, a triple combination cocktail of anti-CD19, -CD22, and -CD38-Saporin immunotoxins, is curative of human B-cell lymphoma in severe combined immunodeficient mice., *Cancer Res.* *57*: 48244829, 1997.

134. Lopes de Menezes, D. E., Pilarski, L. M., and Allen, T. M. In vitro and in vivo targeting of immunoliposomal doxorubicin to human B-cell lymphoma, *Cancer Res.* *58*: 3320-3330, 1998.

135. Bosma, G. c., Custer, R. P., and Bosma, M. J. A severe combined immunodeficiency mutation in the mouse., *Nature.* *301*: 527-530, 1983.

136. Ghetie, M.-A., Richardson, J., Tucker, T., Jones, D., Uhr, J. W., and Vitetta, E. S. Disseminated or localized growth of a human B-cell tumor (Daudi) in SCID mice., *Int. J. Cancer.* *45*: 481-485, 1990.

137. Richardson, D. S. and Johnson, S. A. Anthracyclines in hematology: preclinical studies, toxicity and delivery systems, *Blood Rev.* 11: 201-223, 1977.
138. Bonadonna, G., Monfardini, S., de Lena, M., and Fossati-Bellani, F. Clinical evaluation of adriamycin, a new antitumor antibiotic., *Br. Med. J.* 3: 503-506, 1969.
139. Friesen, C., Herr, I., Krammer, P. H., and Debatin, K.-M. Involvement of the CD95(APO-1/Fas) receptor/ligand system in drug-induced apoptosis in leukemia cells., *Nature Medicine.* 2: 574-580, 1996.
140. Herr, I., Wilhelm, D., Bohler, T., Angel, P., and Debatin, K.-M. Activation of CD95 (APO-1/Fas) signaling by ceramide mediates cancer therapy-induced apoptosis., *EMBO J.* 16: 6200-6208, 1997.
141. Müller, I., Niethammer, D., and Bruchelt, G. Anthracycline-derived chemotherapeutics in apoptosis and free radical cytotoxicity, *Int. J. Mol. Med.* 1: 491-494, 1998.
142. Basser, R. L. and Green, M. D. Strategies for prevention of anthracycline cardiotoxicity., *Cancer Treatment Reviews.* 19: 57-77, 1993.
143. Sommerman, E. F., Pritchard, P. H., and Cullis, P. R. ¹²⁵I labelled inulin: a convenient marker for deposition of liposomal contents *in vivo*, *Biochem. Biophys. Res. Commun.* 122: 319-324, 1984.
144. Zola, H., Macardle, P. J., Bradford, T., Weedon, H., Yasui, H., and Kurosawa, Y. Preparation and characterization of a chimeric CD19 monoclonal antibody, *Immunol. and Cell Biol.* 69: 411-422, 1991.

145. Bradford, M. M. A rapid and sensitive method for the quantitation of microgram quantities of protein utilizing the principle of protein-dye binding, *Anal. Biochem.* 72: 248-254, 1976.
146. Hope, M. J., Bally, M. B., Webb, G., and Cullis, P. R. Production of large unilamellar vesicles by a rapid extrusion procedure. Characterization of size distribution, trapped volume and ability to maintain a membrane potential., *Biochim. Biophys. Acta.* 812: 55-65, 1985.
147. Bartlett, G. R. Phosphorus assay in column chromatography, *J. Biol. Chem.* 234: 466-468, 1959.
148. Mosmann, T. Rapid colorimetric assay for cellular growth and survival: application to proliferation and cytotoxicity assays, *J. Immunol. Methods.* 65: 55-63, 1983.
149. Ishida, T., Iden, D. L., and Allen, T. M. A combinatorial approach to producing sterically stabilized (Stealth) immunoliposomal drugs, *FEBS Lett.* 460: 129-133, 1999.
150. Needham, D., Stoicheva, N., and Zhelev, D. Exchange of monooleoylphosphatidylcholine as monomer and micelle with membranes containing poly(ethylene glycol)-lipid., *Biophysical Journal.* 73: 2615-2629, 1997.
151. Feinstein, A. and Rowe, A. J. Molecular mechanism of formation of an antigen-antibody complex, *Nature.* 205: 147-149, 1965.

152. Lambert, J. M., Goldmacher, V. S., Collinson, A. R., Nadler, L. M., and Blattler, W. A. An immunotoxin prepared with blocked ricin: a natural plant toxin adapted for therapeutic use, *Cancer Res.* 51: 6236-6242, 1991.
153. Press, O. W., Farr, A. G., Borroz, K. I., Andersen, S. K., and Martin, P. J. Endocytosis and degradation of monoclonal antibodies targeting human B-cell malignancies, *Cancer Res.* 49: 4906-4912, 1989.
154. Goulet, A. C., Goldmacher, V. S., Lambert, J. M., Baron, C., Roy, D. C., and Kouassi, E. Conjugation of blocked ricin to an anti-CD19 monoclonal antibody increases antibody-induced cell calcium mobilization and CD19 internalization, *Blood.* 90: 2364-2375, 1997.
155. Lopes de Menezes, D. E., Kirchmeier, M. J., Gagne, J.-F., Pilarski, L. M., and Allen, T. M. Cellular trafficking and cytotoxicity of anti-CD19-targeted liposomal doxorubicin in B lymphoma cells, *J. Liposome Res.* 9: 199-228, 1999.
156. Van Renswonde, A. J. B. M. and Hoekstra, D. Cell-induced leakage of liposomal contents, *Biochemistry.* 20: 540-548, 1981.
157. Bally, M. B., Lim, H., Cullis, P. R., and Mayer, L. M. Controlling the drug delivery attributes of lipid-based drug formulations., *J. Lip. Res.* 8: 299-335, 1998.
158. Straubinger, R. M., Papahadjopoulos, D., and Hong, K. Endocytosis and intracellular fate of liposomes using pyranine as a probe, *Biochem.* 29: 4929-4939, 1990.
159. Pulczynski, S., Boesen, A. M., and Jensen, O. M. Antibody-induced modulation and intracellular transport of CD10 and CD19 antigens in human B-

cell lymphoma cell lines: an immunofluorescence and immunoelectron microscopy study., *Blood*. *81*: 1549-1557, 1993.

160. Lokich, J. J. and Moore, C. Chemotherapy-associated palmar-plantar erythrodysesthesia syndrome, *Annals of internal medicine*. *101*: 798-800, 1984.

161. Balazsovits, J. A., Mayer, L. D., Bally, M. B., Cullis, P. R., McDonell, M., Ginsberg, R. S., and Falk, R. E. Analysis of the effect of liposome encapsulation on the vesicant properties, acute and cardiac toxicities, and antitumor efficacy of doxorubicin, *Cancer Chemother. Pharmacol*. *23*: 81-86, 1989.

162. Flavell, D. J., Noss, A., Pulford, K. A. F., Ling, N., and Flavell, S. U. Systemic therapy with 3BIT, a triple combination cocktail of anti-CD19, -CD22, and -CD38-saporin immunotoxins, is curative of human B-cell lymphoma in severe combined immunodeficient mice, *Cancer Res*. *57*: 4824-4829, 1997.

163. Czuczman, M. S., Grillo-López, A. J., White, C. A., Saleh, M., Gordon, L., LoBuglio, A. F., Jonas, C., Klippenstein, D., Dallaire, B., and Varns, C. Treatment of patients with low-grade B-cell lymphoma with the combination of chimeric anti-CD20 monoclonal antibody and CHOP chemotherapy., *J. Clin. Oncol*. *17*: 268-278, 1999.